<u>ISTANBUL TECHNICAL UNIVERSITY ★ GRADUATE SCHOOL</u>

MULTIPLE OBJECTIVE OPTIMIZATION OF A FUEL-CELL HYBRID ELECTRIC TRUCK USING GENETIC ALGORITHM

M.Sc. THESIS

Baturay GÜRSEL

Department of Electrical Engineering

Electrical Engineering Master's Programm

JUNE 2024

ISTANBUL TECHNICAL UNIVERSITY ★ GRADUATE SCHOOL

MULTIPLE OBJECTIVE OPTIMIZATION OF A FUEL-CELL HYBRID ELECTRIC TRUCK USING GENETIC ALGORITHM

M.Sc. THESIS

Baturay GÜRSEL
504151055

Department of Electrical Engineering

Electrical Engineering Master's Programme

Thesis Advisor: Assoc. Prof. Dr. Murat YILMAZ

JUNE 2024

ISTANBUL TEKNİK ÜNİVERSİTESİ ★ LİSANSÜSTÜ EĞİTİM ENSTİTÜSÜ

YAKIT HÜCRELİ HİBRİT ELEKTRİKLİ KAMYONUN GENETİK ALGORİTMA KULLANARAK ÇOK HEDEFLİ OPTİMİZASYONU

YÜKSEK LİSANS TEZİ

Baturay GÜRSEL
(504151055)

Elektrik Mühendisliği Anabilim Dalı

Elektrik Mühendisliği Programı

Tez Danışmanı: Doç. Dr. Murat YILMAZ

HAZİRAN 2024

Baturay GÜRSEL, a M.Sc. student of İTU Graduate School student ID 504151055, successfully defended the thesis/dissertation entitled "MULTIPLE OBJECTIVE OPTIMIZATION OF A FUEL-CELL HYBRID ELECTRIC TRUCK USING GENETIC ALGORITHM", which he prepared after fulfilling the requirements specified in the associated legislations, before the jury whose signatures are below.

Thesis Advisor : **Assoc. Prof. Dr. Murat YILMAZ** ....
İstanbul Technical University

Jury Members : **Asst. Prof. Dr. Deniz YILDIRIM** ....
Istanbul Technical University

Assoc. Prof. Dr. Nihan ALTINTAŞ ....
Yıldız Technical University

Date of Submission : 24 May 2024
Date of Defense : 26 June 2024

To my lovely spouse, daughter, beloved parents and brother,

FOREWORD

I am deeply grateful to my supervisor, Assoc. Prof. Dr. Murat Yılmaz, for his endless support, patience, and guidance throughout my research journey. His motivation and inspiration have truly shaped my academic endeavor.

Another special thanks to Serhat Sancı and Melih Yördem, for their significant contributions to my study.

I extend my heartfelt appreciation to my wonderful spouse, Büşra Gürsel, for her unwavering patience and support. Additionally, I am thankful to my lovely daughter, who has provided the motivation during these challenging times.

I owe profound thanks to my parents, Filiz and Cengiz Gürsel, and my brother, Kutay Gürsel, for their constant encouragement and support throughout this endeavor.

.

JUNE 2024

Baturay GÜRSEL
(Electrical Engineer)

TABLE OF CONTENTS

Page

ABBREVIATIONS

ICE	: Internal Combustion Engine
BEV	: Battery Electric Vehicle
FCHEV	: Fuel-Cell Hybrid Electric Vehicle
FCHET	: Fuel-Cell Hybrid Electric Truck
EMS	: Energy Management System
GA	: Genetic Algorithm
SOC	: State of Charge
GHG	: Green House Gas
IEA	: International Energy Agency
TTW	: Tank to Wheel
FCS	: Fuel-cell System
UC	: Ultracapacitor
DC	: Direct Current
HV	: High Voltage
NEDC	: New European Driving Cycle
UDDS	: Urban Dynomometer Driving Schedule
ICCT	: International Council of Clean Transport
HDEV	: Heavy Duty Electric Vehicle
LNG	: Liquified Natural Gas
SI	: Spark Ignition
CI	: Compressed Ignition
TCO	: Total Cost of Ownership
OEM	: Original Equipment Manufacturer
GVW	: Gross Vehicle Weight
PTO	: Power Take-off
ESS	: Energy Storage System
NaS	: Sodium-Sulfur
NaNiCl	: Sodium-Nickel Chloride
VRFB	: Vanadium Redox Flow Battery
ZBFB	: Zinc-Bromine Flow Battery

Li-ion : Lithium Ion
NMC : Nickel Manganase Cobalt
LFP : Lithium Iron Phosphate
PEM : Proton Exchange Membrane
PEM FC : Proton Exchange Membrane Fuel-cell
AFC : Alkaline Fuel-cell
PAFC : Phoshoric Acide Fuel-cell
MCFC : Molten Carbonate Fuel-cell
SOFC : Solid Oxide Fuel-cell
DMFC : Direct Methanol Fuel-cell
MEA : Membrane Electrode Assembly
CHG : Compressed Hydrogen Gas
sLH_2 : Subcooled Liquid Hydrogen
CCH_2 : Cryo-Compressed Hydrogen
TRL : Technology Readiness Level
DP : Dynamic Programming
MPC : Model Predictive Control
NN : Neural Networks
RL : Reinforcement Learning
LV : Low Voltage
CO_2 : Carbon dioxide
HDV : Heavy Duty Vehicle
MFFD : Mean Fully Developed Deceleration
SD : Stopping Distance
DoD : Depth of Discharge
LHV : Lower Heating Value
LH_2 : Liquid Hydrogen

SYMBOLS

t	: Time
c_D	: Aerodynamic drag coefficient
c_r	: Air density
A_f	: Frontal vehicle surface
v_{veh}	: Vehicle speed
v_0	: Initial speed
$F_{gravity}$	: Gravitational force
M_{veh}	: Vehicle weight
g	: Gravitational constant
δ	: Mass factor of the vehicle
m	: Mass
a	: Acceleration
η_{colm}	: Coulombic efficiency
Q_{bat}	: Battery capacity
V_{ocv}	: Open circuit voltage of battery
R_{bat}	: Battery internal resistance
P_{bat}	: Battery output power
I_{bat}	: Battery output current
P_{fc}	: Total power generated by FCS
$Pfcs$	: Net output power of FCS
$Paux$	: Auxiliary power demand
η	: Fuel net efficiency
LHV	: Lower heating value of hydrogen
M_{H2}	: Hydrogen molar mass
P_{idle}	: Idle operation output power of FCS
$P_{continuous}$	: Continuous operation output power of FCS
$P_{maximum}$	: Maximum operation output power of FCS
$J_{fitness}$	: Fitness function
$W1$	: Weight of the variable

$\boldsymbol{SOC_{Low}}$ **:** Lowboundry set-point of SOC

$\boldsymbol{SOC_{High}}$ **:** High boundry set-point of SOC

LIST OF FIGURES

Page

LIST OF TABLES

Page

MULTIPLE OBJECTIVE OPTIMIZATION OF A FUEL-CELL HYBRID ELECTRIC TRUCK USING GENETIC ALGORITHM

SUMMARY

The urgency to mitigate CO_2 emissions has driven a significant shift towards electrification in the transportation sector. Heavy-duty 40-tonne long-haul vehicles stand out as a crucial target for electrification due to their substantial contribution to emissions and energy consumption. In this study, a novel approach is presented to optimize the energy management system (EMS) of a fuel-cell electric truck using a genetic algorithm (GA). The primary aim of this research is to optimize the EMS for FCEVs to enhance performance while reducing environmental impact and operational costs.

The study begins with a comparative analysis focusing on lithium iron phosphate (LFP) and nickel manganese cobalt oxide (NMC) batteries. The initial BEV model sets a baseline, helping to facilitate subsequent advancements in FCHEV design. Within the FCHEV's EMS, LFP batteries are specifically chosen for their robust charge retention capabilities under varied operational conditions. Detailed simulations ensure that the EMS aligns with real-world driving conditions and meets industry standards. The algorithm prioritizes battery usage for vehicle start-up, peak loads, and regenerative braking, while the fuel-cell system (FCS) provides the primary energy during lower power demands, also recharging the battery to maintain an optimal state of charge (SOC).

Using a genetic algorithm, the study optimized the operational SOC range to minimize hydrogen consumption and extend battery lifespan. Initial SOC thresholds were set between 40% and 80%. As a result of the optimization, these thresholds were adjusted to 40-60% to achieve lower DoD of the Battery. This adjustment led to a battery life extension, reduction in hydrogen consumption, decrease in overall fuel-cell system usage reflecting in significant energy and packaging volume savings.

The initial optimization phase showed a 3.97% decrease in hydrogen usage (3.21 kg) and a 0.9% drop in unrecoverable energy (5.1 Wh) by keeping the battery's DoD at 35%. Further optimization involved maintaining the FCS operational setpoints at their original levels while adjusting the high and low SOC limits of the EMS using GA. The adjusted SOC thresholds, set at 60% and 40%, led to additional efficiency improvements when integrated into the model. By keeping the battery DoD at 20%, 1.27% reduction in hydrogen consumption (1.02 kg) has been achieved. The final optimization phase involved substituting the initial FCS operating points with those optimized and adjusting the battery's SOC operational boundaries to 40% and 60% following the same GA approach. This final setup reduced hydrogen consumption by 3.96% which equals to 3.17 kg of liquid hydrogen and decreased unrecoverable energy by 5.2 Wh, maintaining the battery DoD at 20%. The management of battery cycling between 40% and 60% SOC significantly extended the battery's lifecycle by reducing electrode degradation and stress on the cells.

This optimized strategy not only improves the FCHEV efficiency but also extends its range by roughly 40 km for every 3.17 kg of saved hydrogen, achieving a fuel economy of about 12.62 km per kilogram of hydrogen. Additionally, it reduces the hydrogen storage requirements by about 51.3 liters, providing space that could be used for extra packaging or system components, thereby enhancing the vehicle’s utility and functionality. This thesis contributes significantly to the field of EMS for fuel-cell electric trucks, offering valuable insights into optimizing such systems for better efficiency and sustainability. The findings suggest that genetic algorithms are an effective tool for achieving significant enhancements in FCEV performance, marking a promising step towards greener heavy-duty transport solutions.

YAKIT HÜCRELİ HİBRİT ELEKTRİKLİ KAMYONUN GENETİK ALGORİTMA KULLANARAK ÇOK HEDEFLİ OPTİMİZASYONU

ÖZET

CO_2 gazı salınımını azaltmaya yönelik belirlenen hedefler, ulaşım sektöründe elektrifikasyona yönelmeye neden olmuştur. Toplam çevresel etkinin %25 lik kısmı yalnızca taşımacılık sektöründen meydana gelmektedir. CO_2 gazı salınımı ve ağır pazar payları göz önüne alındığında, ağır yük taşımacılığında kullanılan 40 tonluk uzun mesafeli araçlar, elektrifikasyonun kritik hedefleri arasında yer almaktadır. Avrupa komisyonu tarafında belirlenen 2035 gaz salınım hedefleri doğrultusunda içten yanmalı motorlara sahip ağır vasıta araçlarının dekarbonizasyon çalışmaları hız kazanmıştır. Batarya elektrikli araçlar (BEV) ve yakıt hücreli elektrikli araçlar (FCHEV) uygulanabilir alternatifler olarak öne çıkmaktadır. Bu çalışmada, hedeflere uygun bir FCHEV araç modeli oluşturulup genetik algoritma (GA) kullanılarak aracın enerji yönetim sistemini (EMS) optimize etmeye yönelik bir yaklaşım sunulmaktadır.

Bu araştırmanın temel amacı, FCHEV için EMS'yi optimize ederek performansı arttırırken çevresel etkiyi ve işletme maliyetlerini azaltmaktır. Çalışma, BEV ve yakıt FCHEV için ortak olarak kullanılacak boylamsal araç modeli ile elektrikli güç aktarım mekanizmasının modellenmesi ile başlamıştır. Bu doğrultuda sürekli mıknatıslı senkron motor, güç eviricisi, soğutma ve aktarma organının entegre yapıda olduğu bir sistem benimsenmiştir. Bu yapının verimi, güç elektroniği ve güç aktarma organlarının verimini içermektedir ve toplam talep gücü bataryadan talep edilen toplam tahrik gücüne eşit olarak kabul edilmektedir. Araç modellemesi için seri üretimde olan bir ağır vasıta uzun yol taşıtının boylamsal modeli kullanılmıştır. Sıcaklık etkisini ve yan yük taleplerini doğru modellemek için mevcut bir araç uygulamasının test ölçüm bilgilerine başvurulmuştur. Oluşturulan ortak elektrikli güç aktarım mekanizmasına sırasıyla lityum demir fosfat (LFP) ve nikel manganez kobalt oksit (NMC) bataryaları entegre edilerek BEV modeli oluşturulmuş ve bu enerji depolama yöntemleri çalışmanın hedefleri doğrultusunda karşılaştırılmıştır. İki BEV modeli, Avrupa Komisyonunun egzoz gazı salınım ölçümleri için belirlediği sürüş çevrimi olan VECTO çevriminde koşturularak enerji geri kazanımı, maliyet ve menzil odaklı kıyaslanmıştır. Karşılaştırma sonucunda LFP batarya, yüksek şarj kabulü ve düşük maliyeti nedeniyle öne çıkmış ve FCHEV araç modellemesinde ikincil enerji depolama sistemi olarak kullanılmaya karar verilmiştir.

FCEV aracı LFP batarya ile modellenerek buna yönelik bir EMS modeli geliştirilmiştir. EMS modeli ile aracın şarj tutan modda çalışması hedeflenmiştir. Bu doğrultuda Batarya şarj durumu (SOC) için batarya ömrünü en uzun sürede tutacak alt ve üst değerler belirlenerek, SOC'nin bu değerler arasında tutulması amaçlanmıştır. Batarya kapasitesini belirleyebilmek için yalnıza bataryadan tahrik edilerek katedilmesi gereken mesafe 35km olarak belirlerek, bu mesafeyi katedebilmek için

gerekli batarya kapasitesi modelleme ortamında tespit edilmiştir. Birincil enerji sistemi olan hidrojen sisteminin devredışı kaldığı durumda aracın yalnızca bataryadan tahrik edilerek en yakın hidrojen dolum istasyonuna ya da atölyeye ulaşması durumu göz önüne alınmıştır. Aracın hidrojeni tamamen tükendiğinde, yalnızca batarya ile istasyona ulaşma durumu göz önüne alınarak gerekli batarya kapasitesi 70kWh olarak hesaplanmıştır. Model, fren homologasyon standartlarına (ECE-R13) uyum ve FCEV sisteminin verimlilik eğrisini optimize etmek için kapsamlı bir şekilde tasarlanmıştır. Homologasyon hedeflerine yönelik olarak Rejeneratif frenleme ile geri kazanılamayan enerji miktarının azaltılması amaçlanmıştır. Algoritmaya göre, bataryanın ve yakıt hücresi sisteminin (FCS) aktivasyonu planlanmıştır. Anlık yük taleplerinde ve rejeneratif frenleme için batarya kullanımına öncelik verilirken, aracın ortalama sürekli yük ihtiyacı ve düşük güç talepleri sırasında FCS'nin birincil enerjiyi sağlaması ve ayrıca optimal bir şarj durumu (SOC) seviyesini korumak amacıyla bataryayı şarj etmesi öngörülmüştür. Algoritmada FCS, aktivasyon kaynaklı oluşabilecek ekstra güç talebini engellemek için sürekli modda çalıştırılmıştır. FCS'nin verim haritasındaki yüksek verim bölgesinde üç çalışma noktası (boşta çalışma, sürekli çalışma, maksimum çalışma) belirlenerek algoritma içerisinde girdi olarak kullanılmıştır. Bataryanın yüksek ve düşük SOC bölgelerinde çalışmasını engellemek amacıyla, algoritma içerisinde yüksek ve düşük sınır noktaları belirlenmiş ve bataryanın bu sınır değerleri arasında çalışması hedeflenmiştir.

GA kullanılarak yapılan çalışmada, hidrojen tüketimini en aza indirmek ve batarya ömrünü uzatmak amacıyla EMS'de yer alan FCS'nin çalışma noktaları ile SOC üst ve alt sınır çalışma aralığı optimize edilmiştir. Yapılan literatür araştırmalarına göre SOC için ilk sınır değerleri %40 ve %80 olarak belirlenmiştir. Optimizasyon sonucu olarak bu sınır değerler %40-%60 olarak güncellenmiştir. Bu güncelleme sonrası yeni FCS çalışma noktaları ile SOC alt ve üst sınır değerleri kullanılarak çevrim tekrarlandığında, batarya deşarj derinliğinin (DoD) azalarak batarya ömrünü iki kata kadar uzattığı, hidrojen tüketiminde ve genel yakıt hücresi kullanımında azalmaya neden olduğu gözlemlenmiştir.

GA uygulanarak öncelikle FCS çalışma noktaları optimize edilmiş ve sistem yeniden koşturulduğunda, 1000 km'lik VECTO çevriminde hidrojen tüketiminde 3.21kg (%3.97) ve geri kazanılamayan enerji miktarında da %0,9'luk bir azalma gözlenmiştir. Diğer yandan bataryanın DoD aralığı %35 oranında kalmıştır. Daha sonra yapılan optimizasyon çalışmasında, FCS'nin giriş değerleri sabit tutularak SOC sınır noktaları optimize edilip model yeni sınır değerler ile koşturulmuştur. Bu çevrim sonucu DoD %20 oranına düşmüş olsa da hidrojen tüketimindeki azalma 1.02kg (%1.27) ile sınırlı kalmıştır. Son olarak optimize edilmiş FCS çalışma noktaları ile SOC sınır değerleri modele entegre edilerek çevrim tekrarlanmıştır. Optimize çalışma noktaları ile tekrarlanan çevrim sonucunda hidrojen tüketiminde 3.17kg (%3.96) ve geri kazanılamayan enerji miktarında 5.2 W düşüş sağlanırken, batarya DoD değeri %22 seviyesinde tutulmuştur. Ortaya konulan strateji sonucu mevcut hidrojen depolama sistemi korunduğunda, 1000km'lik çevrimde aracın menzili 40km artış göstermektedir. Ayrıca menzil korunduğunda, depolama ihtiyacı 51.3 litre azaldığından, bu alan ek paketleme ve sistem bileşenleri için kullanılabilecek bir alan sağlayarak aracın kullanışlılığını ve işlevselliğini arttırmaktadır. Sonuçlar, FCEV'lerde EMS optimizasyonu için GA'nın etkinliğini vurgulamaktadır. Geri kazanılamayan enerjinin ve işletme maliyetlerinin önemli ölçüde azaltılmasını göstermektedir.

Bu tez, yakıt hücreli elektrikli kamyonlar için EMS alanına önemli katkılarda bulunarak bu tür sistemleri daha verimli ve sürdürülebilir hale getirme konusunda önemli fikirler sunmaktadır. Bulgular, genetik algoritmaların FCEV performansında önemli iyileştirmeler elde etmek için etkili bir araç olduğunu göstermekte ve daha çevre dostu ağır yük taşımacılığı çözümlerine yönelik umut vadeden bir adım olduğunu ortaya koymaktadır.

1. INTRODUCTION

In today's world, the primary cause of the climate crisis is the increasing emission of CO_2 gases. The use of fossil fuels has led to a significant rise in CO_2 emissions over the years, resulting in global temperature increases and increased air pollution. Carbon gas emissions from vehicles powered by conventional fuels pose a serious threat to the environment and directly impact climate change [1]. According to the IEA (2021), 24% of CO_2 emissions are solely attributed to transportation. The widespread use of internal combustion engines (ICEs) in the transportation sector is the fundamental reason for the use of fossil fuels. Besides contributing to environmental pollution, these ICEs have very low energy efficiency. Recognizing these negative effects, regulations have gradually restricted carbon gas emissions over the years, making the use of alternative energy sources mandatory today [2]. In 2019, a report published by the UN Secretary-General's office set a target of reducing carbon emissions in the heavy-duty transportation sector by 40% by 2035, in conjunction with regulations, initiating the transformation into carbon-neutral vehicles. Achieving these goals has made the use of alternative energy sources and electrification of vehicles mandatory. Vehicle electrification can be implemented using various technologies.

The transformation in the transportation sector initially began with hybrid vehicles and subsequently continued with electric vehicles. Despite long-standing research efforts in battery electric vehicles, their widespread adoption has taken time due to factors such as low battery energy density, high cost, uncertainties regarding infrastructure, and recycling.

Battery electric vehicles, despite their environmentally friendly and efficient design, have limitations such as power and energy density constraints, which restrict their range and result in long charging times. Efforts are being made to improve charging times and reduce component sizes, both in vehicle systems and infrastructure [3].

Hydrogen electric vehicles have gained importance as an alternative, offering the potential for longer driving ranges and the possibility to convert existing infrastructure for use. However, similar to battery systems, hydrogen systems face various challenges, including operating temperature, efficiency, cost, hydrogen production and storage, and infrastructure.

The hydrogen system operates as an unidirectional system with electricity production following an exothermic reaction. While it serves as the main power source in vehicle applications, to meet the instantaneous power demands of the vehicle and ensure the stable and efficient operation of the hydrogen fuel-cell stack, a hybrid configuration is used with different energy storage systems for the activation of chemical reactions and energy recovery within the hydrogen system. Energy storage systems vary depending on the vehicle application. In heavy-duty and long-haul applications, power transmission systems for hydrogen electric vehicles are commonly built in a hybrid configuration with lithium-based batteries. Despite the lower energy content of hydrogen electric vehicle batteries compared to battery electric vehicles, the system still has both battery-related challenges and advantages because of having batteries [4].

For a hydrogen electric vehicle designed for specific driving cycles with efficient and high-performance driving needs, the choice of battery technology and EMS are very important. In this regard, the following section provides a literature summary of the thesis's objectives and the related topics.

1.1 Purpose of Thesis

Within the scope of this master's thesis, the objective is to convert a long-haul heavy-duty tractor vehicle into a Fuel-Cell Hybrid Electric (FCHEV) structure using the most suitable topology, system voltage, and energy storage systems.

When constructing the FCHEV structure, the goals of hydrogen consumption minimization and battery and fuel-cell system's lifetime optimization have been taken into consideration.

For this study, a 44-ton heavy-duty tractor with a 4x2 chassis configuration has been taken as a basis. Initially, a battery electric vehicle (BEV) has been modeled at a 800V system voltage with different lithium based battery technologies which vary in terms of energy and power densities. These BEV's are assessed in terms of system lifespan and range performance according to the Vehicle Energy Consumption Calculation TOol (VECTO).

Building upon the reference of the battery electric vehicle model, a FCHEV structure is developed by integrating a designated fuel cell system with research-based operation set-points. Batteries are sized according to the design concerns of a FCHEV. The proposed vehicle is first driven according to rule-based EMS algorithms for design verification. The rule-based EMS algorithm parameters are further optimized using a multi-objective Genetic Algorithm (GA) to achieve minimum hydrogen consumption and maximum system lifespan. The results obtained through optimization with GA are compared with the initial state of the rule-based EMS.

Vehicle simulation is performed in the MATLAB/Simulink environment, where hydrogen consumption, fuel-cell system durability, and battery DoD are optimized using the GA framework.

In the initial phase of this study, rule-based EMS has been considered to make fundemental comparisons and topology selections. GA is proposed for offline multiple objective optimization scenarios and combined with rule-based EMS.

1.2 Literature Review

With the increasing impact of greenhouse gas (GHG) emissions on global warming, the importance of low-emission transportation technologies is growing worldwide. The population growth in large cities and the widespread use of fossil fuel-powered vehicles have become a major source of local air pollution and a concerning issue for public health today [5].

In Europe, heavy-duty vehicles constitute approximately 25% of the total CO_2 emissions in road transportation, contributing to 6% of all greenhouse gas emissions. Due to the nature of their usage, they present a significant challenge for pollution reduction efforts. Without any mitigation measures, it is expected that the contribution of heavy-duty vehicles to CO_2 emissions will increase by 9% between 2010 and 2030 [6].

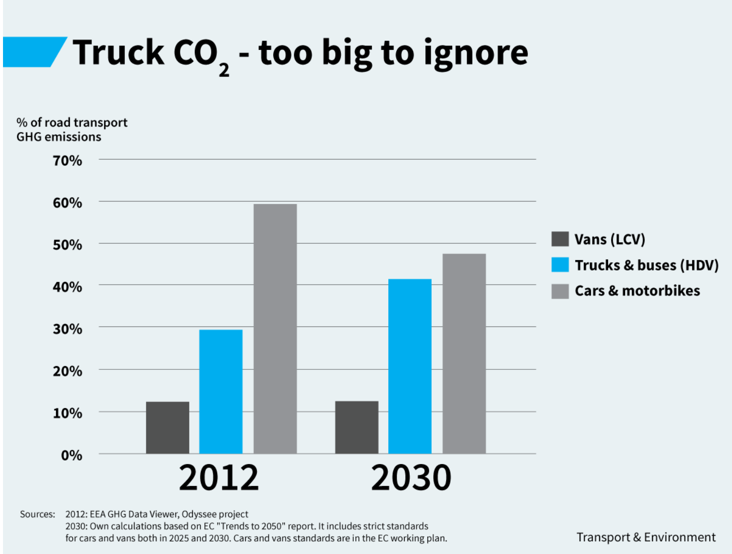

Figure 1.1: CO_2 emission impact of the heavy-duty vehicles [6].

With the increasing impact of GHG emissions on global warming, the importance of low-emission transportation technologies has grown worldwide. Among other applications, long-haul trucks account for approximately 65-70% of these emissions which make them a primary focus in the EU's carbon footprint reduction plans to achieve the goals of the Paris Agreement. With a target of a 90% reduction in net emissions by 2050, the EU has established the CO_2 Emission Standards Regulation ((EU) 2019/1242) for new heavy-duty vehicles. This regulation aims to achieve a fleet-wide reduction of 15% by 2025 and 30% by 2030 compared to the 2019-2020 baseline [7]. According to McKinsey's (2022) global road transportation roadmap report, medium and heavy-duty transport accounts for approximately half of the transportation carbon footprint associated with global trade and about 15% of total European CO_2 emissions, with 70% of this attributed to heavy-duty trucks. The International Energy Agency (IEA) anticipates a 14.8% increase in global CO_2 emissions from heavy-duty vehicles by 2030 [8]. Among various approaches to achieving fuel carbon neutrality, the electrification of heavy-duty vehicles holds a crucial position. Zero-emission zones within cities aim to mitigate urban air pollution, while long-haul applications aim to reduce exhaust gas emissions through electric and plug-in applications [9].

In the process of determining the vehicle configuration to be referenced in the thesis, 17 distinct vehicle groups which have been outlined by Commission Regulation (EU) 2017/2400 have been considered. This categorization is based on criteria such as axle configuration, chassis setup, and maximum allowable gross weight. Among these vehicle groups, the 4x2 Tractor Heavy-Duty Vehicle is distinguished with the highest sales share (43%) and based on 2016 data, the highest CO_2 emission share (over 50%) as presenden in Figure 1.2 [10].

While battery electric propulsion systems are feasible for long-haul applications, there are several constraints limiting their common usage. Key limitations include limited range and long charging times, which affect delivery schedules and operational efficiency. Additionally, the economic and environmental impacts of battery production, together with increased vehicle size and towing weight, reduce cargo capacity, limiting economic viability for the market [11].

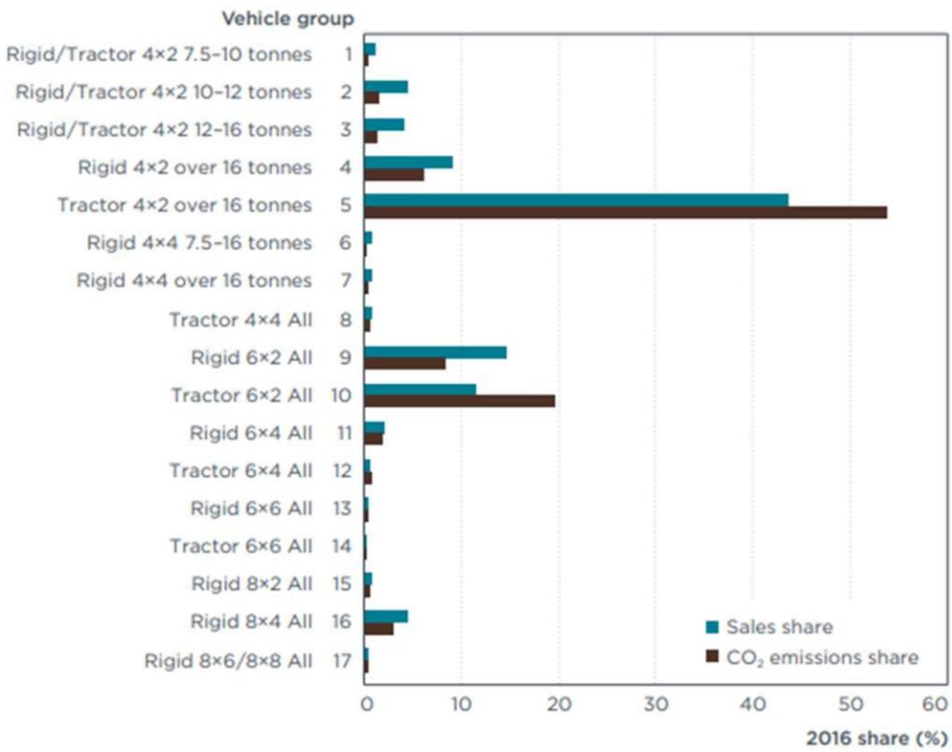

Figure 1.2: CO_2 emissions and sales share for the EU 2017/2400 [10].

FCEV's offer a good alternative for long-haul propulsion compared to BEVs due to their advantages, such as rapid refueling, lower infrastructure requirements, reduced drive system weight, increased cargo capacity, economic benefits, and feasibility. Furthermore, despite lower tank-to-wheel (TTW) efficiency, they are a preferred option in achieving zero exhaust emissions [12]. The fundamental advantage of the fuel-cell systems (FCS) compared to electrochemical batteries is the separation of power generation and portable energy storage, enhancing both aspects and minimizing dependencies [13]. Verbruggen and his fellows demonstrated that for a long-haul 40-ton truck with a 600 km range, a battery pack energy density of 150 Wh/kg and an average energy consumption of 1.72 kWh/km resulted in a minimum reduction of approximately 4 tons in payload capacity [14]. In contrast, a typical heavy-duty fuel-cell electric vehicle (FCEV), equipped with two hydrogen tanks carrying 40-60 kg of hydrogen at 350-bar pressure, can achieve an 800 km range with a single fueling session [15]. In FCEV, the small size of the FCS and the low weight of hydrogen as a fuel lead to a higher payload capacity. However, the need for on-board hydrogen storage tanks and the restrictions from packaging requirements make the Hydrogen technology crucial. In the context of hydrogen storage for heavy-duty vehicles, Subcooled Liquid Hydrogen (sLH_2) systems offer a higher hydrogen storage density (up to ~62 kg/m^3) at lower pressures (-245 °C and approximately 16 bar) compared to Compressed Hydrogen Gas (CHG) systems, resulting in a more compact refueling infrastructure and quicker refueling times under 10 minutes. sLH_2 technology also affords a significant reduction in weight per kg of hydrogen stored and operational costs, potentially increasing the range of heavy-duty trucks to over 1000 km [16].

Hydrogen fuel-cells are emerging as a clean alternative to traditional ICEs, offering similar vehicle performance without emitting greenhouse gases or carbon emissions. Despite their potential, fuel-cell vehicles face challanges related to performance and high costs that limit wider adoption by the customers [17]. FCS of the vehicle brings about further requirements and challanges to the system which are charge of compressor, warming up of fuel-cell stacks and humidification of hydrogen and oxygen and slow dynamic response of FCS. The low dynamic response of FCS shows an important challenge in terms of providing immediate power to the vehicle during acceleration, which leads to an ineeficient fuel usage and increase wear on system component. Besides, due to the unidirectional power flow of the FCS, vehicle necessitates additional measure to recover the braking energy. In order to meet all these requirement, fuel-cell system must be hybridised with secondary energy sources such as batteries or supercapacitors. As a result, vehicle powertrain can be configured via varying combinations of fuel-cells, supercapacitors, and batteries. Figure 1.3 shows the first hybrid fuel-cell vehicle with fuel-cell system and battery. This kind of configuration could lower fuel-cell system prices and the fuel-cell's power. On the other hand addition extra weight, volume and complexity to the system. Vehicle must regulate the operation status of two power supplies [18, 19]. Recently, the cost of fuel-cell vehicles is significantly higher due to the advanced technology involved. An important factor in enhancing both performance and affordability is the optimization of the vehicle's drivetrain design. Various studies have been conducted aiming to find the most suitable vehicle architecture, considering system costs and technical requirements.

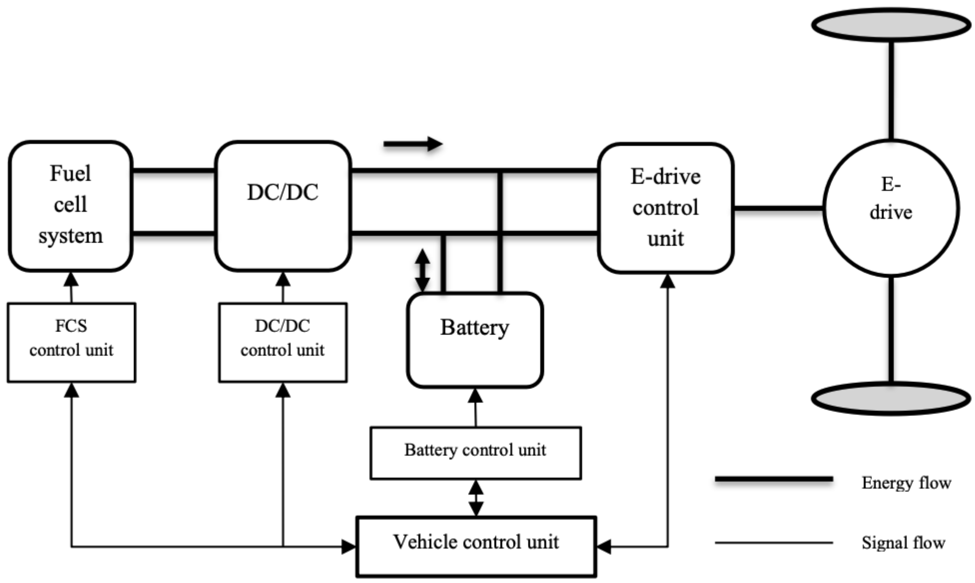

Figure 1.3: Powertrain configuration of fuel-cell and battery.

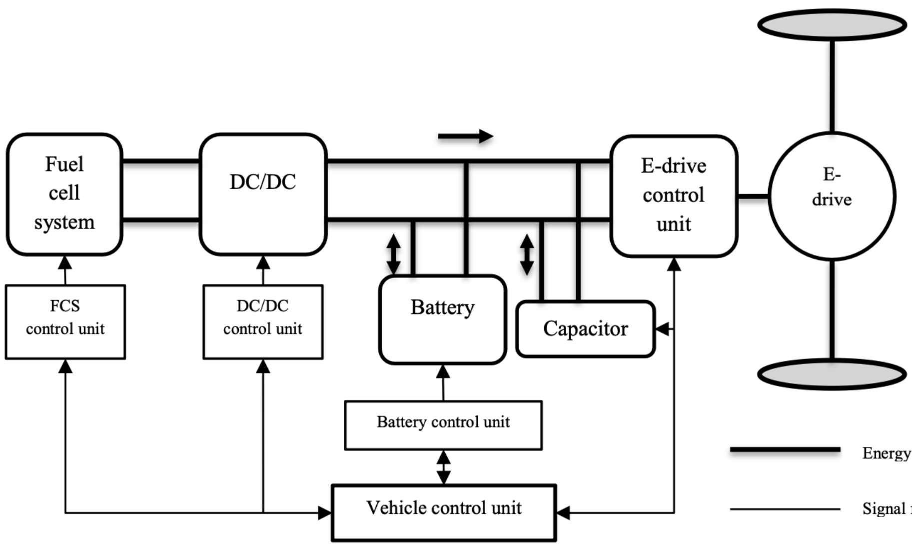

Figure 1.4: Powertrain configuration of fuel-cell and battery and ultracapacitor.

Jennifer Bauman (2008) compared three different powertrain arrangements for FCHEVs to determine the optimal architecture. Three configurations with fuel-cell system with batteries, fuel-cell system with supercapacitors, and combinations of fuel-cell system with batteries and supercapacitors have been evaluated. The analysis reviews power transmission component prices, fuel efficiency, and performance to identify the most effective setup. This study determines the optimal power level for hydrogen systems in vehicles based on minimum power requirements, considering high current and future costs. Among the configurations, the hydrogen-supercapacitor configuration is found to be least favorable due to high costs and poor fuel economy from increased weight and low energy density of supercapacitor. On the other hand, FCS-battery and FCS-battery-supercapacitor show similar performances, having better fuel efficiency and extended battery life but at potentially higher costs [20].

Supporting the findings of Jennifer Bauman (2008), Naylor S. M. et. al. (2006) have researched on various drivetrain configurations which are shown in Figure 1.6, analyzing their performance through simulations in standard vehicle models. This approach involves testing different components and drive cycles to identify optimal configurations for performance and efficiency. They designed a vehicle topology in a modular structure and replaced each component to generate different topologies. Example topology is inherited from an existing BEV. The example configuration is given in Figure 1.5.

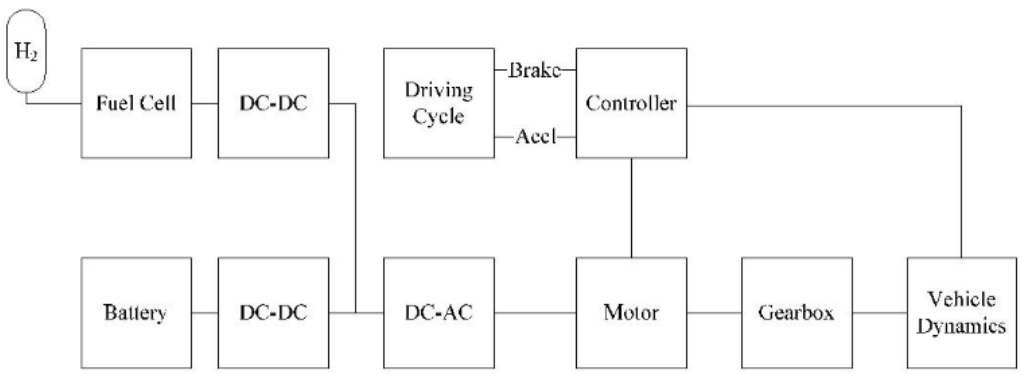

Figure 1.5: Schematic of simulation model [17].

Vehicle model has a Polymer Exchange Membrane Fuel-cell (PEMFC) system with 80 kW power output and a 4 kg hydrogen storage tank. As a battery system, lithium-ion polymer battery packs are used managed due to their favorable energy-to-weight ratio and cycle life. The model is controlled by an embedded controller block. Their Study concluded that having the secondary energy storage system is very crucial to reach the target range and the efficiency of the fuel cell system. Additionally, results indicated that different topologies perform better under different conditions [17].

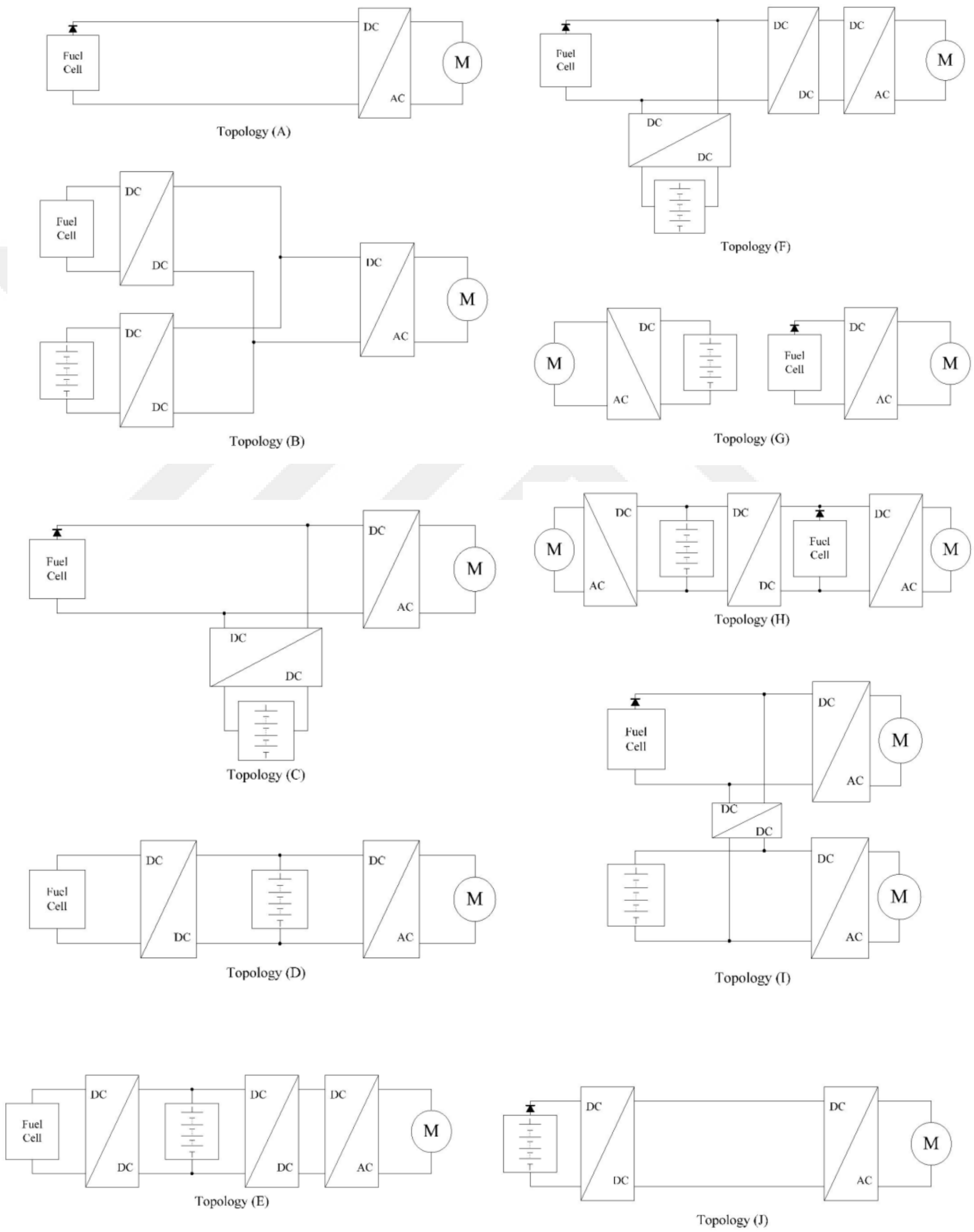

Figure 1.6: Fuel-cell drive train topologies [17].

Possible topology configurations are presented in Figure 1.6. Based on energy storage system connections to the HV-bus, in another research, the benefits and drawbacks of each hydrogen electric vehicle topology are analysed. This includes the topologies of Hydrogen-Supercapacitor, Hydrogen-Battery hybrids, and Hydrogen-Battery-Supercapacitor architectures. The Hydrogen-Battery-Supercapacitor combination found to be ideal for power demands during different vehicle modes, but the Hydrogen-Supercapacitor hybrid was judged inappropriate for large-scale use due to limits on charge and discharge control. Its complicated EMS, high production costs, and difficulties matching energy source parameters prevent it from being commercially viable in the near term. As it is shown in Figure 1.7, since 2012, statistics show that hybridization of a FCS with a battery has attracted more attention than FCS + battery + ultracapacitor (UC). Alternative integration method of these energy sources are shown in Figure 1.8. The study finds that while directly connecting the battery to the high-voltage DC bus optimises lifetime and fuel economy, it also demands higher battery performance, which calls for optimal battery design to keep up with the demands of ever-increasing performance needs.

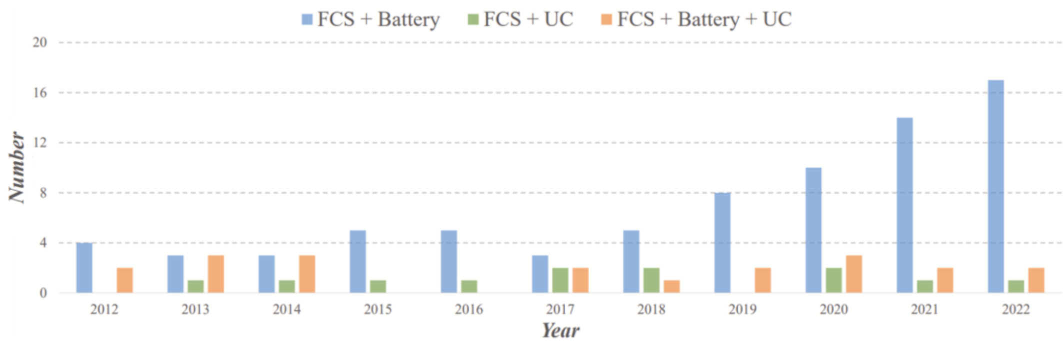

Figure 1.7: Distribution of each topology since 2012 [21].

It is concluded that hybrid system in which the battery is directly connected to the high voltage DC-bus is more advantageous in terms of fuel economy and lifetime optimization compared to other configurations. However, it should be noted that by the direct connection performance demand on the battery increases. With respect to the increasing performance requirements, an optimal battery should be carried out [21].

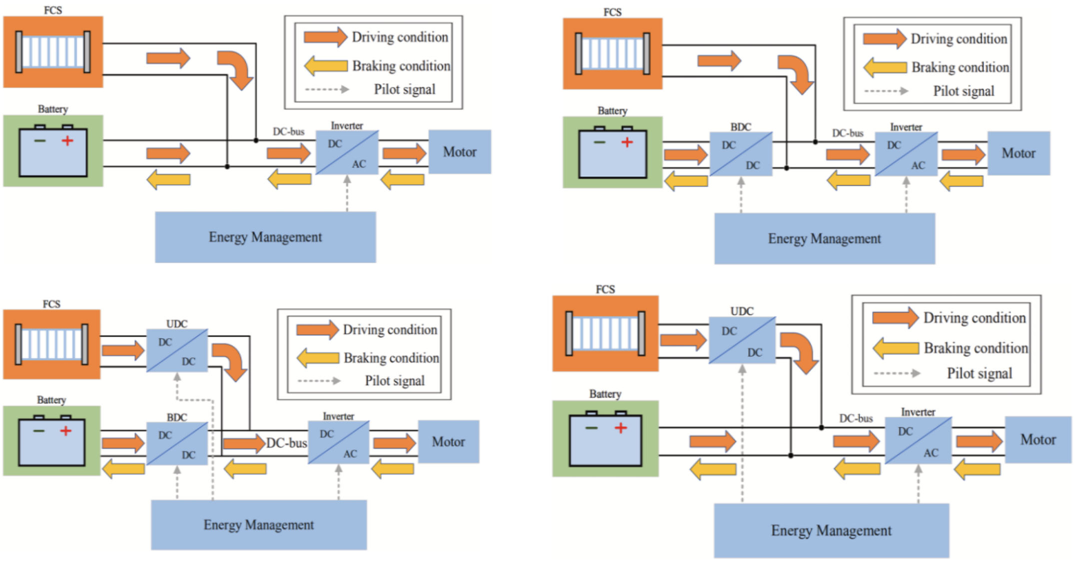

Figure 1.8: Different integration methods of energy sources [21].

According to Pardhi's et. al. (2022) research, in heavy-duty vehicles, the system voltage is determined to be 650V or higher to meet system efficiency and instant peak power demands. In long-haul applications, hydrogen fuel-cells are sized as the primary energy source to power the vehicle's traction and auxiliary loads. Additionally, the use of secondary energy systems enables efficient operation of the hydrogen fuel-cell system and facilitates energy management that allows different subsystems to work efficiently together.

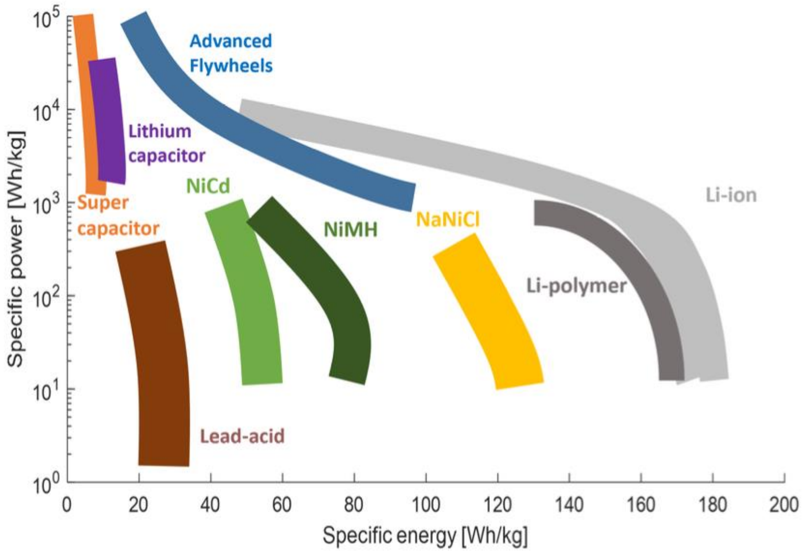

Figure 1.9: Comparison of energy storage systems (ESS) in terms of specific power and specific energy capacities [18].

Electrochemical batteries are used as the secondary ESS. Batteries are suitable for heavy-duty vehicle targets in terms of specific energy, specific power, durability, reaction rate, and cost. Among all electrochemical battery technologies (NiCd, NiMH, NaNiCl) lithium batteries offer the best performance and more choices in a wide range of power and energy. Figure 1.9 presents the comparison of different energy storage systems (ESS). Moreover, they are also commonly preferred thanks to their price-performance index [18].

The fuel-cell hybrid system addresses issues such as slow dynamic response and the inability to efficiently capture braking energy regeneration seen in pure fuel-cell vehicles. However, this introduces a new complexity in managing power distribution within the system. The EMS is important for allocating power effectively, requiring improvements for optimal performance. EMS's that employ rule-based strategies coupled with multi-objective optimization algorithms are designed to primarily adjust the power output in response to varying load demands, effectively managing the slow response of the PEMFC and optimizing the power split between the fuel-cell and the hybrid battery system. By doing so, the EMS can maintain the FCSs such as proton exchange membrane fuel-cell (PEMFC) within its optimal operating range, reduce the occurrence of fast load changes that contribute to mechanical stress, and thus enhance the overall efficiency and durability of the FCHEV [21]. Yuan Hai-Bo et. al. (2022) study focuses on designing an EMS for FCHEVs to improve fuel-cell durability, battery life, and fuel efficiency.

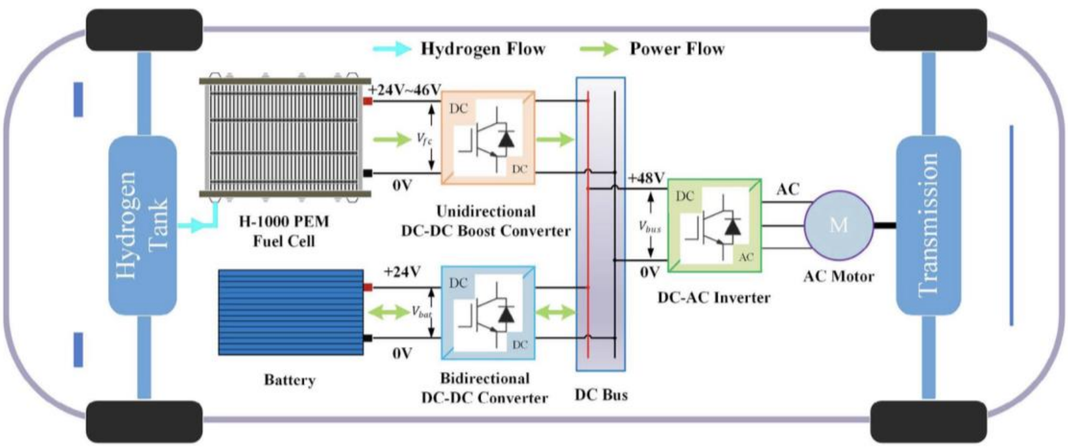

Figure 1.10: Power flow in a FCHEV [22].

Figure 1.10 illustrates the powertrain configuration of a FCHEV system. In this setup, the PEMFC is connected to a DC bus through a unidirectional DC-DC boost converter, which serves as the primary power source. Additionally, a battery pack, linked via a bidirectional DC-DC converter, provides supplementary power and captures energy from braking. The efficiency curve for the PEMFC, derived from experimental data, is shown in Figure 1.11. As a secondary energy supply, battery package is connected in series to a bi-directional DC-DC converter which provides supplementary power and recover the energy from regenerative braking [22].

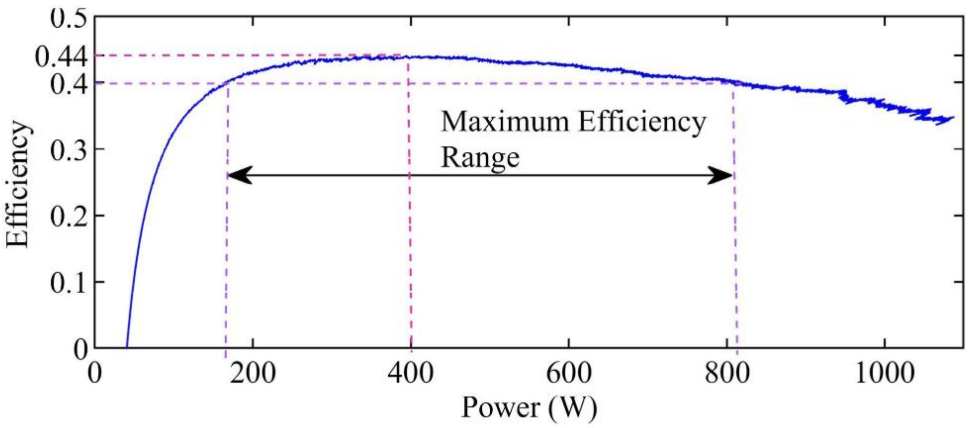

Figure 1.11: PEMFC system efficiency curve [22].

A rule-based EMS utilizing a GA optimized real-time power distribution for FCHEVs, focusing on reducing hydrogen consumption and maintaining battery life among different driving scenarios. This approach adjusted battery charging based on urban, suburban, and highway driving patterns and evaluated the battery's State of Charge (SOC) impact on the system. The study compared its effectiveness with dynamic programming and fuzzy logic methods under identical conditions. The EMS was enhanced with multi-objective GA optimization to balance fuel-cell durability, hydrogen consumption, and battery preservation, acknowledging the challenge of optimizing these objectives simultaneously. This optimization aimed for a trade-off among all objectives, terminating when specific criteria were met. Consequently, this EMS improved the fuel-cell system's operation, supported power demands efficiently, and minimized hydrogen consumption. Moreover, it has been concluded that in rule-based and fuzzy logic EMSs, the battery SOC experiences significant fluctuations as a result of the absence of optimization, resulting in a reduced battery life. Without optimization, both EMS systems show excessive hydrogen consumption during New European Driving Cycle (NEDC) and Urban Dynamometer Driving Schedule (UDDS) tests, mainly due to the fuel-cell operating in an inefficient working zone. Furthermore, the absence of optimization leads to increased energy storage within the battery [22].

In another study, Salek et. al. (2023) has performed a multi-objective optimization using Genetic Algoritm to find optimum range and hydrogen consumption of a DAF 44 tons Heavy-Duty FCHEV which consists of 8.5 tons of truck cab and 35.5 tons of trailer. The model considers the primary variables of the powertrain control system, and the optimization process utilizes a real road driving cycle. This cycle is designed based on a high-altitude climb scenario for a truck with an average power requirement of 300 kW. Following the optimization, five distinct design points were recommended and transient results were generated for these operational points to determine the optimal scenario. At the chosen design point, the specifications for the H_2 storage tank, fuel-cell, and battery packs were determined as follows: 65 kg of H_2 for onboard storage, a 270 kW fuel-cell, and 257 kWh for the battery packs, respectively. The technical parameters of the truck body and rolling resistance applied to the truck wheels are presented in the Table 1.1.

Table 1.1: Truck and trailer body technical parameters [23].

Component	Parameter	Value
Truck body dimensions	Distance from hitch to front axle [23]	6200
	Height of support point at bench test [23]	1050
	Wheel-base [23]	4550
Trailer body dimensions	Distance from hitch to axle [m]	7.7
	Pitching moment coefficient	1
Truck nominal weight	Curb Weight [kg]	8000
	Gross weight [kg]	8500
Trailer nominal weight	Curb weight [kg]	19000
	Gross weight [kg]	35500
Aerodynamic parameters	Drag coefficient	0.7

The efficiency map of the electric motor is utilized for both driving and recuperation power. The estimated sizing of the main powertrain components of the FCET is given in Table 1.2.

Table 1.2: The estimated sizing of the main components of the FCET powertrain.

Parameter	Value
Number of Fuel-cell stacks	3
Fuel-cell total power [kW]	270
Number of Battery Packs	4
Battery Packs total capacity [kWh]	257
Electrical drive power [kW]	300
Hydrogen storage capacity [kg]	65

For the control of the power distribution of the FCHEV Powertrain, a rule-based control strategy is designed. There have been four operation modes are defined, respectively Power, Boost, Charge and Battery mode. These modes are based on the states and the comparison between average vehicle power, fuel-cell activation threshold, battery SOC. The proposed rule-based control strategy for this study is given in Figure 1.12.

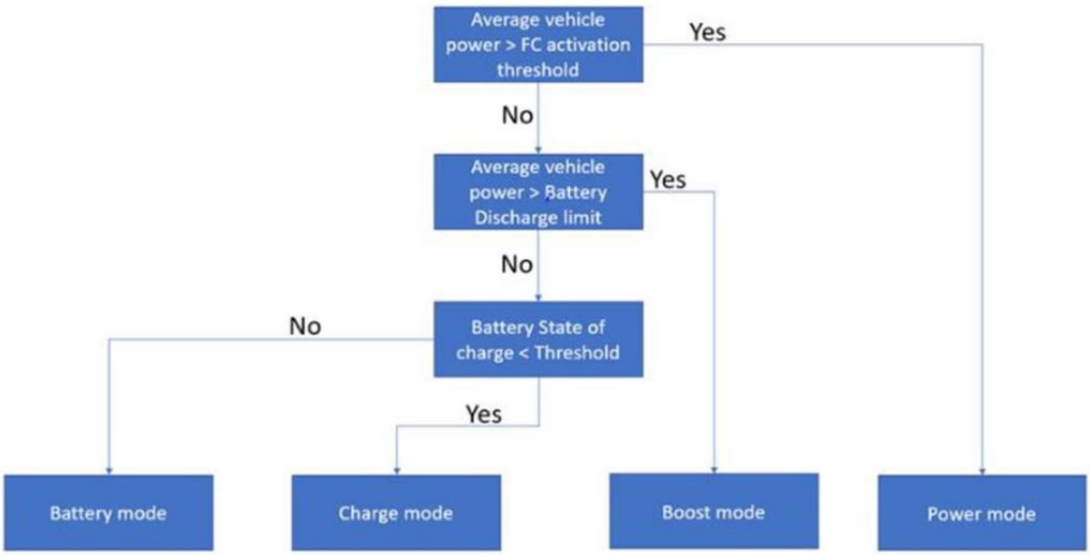

Figure 1.12: The Rule-Based control strategy for power distribution management of the FCHEV [23].

To optimize the powertrain, key parameters of the control system such as fuel-cell activation power, SOC charge on and off set-points are selected as variables. The optimization aims to minimize H_2 consumption while maximizing the remaining battery range. The SOC off and on parameters represented the state-of-charge levels of the battery pack at which the fuel-cell begins to charge them on or off respectively. When the electrical power demand reaches the fuel-cell activation power value, the fuel-cell initiates the direct parallel power supply to the electric motor, in conjunction with the battery packs. The genetic algorithm is utilized to identify the optimal design point, which comprises the most favorable combination of control strategy values. The primary objective is to maximize the total estimated range while simultaneously ensuring stable performance of both the fuel-cell and the battery.

UN-ID	Best Points	FC Activation Power [kW]	SOC off	SOC on	Remained Battery Range [km]	H2 Consumption [kg/100km]	Estimated Total Range [km]
1	1-BR	103.7	71.90	10.03	50.92	12.740	561
2	2-BR	185.1	75.67	39.17	60.39	13.332	548
3	3-BR-H2C	86.82	70.37	37.93	55.52	13.032	554
4	1-H2C	152.1	82.84	48.30	68.82	13.837	539
5	2-H2C	275.2	64.06	25.40	40.99	12.290	570
Base	NA	250	70	30	47.128	12.727	558

Figure 1.13: Optimum design points and responses.

As a result, the proposed FCHEV with an optimized control strategy achieves a range of 570 km with the most stable fuel-cell and battery performance as shown in Figure 1.13. In comparison, a battery-electric vehicle with a total battery capacity of 516.16 kWh only achieves a range of 211 km [23].

In conclusion, the ongoing transition towards sustainable transportation is a critical component in the global effort to mitigate climate change impacts, particularly those arising from CO_2 emissions in the heavy-duty transport sector. This thesis has outlined the considerable potential of FCHEVs in achieving these environmental targets. With their capacity for long ranges, rapid refueling, and significant reductions in vehicle weight and emissions, FCHEVs represent a powerful alternative to conventional and battery electric vehicles, particularly in long-haul applications. The study presented herein demonstrates that through careful selection and optimization of energy storage systems and energy management strategies, notably the integration of rule-based and genetic algorithm-based optimization, FCHEVs can effectively minimize hydrogen consumption and extend the lifetime of batteries. This optimization not only enhances vehicle performance but also contributes to the broader goals of reducing greenhouse gas emissions and advancing the adoption of zero-emission vehicles. By addressing the technical challenges and leveraging advanced EMS, this research contributes to the improvement and viability of FCHEVs as a sustainable solution in heavy-duty transportation, aligning with global emission reduction requirements and advancing the cause of environmental sustainability.

2. HEAVY DUTY TRUCK APPLICATIONS AND ENERGY STORAGE SYSTEMS FOR TRANSPORTATION

Heavy-duty trucks are an indispensable part of daily life by serving as essential tools for the transportation of goods and materials to diverse locations, while simultaneously playing a vital role in the economy. There exists a wide range of heavy-duty truck types in the market, each possessing its unique advantages. Trucks are divided into several categories, including long-haul, regional delivery, urban delivery, and construction [24].

Heavy-duty trucks significantly contribute to environmental pollution. The International Council of Clean Transportation (ICCT) reports that transitioning to battery-electric trucks has the potential to reduce GHG emissions by as much as 63% when compared to diesel, hydrogen, and natural gas-powered trucks throughout the entire lifespan of the vehicle. This figure already signifies a substantial reduction in emissions, under the assumption that the electricity used to charge these electric trucks is derived from today mixed power sources.

The European Commission is planning to mandate 45% reduction in emissions by 2030 and an even more ambitious 90% reduction by 2040, both compared to 2019 levels. This legislative initiative doesn’t solely focus on trucks; it also extends to specify that all new urban buses must adopt zero-emission technology by 2030. Significant truck manufacturers have already started to take proactive steps by committing to having heavy-duty electric vehicles (HDEVs) account for up to 70% of their European sales by 2030.

Large transportation companies are also preparing for a future with zero emissions. They commit to the adoption of zero-emission freight trucks by 2035. In December 2022, 44 major transportation operators jointly addressed an open letter to the European Commission, advocating for the adoption of zero-emission freight trucks by

2035. Due to the regulatory reasons, the transition is happening more rapidly than originally anticipated [25].

2.1 Heavy Duty Truck Application and Types

Heavy duty trucks can be categorized into three main groups based on their primary energy storage systems. These are conventional heavy duty trucks, battery electric trucks, and fuel-cell hybrid electric trucks.

2.1.1 Conventional and hybrid heavy duty trucks

Conventional Heavy Duty Class 8 Trucks are powered by non-renewable energy sources such as natural gas and diesel. These trucks deploy commonly ICE or a LNG engine with spark ignition (SI) or compression ignition (CI) combustion. Diesel engine trucks are considered as conventional baseline. Major problems of these applications are high environmental impact and low system efficiency. The maximum efficiency of an ideal diesel engine with 18:1 ration compression can be 63.2%. Nevertheless, the efficiency could not be reached because of limiting factors such that of energy losses through friction, cooling and pumping, thermal insulation. The average efficiency of a diesel cycle is 30% at optimal operating point. The primary indicator for a sustainable and profitable transportation economy is the Total Cost of Ownership. The most significant component of TCO is the expense of fuel, prompting Original Equipment Manufacturers (OEMs) to focus on developing fuel-efficient diesel engines. Ultimately, engines with higher fuel efficiency consume less fuel, leading to reduced emissions. Figure 2.1 and Figure 2.2 respectively show a conventional powertrain topology and architecture.

Figure 2.1: Volvo HD 4x2 diesel powertrain topology [26].

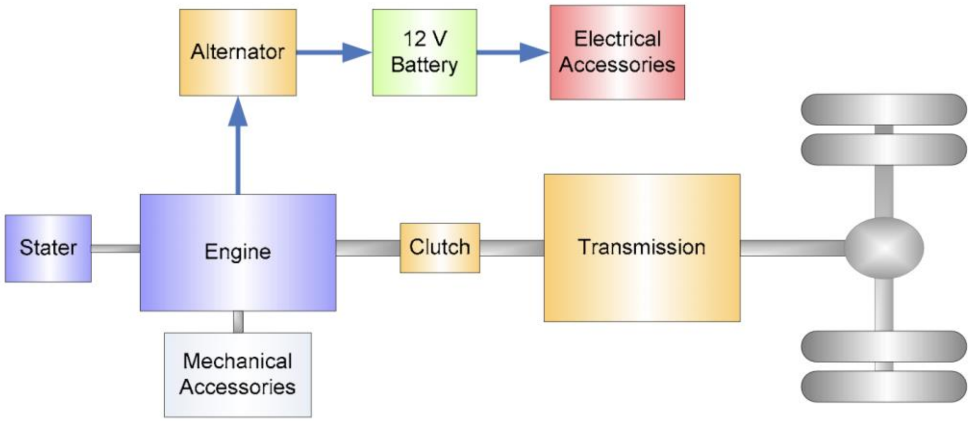

Figure 2.2: Conventional heavy-duty truck powertain architecture [27].

Figure 2.3: Conventional heavy-duty truck [26].

In order to reach the most efficient and more environment friendly way of deploying non-renewable energy sources, hybrid architectures are also available. Hybrid-electric configurations incorporate a diesel engine or an LNG engine with either SI or CI combustion, an electric motor and a lithium-ion battery. The best hybrid architecture is considered as parallel hybrid powertrain as shown in Figure 2.4. In this architecture, the vehicle has the capability to be driven by either the engine, the electric motor, or both simultaneously. In contrast to the typical conventional tractor-trailer, where a majority of accessories rely on the engine for power, the hybrid electric drive system offers the possibility to convert engine-driven accessories, like the air conditioner and air compressor, into electric power sources.

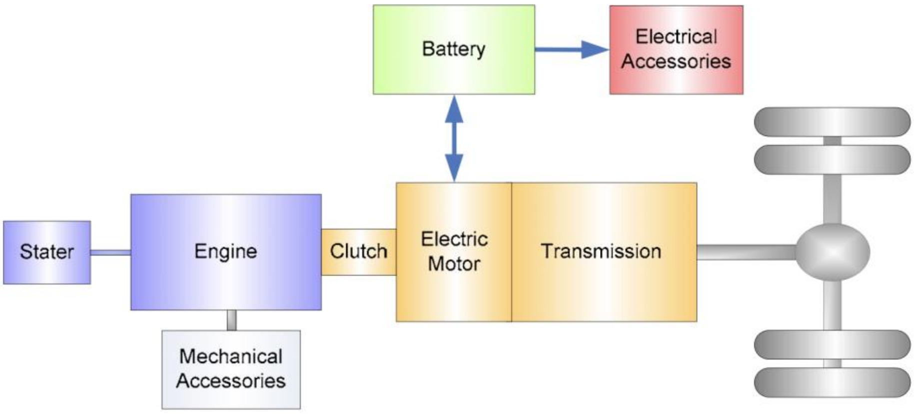

Figure 2.4: Hybrid heavy-duty truck powertain architecture [27].

In comparison to traditional diesel trucks, LNG-SI trucks exhibit 22-28% lower diesel-equivalent fuel economy, while LNG-CI trucks showed nearly the same fuel economy across various drive cycles. When conventional trucks are hybridized with diesel, LNG SI or LNG CI engines, fuel economy improvements of 24%, 33%, and 18% were observed for day drive cycles, and 10%, 14%, and 8% for short haul cycles, respectively. In long haul applications, hybridizing diesel and LNG trucks led to a 3-6% increase in fuel economy. Battery electric trucks (BETs) demonstrated a diesel-equivalent fuel economy 2.2-2.7 times higher than conventional trucks, while hydrogen fuel-cell trucks improved fuel economy by 27-39% across day drive, short haul, and long-haul cycles, according to simulation results. The studies show that introducing hybrid and electric technologies into truck powertrains can substantially enhance fuel efficiency and decrease the carbon dioxide emissions of traditional diesel and LNG trucks [27].

In the scope of this study, viable alternative vehicle applications are examined to replace combustion engine heavy-duty long-haul vehicles. Therefore, it is important to give a precise long-haul vehicle definition in order to set vehicle targets. Table 2.1 lists the aspects of a long-haul truck.

Table 2.1: Definition of long-haul truck [29, 31].

Parameter	Long-haul Truck
Gross vehicle weight (GVW)	30-40 tonne
Daily Range	800-1,500 km
Typical operation	(Inter)national
Fuel Consumption	32/100km

In the subsequent parts of this thesis, a study will be conducted on a 40-tonne heavy-duty truck application. Therefore, various technical specifications of the conventional vehicle are given in Table 2.2.

Table 2.2: Technical specifications of a 40-tonne conventional distribution truck [31].

Parameters	Value	Unit
Energy consumption (kWh/100km)	207	Diesel
Useful fuel storage capacity	1300	l
Engine Power	375	kW
Energy carrier volume	1420	l

2.1.2 Battery electric trucks

BETs are electric traction vehicles powered by batteries and driven by electric motors. Required energy for the traction comes from the electricy stored in the batteries.

BETs can be divided into two categories in terms of electric motor configuration within the system architecture. These are centralized (single motor) and distributed (multiple motor) configurations. BET's were first configured with centralized configuration because of its similarity with the conventional vehicle configuration. An example central drive unit is shown in Figure 2.7. Lately, multi-motor configurations became a very good alternative among OEMs because they can work in different operationg modes and enhance the power system. Figure 2.5 shows the long-haul BET of Daimler Truck with a multi-motor configuration presented in Figure 2.6. In the Tesla Semi, the propulsion system consists of a three electric motors, each operating independently to enhance the vehicle's efficiency. This configuration features one motor that consistently runs to optimize efficiency, while the supplementary two motors are activated to support power during situations that demand more robust acceleration or when driving uphill. This design is crucial to ensure the Semi's high performance while also maintaining energy efficiency [32]. Volvo has also launched a fully electric rear axle that integrates two electric motors [33].

Figure 2.5: Battery electric long-haul truck: Mercedes-Benz eactros 600 [32].

BETs have the highest efficiency in converting the available energy into the energy at the wheel. BETs primarily rely on lithium-ion batteries to store energy for propelling the vehicle. This electrical energy is transformed into mechanical power at the wheels through the powertrain components of electric motor, on-board power electronics and transmission [28].

Heavy duty diesel-powered commercial vehicles and BEV heavy duty commercial vehicles share a common powertrain topology. Except the power source, both diesel and BEV vehicles are equipped with essential components such as gearboxes, propeller shafts, and axles. OEMs benefit from leveraging their established technologies in gearboxes, propeller shafts, rear axles and Power Take-Off (PTO) systems for BEVs. Some of the available BETs in the market has been listed with key aspects in Table 2.3.

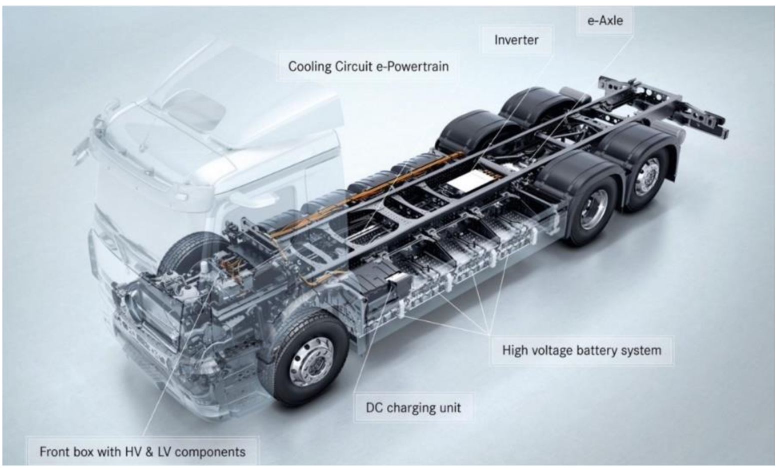

Figure 2.6: Battery electric truck with a near-wheel drive/distributed configuration [30].

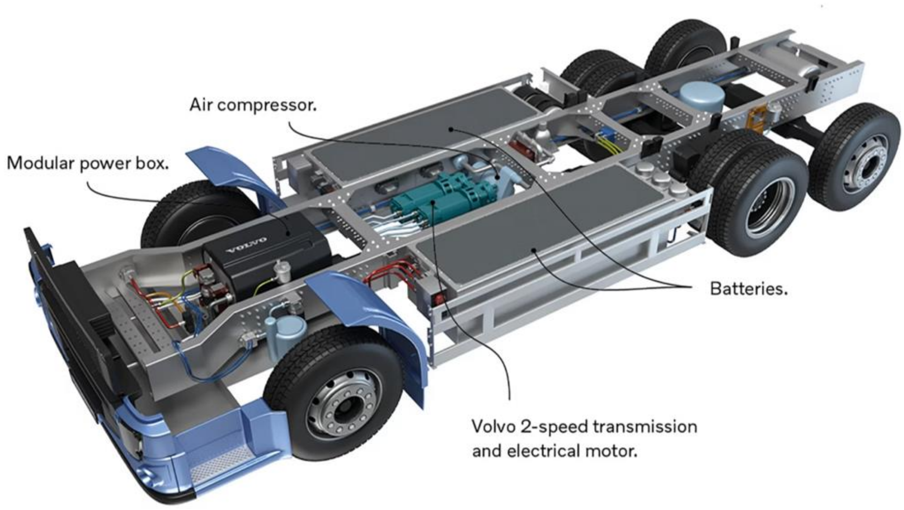

Figure 2.7: Battery electric truck with central drive unit [24].

Table 2.3: List of some available battery electric trucks in the market.

Brand	Model	Range (km)	Battery Capacity (kWh)	Reference
Mercedes-Benz Trucks	eActros 600	500	621	[34]
Volvo	FL	450	565	[33]
MAN	eTGX	400	480	[35]
SCANIA	-	<400	624	[36]
IVECO	S-Way	500	738	[37]
TESLA	Semi	<800	900	[32]
BYD	8TT	269	400	[38]

When looking at today's battery electric truck specifications, for BEVs to achieve the conventional long-haul daily range target, they need to be charged at least once between their haulage.

2.1.3 Fuel-cell hybrid electric trucks

In the context of Fuel-Cell Electric Trucks (FCETs), the energy for vehicle operation is stored as hydrogen, typically in compressed gaseous or liquid form within special tanks. Within the fuel-cell stack, the hydrogen is supplied to the anode, while air is simultaneously supplied to the cathode. An anode-located catalyst triggers the separation of hydrogen molecules into protons and electrons, with each component migrating autonomously towards the cathode. The flow of electrons through an external circuit generates electric energy. This electric energy is then transformed into mechanical propulsion at the wheels of the vehicle, as similar process as observed in BETs [25, 26]. Additionally, like HEVs, FCEV include additional energy storage systems such as battery and ultracapacitors to handle both transient power demands and regenerative power. The regeneration process requires the presence of a battery system because power cannot be directly regenerated into the fuel-cell. However, with a significantly reduced capacity when compared to BETs [38]. A simplified FCEV architecture is shown in Figure 2.8.

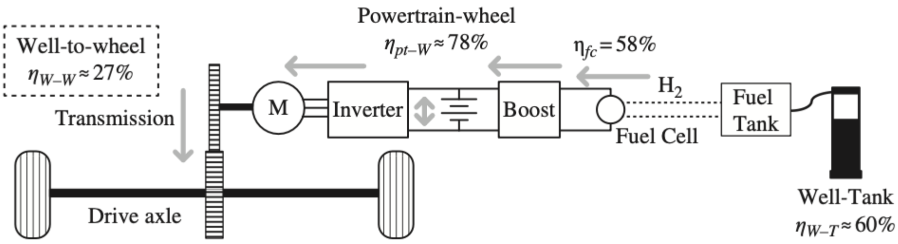

Figure 2.8: FCEV architecture and energy flow [39].

FCETs generally have a weight comparable to that of conventional diesel trucks. However, in scenarios requiring a 700-kilometer range for long-haul applications, the powertrain of a 44-ton BET can frequently exceed twice the weight of an equivalent FCET powertrain. This difference mainly comes from the relationship between battery size and the energy requirements of the vehicle [40]. The impact of the range increase on the weight of the powertrain is shown in Figure 2.9.

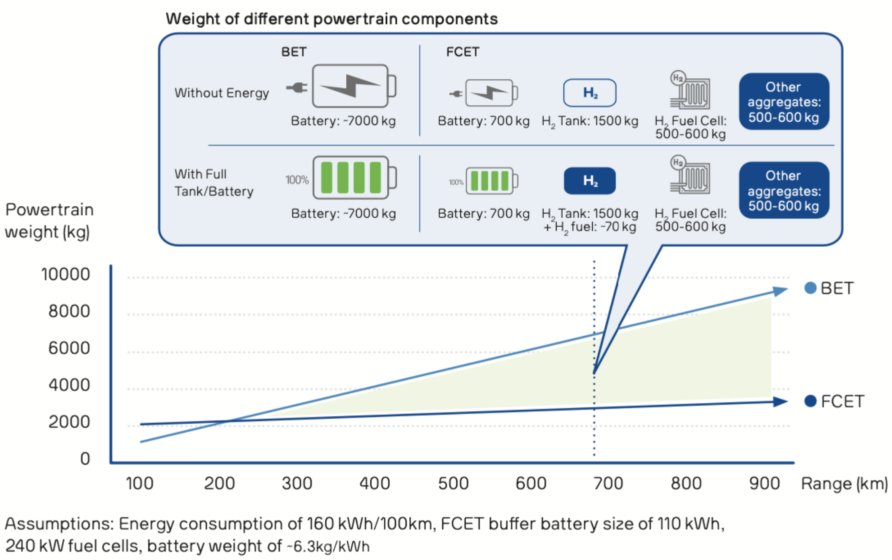

Figure 2.9: Variation of BET and FCEV powertrain weights for a 44-ton tractor with increasing range on single charge [40].

For example, TESLA's heavy-duty trucks require a battery pack weighing approximately 4.5 tons. Furthermore, the recharging process is exceedingly time-consuming, sometimes taking up to 7 hours per charging cycle.

Figure 2.10: Fuel-cell electric truck – Nikola Motors - Tre with compressed gaseous hydrogen [42].

In contrast, FCEVs do not encounter this issue because the amount of hydrogen they carry on board is significantly lighter than the battery pack of BEVs, and it yields a higher specific energy—around 120 MJ/kg compared to 44 MJ/kg for gasoline. However, the density comparison tells a different story. Hydrogen's density is about four times lower at 8 MJ/L, compared to gasoline's density of 32 MJ/L. Hence, for light vehicles aiming for a range of 300 miles, a hydrogen storage system ranging from 5 to 13 kg becomes imperative. However, this could seem as a challange. This challenge could be overcomed via different fuel cell storage system technologies [41].

Figure 2.11: Fuel-cell electric truck – Mercedes-Benz - GenH_2 with liquid hydrogen storage [43].

Table 2.4: List of current and upcoming fuel-cell electric long-haul heavy-duty vehicle initiatives [18].

Manufacturer	Initiative	FCS [kW]	eDrive Power [kW]	Battery Capacity [kWh]	Tank Capacity [kg]	GCW [ton]
Hyundai	Xcient	95x2	350	73.2	32	36
ESORO (MAN)	Coop logistics	100	250	120	31	34
VDL	Medium H_2-Share	88	210	84	30	27
VDL	Heavy H_2-Share	88	210	72	30	44
IVECO	7H_2Hau1	100x2	480	80x2	65	42
US Hybrid	Class 8 Drayage	80	320	36	38.56	36
Toyota-Kenworth	Alpha, Beta	226	500	12	40	36
Scania-Asko	-	90	290	56	33	27
Cummins	Class 8	90-180	330	100	23.5	36
Nikola Motors	Tre	120	480	70	80	40
Transpower BAE	ZECT Electric	100	300	100	30	36
VDL (DAF)	Waterstofregio 2.0	60	-	-	30	44
AVL	FC4HD	310	540	52	30	42
Mercedes-Benz	GENH_2	150x2	330	70	88-liquid	40

Nikola Motors Tre and Mercedes-Benz GENH_2 are some of the leading FCEVs for heavy-duty long-haul application. They are shown in Figure 2.10 and Figure 2.11.

2.2 Energy Storage Systems for Heavy Duty Electric Trucks

In the electrification of heavy-duty vehicles, various energy storage systems can be deployed, including batteries, ultracapacitors, fuel cell systems, and hybrid systems that combine these technologies.

2.2.1 Battery technologies

Batteries serve as the predominant ESS in the current market due to their cost, ease of transport, and durability. There are number of battery technologies in the market differenciating by the ion compositions such as lead-acid, NaS (Sodium-Sulfur), NaNiCl (Sodium-Nickel Chloride), NiCd (Nickel-Cadmium), VRFB (Vanadium Redox Flow Battery), ZBFB (Zinc-Bromine Flow Battery), and Li-ion (Lithium-ion). They generate electrical energy by harnessing the latent energy stored within their chemical composition. Table 2.5 demonstrates different battery technologies.

A battery usually consists of three main parts: an electrolyte, two electrodes (one positive and one negative), and a separator. These electrodes are made from different materials and react chemically with the electrolyte through different types of bonding.

Important factors for automotive use include how long the battery lasts, how much power and energy it can provide, how cost-effective it is, and how safe it is [48].

In the past decade, there have been important progress made in battery technology, primarily regarding passenger vehicles batteries. This progress has led to significant investments in the establishment of large-scale battery gigafactories worldwide to meet the growing demand for electric passenger vehicles. Nevertheless, it is important to examine the arising demand of the battery technologies for heavy duty trucks. It is estimated that there will be additional demand of approximately 275-300 GWh for BETs by the year 2030.

Table 2.5: The main characteristics of different battery technologies [44].

Battery Type	Energy Density (Wh/kg)	Power Density (W/kg)	Cycle Life (100% DoD)	Capital Cost ($/kWh)	Round-trip efficiency (%)	Self Discharge
Lead-Acid	25-40	75-300	200-1000	100-300	75-85	Low
NiMH	60-120	250-1000	180-2000	900-3500	~65	High
Li-ion	75-200	500-2000	1000-10000	300-2500	85-97	Medium
NaS	150-240	150-230	2500-4000	300-500	75-90	-
VRB	10-30	80-150	>12000	150-1000	75-90	Negligible

Recently, lithium-ion batteries are the dominant choice for electric vehicles, with a particular focus especially on two cathode chemistries. The first one is Nickel-Manganese-Cobalt (NMC) cathodes, which have experienced remarkable progress over the past decade. Battery manufacturers have actively worked to reduce the Cobalt content due to supply chain concerns, while simultaneously increasing the Nickel content to enhance energy density. Recent price fluctuations in materials affaced the battery with NMC cathodes and shift the interest in more cost-effective battery chemistries such as Lithium Iron Phosphate (LFP) cathodes. In comparison to NMC, LFP technology tends to be relatively heavier and has lower energy density. LFP has an important role especially in the bus sector and is used for battery electric passenger cars, light commercial vehicles, and heavy-duty trucks with lighter cargo requirements, particularly for return-to-base operations.

Table 2.6: The main characteristics of various Li-ion batteries [45, 46].

Battery Type	Energy Density at pack level (Wh/kg)	Charging/ Discharging (C-rate)	Discharge cycles	Capital Cost ($/kWh)	Thermal Runaway °C	Discharge recommenddation
LFP	160	1C/1C	2500	90	270	100%
NMC (LNMC)	200	0.7-1C/1C	1000	130	210	80-90%
NCA (LNC)	200	0.7C/1C	1000	130	150	80-90%

To enhance the energy density and range of BEV, ongoing research explores various technological advancements, including cathodes with even higher Nickel content, silicon anodes, Na-ion and solid-state batteries. However, it is crucial to acknowledge that these technologies are still in their early stages and currently lack the industrial readiness required for widespread adoption, potentially leading to higher costs in the foreseeable future [39].

Within the scope of this thesis, NMC, and LFP have been analysed to find the most suitable battery technology for a FCHEV. According to the Knibbe R. and his fellows, NMC stands out for its energy density, yet it falls short in terms of lifecycle costs due to its comparatively limited cycle life. NCA batteries show similar performance as NMC in terms of high energy density and have good thermal stability up to 55°C. Altough their large-scale use in automative sector, due to cost fluctuation of aluminium and cobalt in the global commodity market, battery cell price are not stable. On the other hand, the LFP chemistry has lower energy density and concurring higher weight but it seems to be the most suitable choice, offering a balance between decent cycling stability and affordability. Besides, LFP batteries have excellent chemical stability offering a safe operation between -20°C and 60°C with lower risk of Thermal Run-away. LFP is suitable for larger vehicles like buses, trucks, rail, and stationary setups, as well as other applications needing affordability and where size is not a limiting factor [47, 49]. Table 2.6 shows the main differences between these technologies.

2.2.2 Ultracapacitors

Capacitors store electrical energy by physically separating and combining opposite electrical charges. Energy storage is primarily provided in the form of an electric field between two electrons. The electric charges stored between parallel plates are separated by an insulating material. The energy stored in a capacitor is measured in Coulombs units, as shown in equation 2.1:

$$Q=C.V=\frac{A\varepsilon}{d}V \tag{2.1}$$

The ability of a capacitor to store energy is directly proportional to the area of the plates (A) and the dielectric constant (ε) of the plate, while it is inversely proportional to the distance (d) between the plates. Ultracapacitors are a specialized type of capacitor that can store high amounts of energy at low voltages. This capability comes from their large plate area and high electrical conductivity coefficient.

The ability of ultracapacitors (UCs) to store energy through the accumulation of opposite electrical charges has significant impacts to their life-cycle, efficiency, energy storage capacity, power density, and voltage. Due to the absence of chemical changes between electrodes during nominal operation, ultracapacitors have long lifetime. Their efficiency is high as it is primarily dependent on the resistance along the conduction path. With electrical charges physically stored on the electrodes, ultracapacitors have high power densities. However, since electrons do not physically bond, their energy densities are relatively low. Due to the lack of chemical bonds, ultracapacitors can discharge completely, leading to high voltage fluctuations as a function of SoC [48].

Figure 2.12: Ultracapacitor cell [50].

Figure 2.13: 48V Ultracapacitor module with 53Wh energy storage [51].

In heavy-duty vehicle applications, due to reasons such as limited mounting space, weight restrictions, and cost considerations, it is important for energy storage systems to have high energy density. Research efforts are currently underway to explore the utilization of UCs in electric vehicle technologies for situations requiring low energy demand [52].

2.2.3 Fuel-cell systems

Fuel-cells are commonly assumed as the next-gen power providers due to their remarkable efficiency and low pollutant emissions, as they directly transform the chemical energy contained in fuels into electricity through electrochemical processes [53].

2.2.3.1 Fuel-cell technologies

Fuel-cells can be categorised into six primary categories based on their electrolyte composition. These categories are shown in Table 2.7 including proton exchange membrane (PEM) or polymer exchange membrane fuel-cells (PEMFCs), alkaline fuel-cells (AFCs), phosphoric acid fuel-cells (PAFCs), molten carbonate fuel-cells (MCFCs), solid oxide fuel-cells (SOFCs), and direct methanol fuel-cells (DMFCs).

Table 2.7: Operational data of fuel-cell systems [53].

Cell System	Temperature °C	Electrolyte State
Proton exchange fuel-cell	60-100	Solid
Alkaline fuel-cell	100	Liquid
Phosphoric acid fuel-cells	60-200	Liquid
Molten carbonate fuel-cells	500-800	Liquid
Solid oxide fuel-cells	1000-1200	Solid
Direct methanol fuel-cells	100	Solid

Among these technologies PEM stands out as the most common option for vehicle applications [53].

They differ from their electrolyte membranes. Fuel-cell assemblies consist of the membrane electrode assembly and the bipolar plates. The membrane electrode assembly (MEA) serves as the central element within a fuel-cell unit, facilitating the oxidation-reduction reactions [55]. The MEA is composed of three primary elements as presented in Figure 2.14. They are the electrolyte membrane, the catalyst layer, and the diffusion media. The primary role of the electrolyte membrane is to separate the reactant gases, specifically hydrogen and oxygen, while facilitating the transfer of electric charges between the anode and cathode,

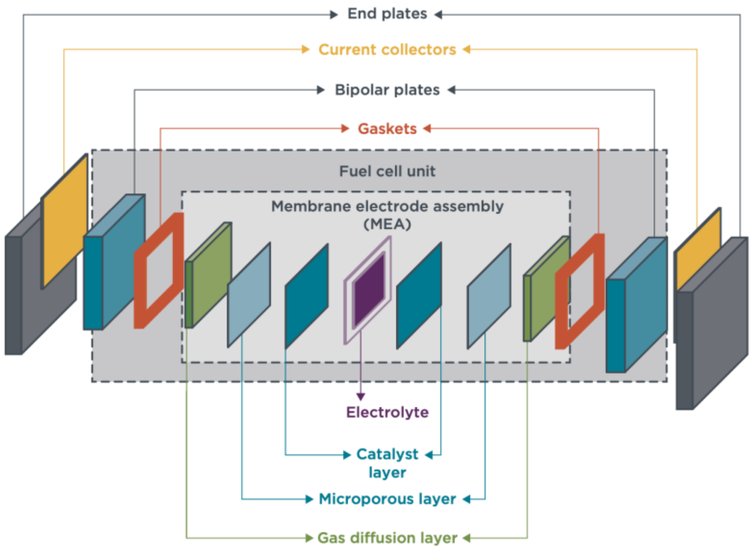

Figure 2.14: Schematic of a fuel-cell stack [53].

In the development of electrolyte membrane, various competing attributes must be considered such as electrical conductivity, gas tightness, electron insulating properties, as well as chemical, mechanical, and thermal stability [53].

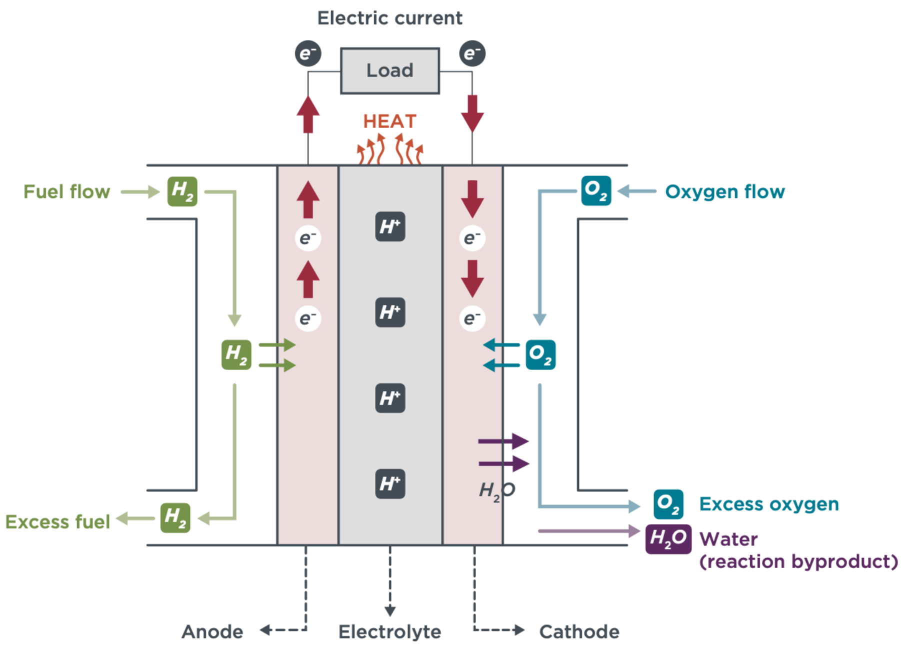

Figure 2.15: Working principle of a fuel-cell unit [53].

In practical implementation, fuel-cell systems require supplementary components to facilitate their function. Principle view of FCS is shown in Figure 2.15.

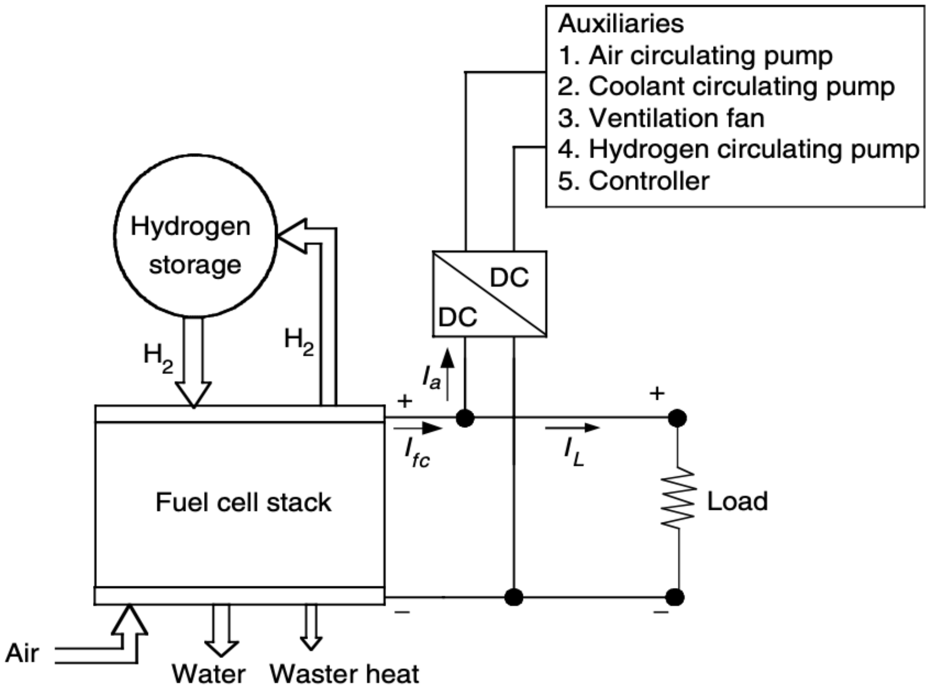

Figure 2.16: Fuel-cell system layout [54].

These supplementary components typically are an air circulation pump, a coolant circulation pump, a ventilation fan, a fuel supply pump, and a set of electrical control devices. It is worth noting that among these auxiliary components, the air circulation pump stands out as the most significant energy consumer. The power consumed by the air circulation pump, including its driving motor, can amount to approximately 10% of the total power output generated by the fuel-cell stack. In contrast, the remaining auxiliary components consume considerably less energy when compared to the air circulation pump [54]. Figure 2.17 presents the system components of Toyota Mirai FCS.

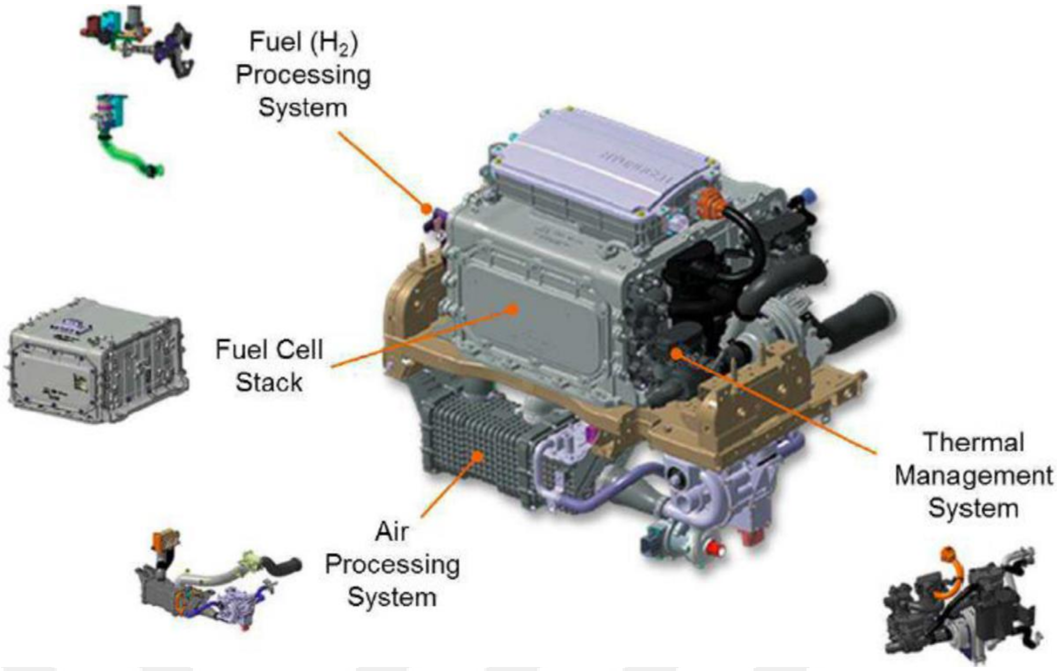

Figure 2.17: Toyota Mirai fuel-cell stack with BOP components [53].

2.2.3.2 Hydrogen storage system

In a FCEV, a critical element is the hydrogen storage system located onboard. While hydrogen offers a significant gravimetric energy density, its volumetric density is low at ambient temperature and corresponding pressure. In order reach range targets, hydrogen must be either stored at high pressure or lower temperatures [16]. Various technologies are available for this purpose, but the most common approach for vehicles deploying hydrogen storage as compressed hydrogen gas (CHG) at either 350 bar or 700 bar. While 350 bar compressed hydrogen is suitable for fuel-cell buses, it presents limitations for long-haul trucks due to space constraints. Using 350 bar storage results in a shorter driving range of less than 400 km due to the low hydrogen density in the tank. In contrast, 700 bar compressed hydrogen allows for an extended driving range due to its higher hydrogen density but resulting to a higher cost per unit of usable hydrogen.

Another alternative is liquid hydrogen storage. Subcooled Liquid Hydrogen (sLH_2) requires extremely low temperatures up to -253°C and which necessitats thermally insulated tanks. This method is drawing attention, particularly for long-haul trucks, as it offers an extended driving range due to its high hydrogen density. It is also more cost-effective per unit of usable hydrogen compared to the 350 bar storage option [10].

Cryo-compressed hydrogen storage combines compressed gas and liquid hydrogen, delivering advantages such as higher density, cost-effectiveness, reduced weight, and enhanced safety. While this technology is still in the development phase, it is expected to offer a high hydrogen density [56]. Figure 2.18 provides an overview of the hydrogen storage densities in various onboard HSS.

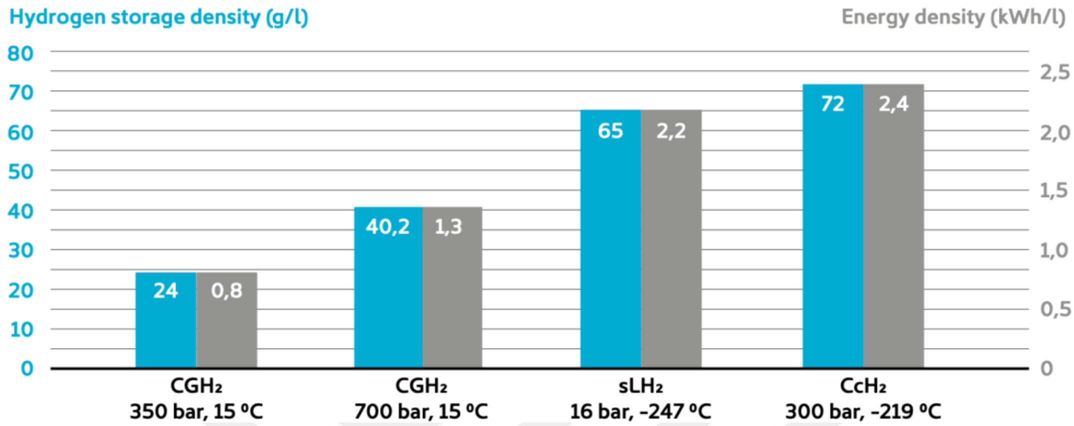

Figure 2.18: Comparison of various H_2 fuel onboard storage techniques for long-haul heavy duty road mobility [57].

The choice of onboard HSS is also influenced by the availability of hydrogen refueling infrastructure. The 350 bar and 700 bar compressed refueling systems are well-established technologies, while liquid hydrogen and cryo-compressed hydrogen refueling systems are still in the experimental stages. However, the energy required for compressing and cooling hydrogen varies, impacting fuel costs. Although onboard HSS does not increase payload weight for long-haul trucks in comparison to diesel counterparts, but it will lead to space concerns [57]. While CHG typically achieves storage densities of approximately ~40 kg/m^3 (at 700 bar and 15°C), sLH_2 can achieve densities of up to ~62 kg/m^3 (at around 16 bar and -245°C). By combining higher pressures, such as 350 bar, with low-to-cryogenic temperatures (e.g., -250/-200°C), it becomes feasible to achieve even greater energy densities, reaching approximately ~72 kg/m^3. However, Cryo-Compressed Hydrogen (CcH_2) storage technologies are more complex and currently shows a lower Technology Readiness Level (TRL) compared to the other methods. This is due to the necessity of managing both extremely low temperatures and high pressures within both the tank system and the refueling infrastructure (such as pipes and connectors).

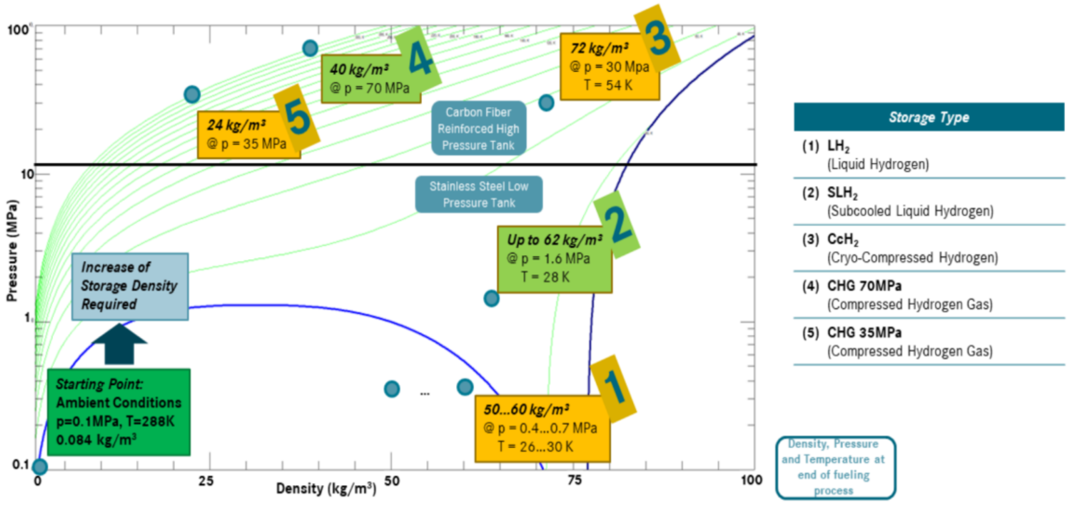

Figure 2.19: Summary of hydrogen storage systems technical specifications in terms of density vs. pressure as reported in the literature [16].

Key Assessment Criteria		
Capacity on Truck	> 80 kg (4x2)	~60 kg (4x2)
Operating pressure	4-8bar	20-700bar
Target pressure	16bar	700bar (p_target depend on p-initial and Tamb)
Range	> 1000 km	~600-700 km
Hold Time (w/o Boil off)	SOC 100% ≈ 10 h [(1)] **SOC 80% ≈ 130 h [(1)]** SOC 50 % ≈ 200 h [(1)]	n.a.
Handling / Refueling	**Multiple tank filling possible, no return gas, no communication**	Multiple tank filling possible, no return gas, **communication required**
Tank Type	Stainless steel without additional reinforcement, vacuum insulated	Typ IV (liner + carbon/glass fibers)

[(1)] Assuming 5W heat transfer and depending on operating pressure

Figure 2.20: Comparison of two heavy duty trucks equipped with sLH_2 and CHG700 [16].

sLH_2 achieves about 50% higher density, up to 62 kg/m^3 at 16 bar and 28 Kelvin, compared to CHG700's 40 kg/m^3 at 700 bar and ambient temperature. An insulated stainless-steel, low-pressure tank is sufficient for storing sLH_2, unlike Type IV high-pressure tanks reinforced with carbon fibers used in CHG700 configurations. The differences between hydrogen storage systems can be observed in Figure 2.19. The Figure 2.20 compares the key assessment criteria for two types of hydrogen storage systems used in trucks. The figure highlights the impacts of the CHG700 and sLH_2 in terms of capacity, operating pressure, target pressure, range, and handling/refueling requirements.

One of the most important challenges with sLH_2 at the vehicle is the boil-off onboard. But the studies show that boil-off may occur when staying 10h at 100% SOC (full tank) or stayin 160h when the tank is half empty (50% SOC). Nevertheless, under the normal drive conditions of heavy-duty trucks, the risk of Boil-off is considered very low [16]. Overall, sLH_2 is more advantageous in terms of range, vehicle investment costs and payloads compared to CHG technology. Therefore, in this study, the use of Liquid Hydrogen technology has been assumed for storage and refueling purposes. Hybrid energy storage system topologies

FCHEV topologies are classified into three groups according to their auxiliary source configurations which are FCS with battery hybridization FCS with UC hybridization, and FCS with battery and UC hybridization. The designs of hybrid topologies are tailored to different conditions such as the amount of energy required, and the type of energy needed by the systems they are employed in.

2.2.3.3 Hydrogen with battery hybridization

The common FCHEV topology is the combination of FCSs with batteries. They perceived to be cost-effective thanks to their established industry chain. This configuration utilizes the fuel-cell as the primary energy source, supplemented by the battery during peak demand or regenerative braking, reducing the impact on the FCS during high-load conditions and enhancing overall efficiency. Figure 2.21, Figure 2.22, Figure 2.23 and Figure 2.24 show different connection methods between the FCS and battery such as direct parallel connection and indirect parallel connection, each has unique features affecting the durability and cost of FCHEV. Advantages and disadvantages of each connection method is analyzed in Table 2.8.

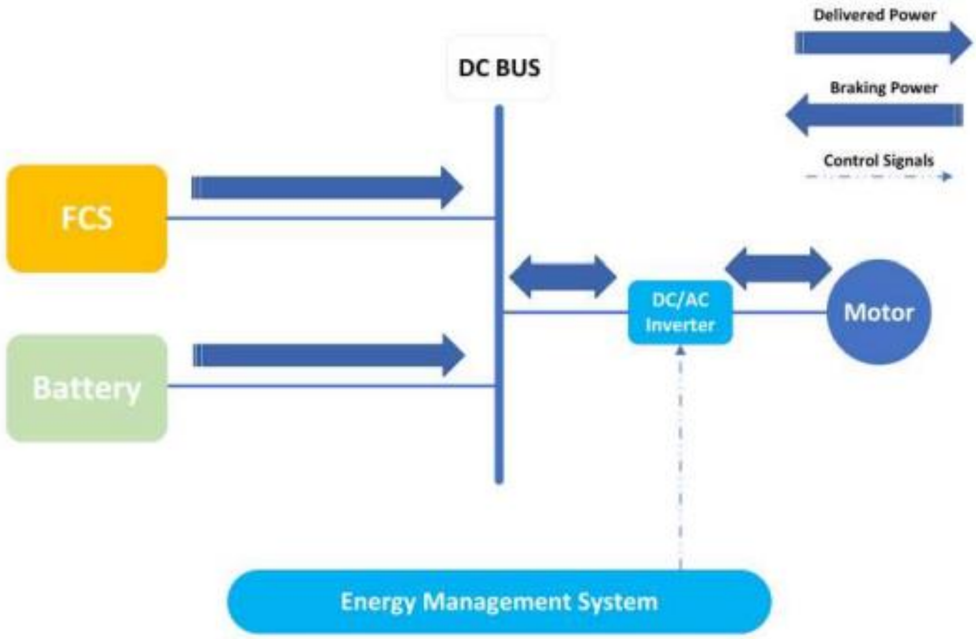

Figure 2.21: Direct parallel connection of both FC and battery.

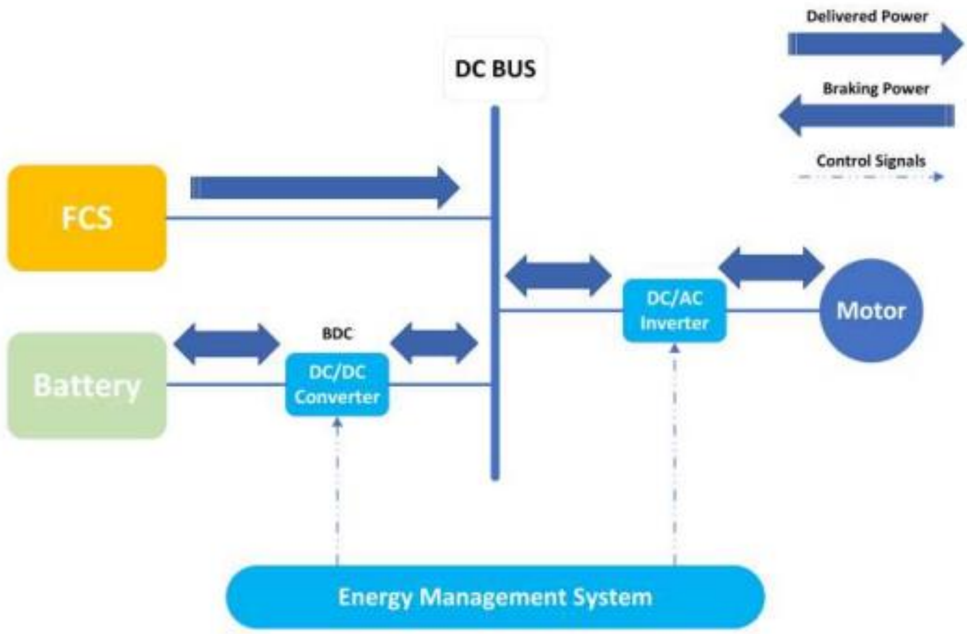

Figure 2.22: Direct connection of FCS [19].

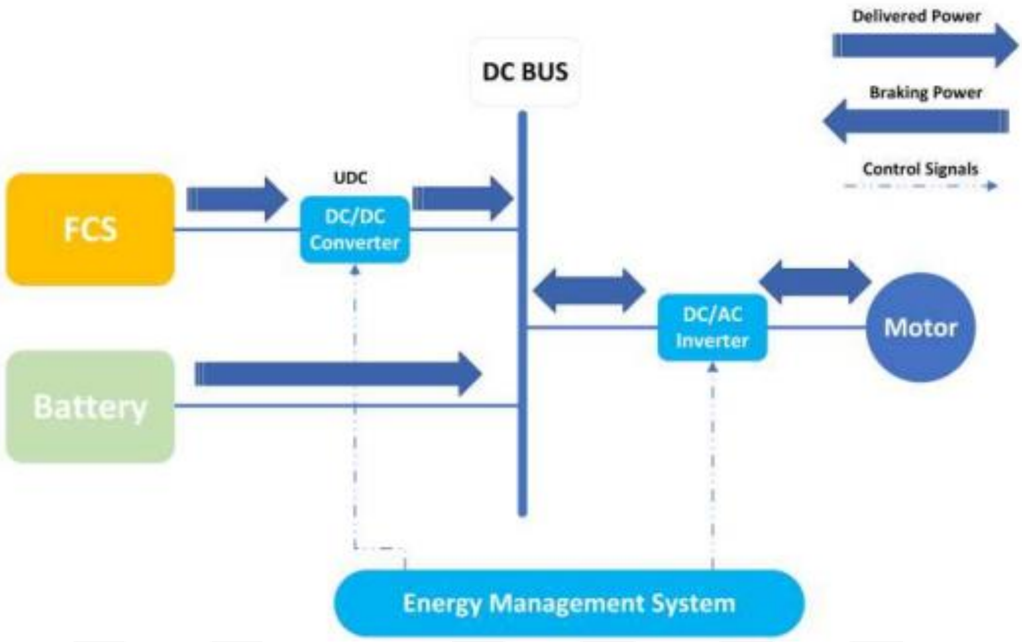

Figure 2.23: Direct connection of battery packs**.**

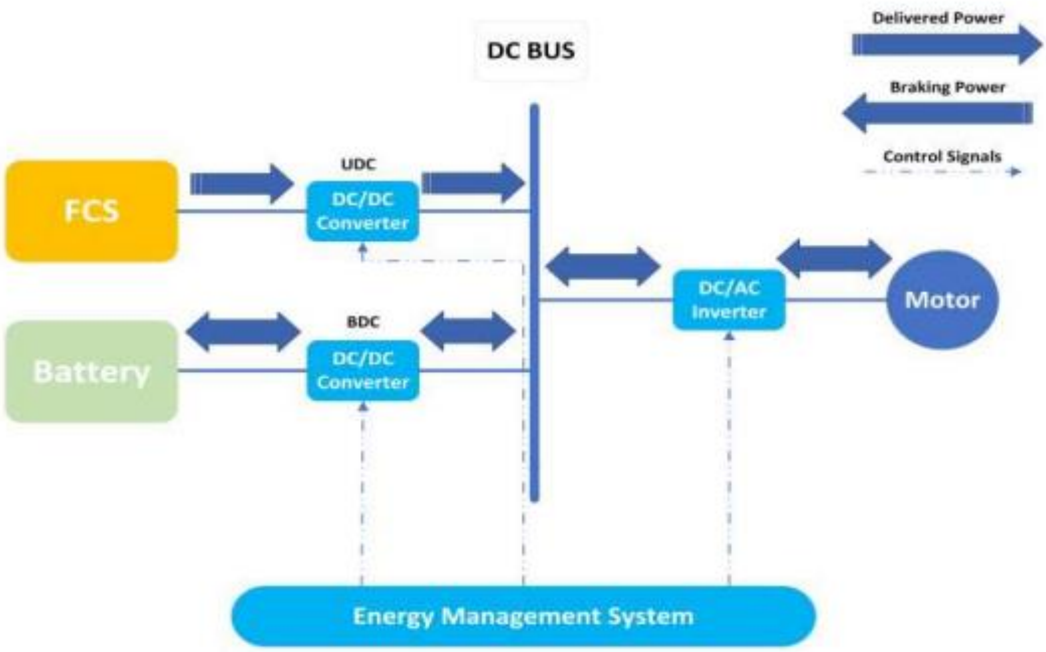

Figure 2.24: Indirect connection of both FC and battery [19].

Table 2.8: Comparison of various FCS+Battery hybridization layouts [19].

Type	Advantage	Disadvantage
Direct parallel	-Simple, cost-effective design -Easy handling -No complexity due to Converters	-High requirements for components -High Voltage fluctuations -Complex Component Management - Lower Efficiency
FC direct	-Less complex -Easier handling -Less battery dependency -Boosts battery efficiency	-High voltage fluctuation -Reduced total energy usage -Poor transient response
Battery direct	-Prolongs FC System life -Reduced Voltage fluctuations -Enhance FC Efficiency	-Reduced total energy usage -Higher requirements for batteries
Indirect connection	-Stable DC bus voltage -Simplified management -Better operational stability	-Requires larger filter capacitors -Increased costs -Lower efficiency -More complexity in system

2.2.3.4 Hydrogen with ultracapacitor hybridization

The ultracapacitor offers advantages over batteries, including higher power density and efficient cold start operation, making it suitable for hybridization with fuel-cell systems (FCS + UC). However, UCs have drawbacks like lower energy density and safety voltage, along with challenges in controlling high discharge rates and rapid charging, crucial for wider adoption [19]. Because of their extremely low energy density (10 Wh/kg) [58], it has been demonstrated that ultracapacitors are unsuitable for design topology.

2.2.3.5 Hydrogen with battery and ultracapacitor hybridization

For optimal vehicle acceleration, it is important to have both high power and high energy density. A system combining a Fuel FCS, a battery, and an UC is effective for managing energy in different situations. Research indicates that this triple hybrid vehicle reduces size and weight, boosts efficiency, and extends battery life while delivering power comparable to the FCS alone. This setup uses the FCS for regular power needs, the battery for extra power during peak demand, and the UC for quick bursts of power and to keep the bus voltage steady. Figure 2.25, Figure 2.26 and Figure 2.27 show different connection methods between the FCS, battery and UC. As explained in Table 2.9, although this system is good at recovering energy and meeting power requirements, its high cost and the complexity of its energy management limit its commercial use. Consequently, this potential configuration is not considered.

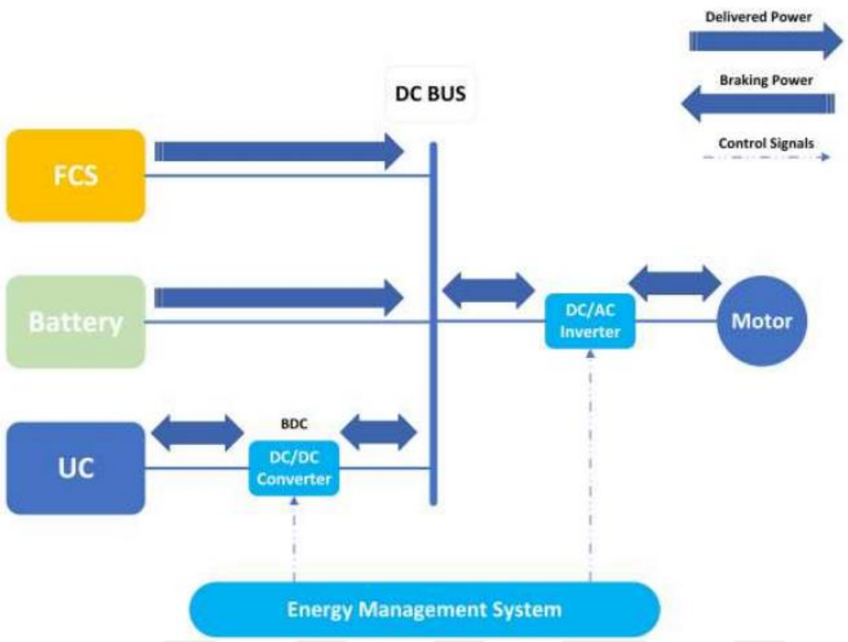

Figure 2.25: Battery and FC direct connection [19].

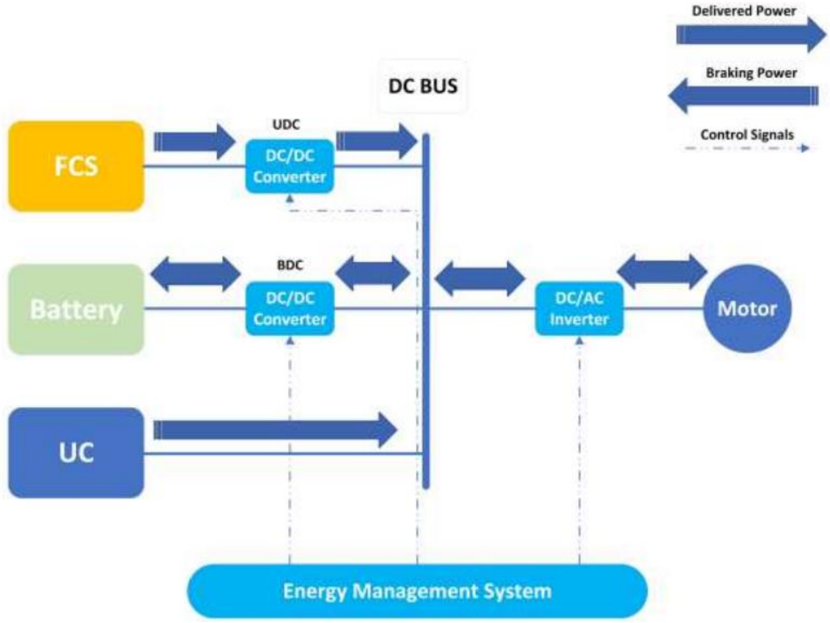

Figure 2.26: Direct connection of UC.

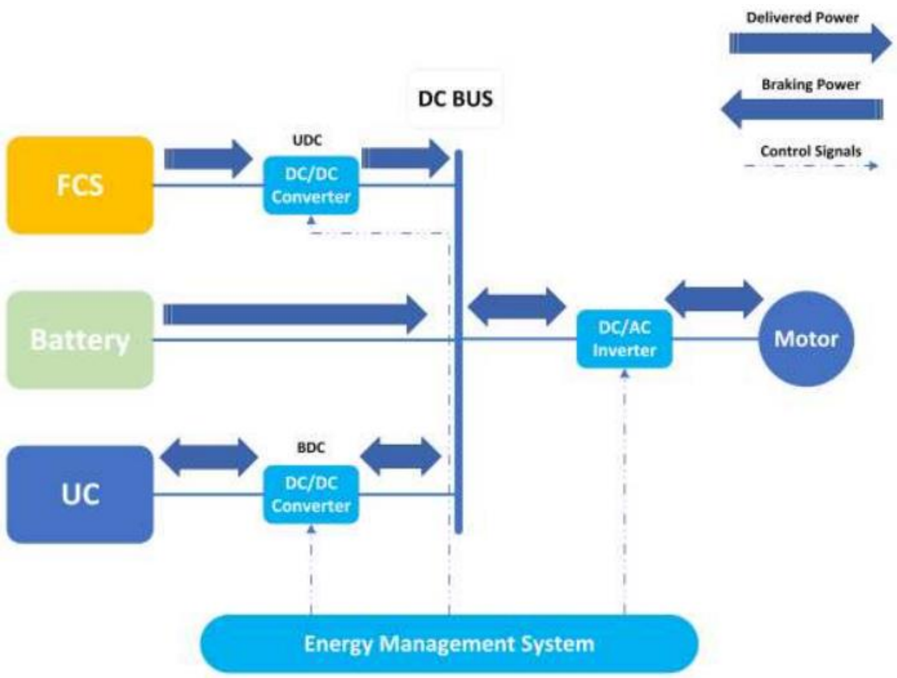

Figure 2.27: Direct connection of battery [19].

Table 2.9: Comparison of different hybridization topologies considering their corresponding models.

Type	Advantage	Disadvantage	Model
FCS+ Battery	Low manufacturing costs, suitable for basic performance needs, improved cold-start capability	Not sufficient for prolonged high-power needs	Hyundai Nexo, Toyota Mirai, Honda Clarity
FCS + UC	Better peak power management, efficient energy use	Limited performance under extended high-load conditions, complex current regulation	Honda FCX-Clarity
FCS+ Battery +UC	Dynamically adapts to driving conditions for optimized performance	Higher complexity in energy management and more expensive to manufacture	No data

Table 2.10 gives a summary of the secondary energy storage systems based on power and energy densities.

Table 2.10: Mass and volume comparison of energy storage systems [59].

Type	Lead Acid	Lithium-ion	UC
Energy density (Wh/kg)	35-40	50-220	2.5-55
Power density (W/kg)	69-154	50-5100	5000-10000
Cycle life	800	3000	>50000
Cost	55-168	385-1005	103k-220k

2.2.4 Hybrid energy storage system management

EMSs play an important role in the power regulation of FCHEVs, utilizing different strategies to balance the load between fuel-cells and batteries. The Figure 2.28 shows rule-based, optimization-based and learning-based energy management strategies. Rule-Based EMS strategies are recognized for their simplicity, requiring minimal computational resources, and providing robust real-time performance, which makes them a preferred choice for commercial applications. Despite their direct implementation, they may not provide optimal energy management across variable conditions due to a lack of adaptive capabilities.

Optimization-Based EMS strategies, on the other hand, leverage mathematical algorithms to minimize both fuel consumption and cell degradation. Techniques like Dynamic Programming (DP) and Model Predictive Control (MPC) are applied to forecast and optimize energy distribution, aiming at cost-effective operation. While offering precise control, these strategies are often challenged by their computational demands, which can limit their real-time application.

Lastly, Learning-Based EMS strategies harness the potential of Neural Networks (NN) and Reinforcement Learning (RL) to adaptively optimize energy management. These systems continuously learn from operational data, improving their decision-making processes over time. Even though they could be very flexible and effective, their success depends on having a lot of data and they need a lot of initial learning time to work their best [19].

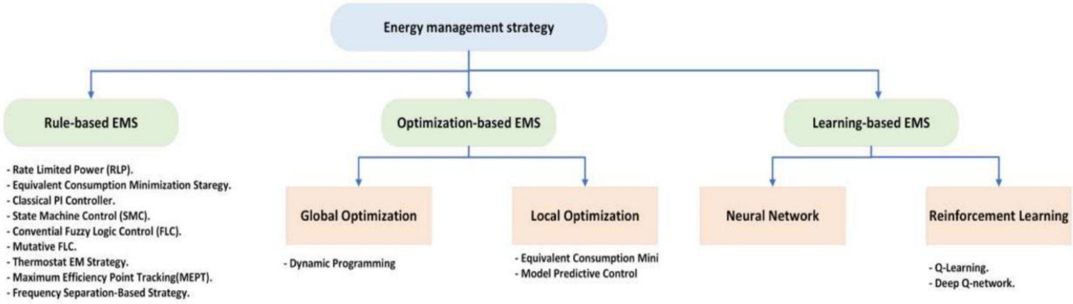

Figure 2.28: FCHEV energy management strategies [19].

3. MAIN CONSIDERATIONS FOR ELECTRIFICATION AND HYBRIDIZATION FOR TRUCKS

When electrifying Heavy Duty Truck applications, there are various factors to consider. Some of these factors include customer demands, environmental conditions, technological advancements, and regulatory requirements. Due to OEMs' preference for constructing battery electric and fuel cell electric vehicles on existing vehicle platforms to leverage existing technologies, this study initially conducted verification work on the battery electric vehicle platform before fuel cell electric hybridization. Subsequently, a hybridization of fuel cell and battery was performed, considering hydrogen consumption and battery lifespan, followed by optimization efforts.

3.1 Vehicle Targets

Based on the results of literature research, a daily range of 800 km is required for Long-Haul Heavy-Duty Truck applications. In almost all applications, the battery needs to be charged along the way to reach this target. Among these applications, considering the weight and volume constraints from truck applications the vehicles with 40-tonne Gross Vehicle Weight has been used as a reference for assessing CO_2 emissions among heavy-duty vehicles. Based on the literature review, 40-tonne Heavy-Duty Trucks are considered to be one of the most challenging categories to achieve these targets for OEM's.

According to the summer and winter testing datas from various OEMs, ambient temperature range has been assumed between -9°C and 52°C. Considering the interactions between high voltage components, cooling systems, and different operating conditions, battery temperatures vary between -32°C and 40°C. It is assumed that regardless of environmental effects, after routine pre-conditioning of the vehicle, the battery temperature at the start will always be 23°C. Based on the technical premises of the high voltage components and the collective data from road tests, climatic conditions of the vehicle and their distribution to the cycle has been given in

Table 3.1. The vehicle specifications for BET and FCHEV applications are determined as shown in Table 3.2.

Table 3.1: Assumption for temperature distribution.

Temperature in °C	Distribution %
-32	6
23	30
40	63
44	1

Table 3.2: Main vehicle specifications.

Definition	Battery Electric Vehicle	Fuel-cell Electric Vehicle
GVW	40t	40t
Target Range	500km	1000km
Max. speed	90km/h	90km/h
Environment Temperatures	-32°C - 60°C	-32°C - 60°

3.1.1 Electric powertrain

The vehicle topologies of FCHEV and BET are designed at a 800V of system voltage. In both Vehicle Models, the similiar powertrain architectures will be deployed. Considering the literature reviews in Chapter-2, for FCHEV vehicles, the EMS's have been designed with direct connections to the HV DC-Bus for the battery, while the FCS has been modeled based on an indirect connection. The Powertrains have a central motor where the motor and inverter are integrated into a modular design as presented in Figure 3.1. This type of integrated electric axle presents unified solution that allows vehicle manufacturers to optimize the vehicle design weight to add packaging space and to improve aerodynamics and function [60].

Figure 3.1: Integrated and modular electric axle [60].

In addition to auxiliary high voltage consumers for the hydrogen system like the hydrogen recirculation blower and coolant pump, the high voltage components in the powertrain are identical. These are namely water pumps, DC/DC converter, heat pump, air compressor and heaters which all work at 800V DC voltage. Vehicle topologies of FCHEV and BET are demonstrated in Figure 3.2 and Figure 3.3.

In both models, the load demand created by the Low Voltage (LV) board net, operating at 24V voltage, on the HV battery is integrated into the system depending on the power requested from the DC/DC converter. Power demands of the auxiliary components are listed in Table 3.3.

Table 3.3: High voltage auxiliary load demands.

Definition	Power Demand at Maximum Continuous (kW)	Quantity
PTC	10	3
Air Compressor	12	1
Heat Pump	10	1
Water Pump	2	2
DC/DC Converter	6	2

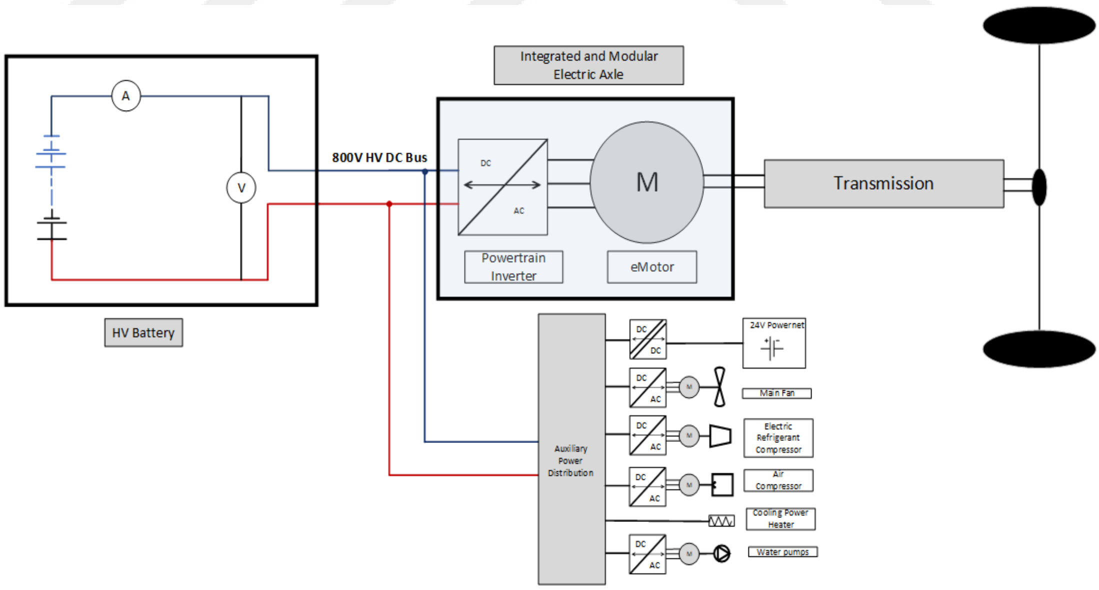

Figure 3.2: Battery electric truck topology.

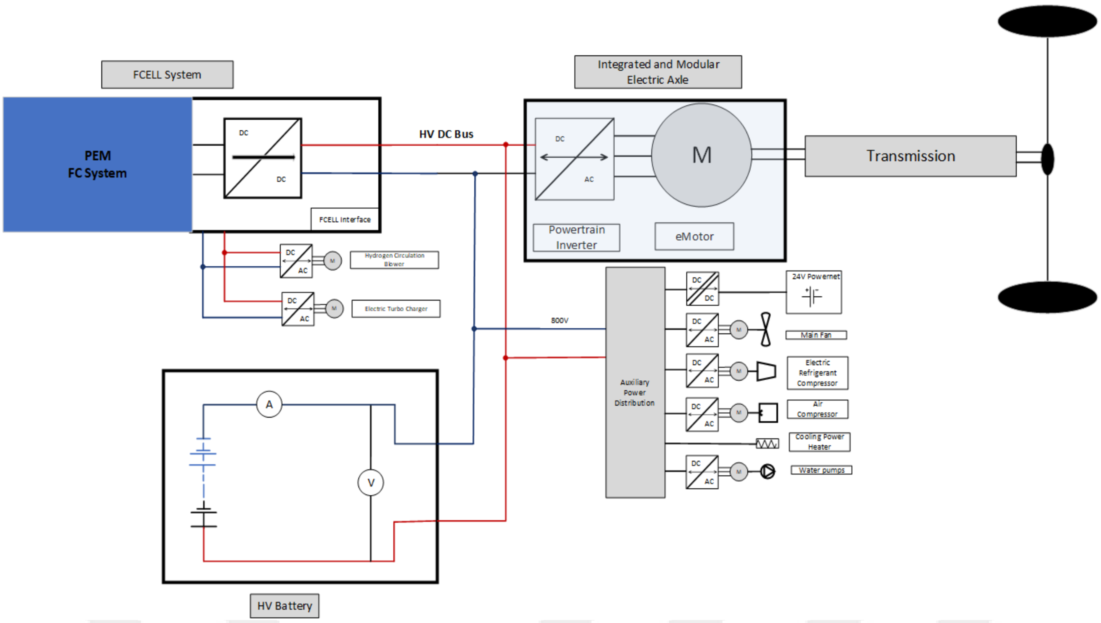

Figure 3.3: Fuel-cell hybrid electric truck topology.

Table 3.4: Design aspects of a 40-tonne fuel-cell electric truck.

Parameters	Value	Unit
Target Range	1000	km
Battery Cell Technology	LFP	-
Battery Electric Drive Distance	35	km
FCELL Storage Technology	Liquid H_2	-
FCELL System	PEM	kW
Target H_2 Consumption/1000km	< 80	kg

3.1.2 Secondary energy source desing aspect for FCEV

To determine the battery capacity for the FCEV, the distance that the vehicle needs to reach the nearest refueling station when the hydrogen reserve is depleted has been considered. For the scenario, where the hydrogen system is completely inactive and the vehicle operates solely on battery power, sufficient battery capacity must be available to cover the required distance. The planned battery technology for the FCEV has been simulated, and the required battery capacity has been calculated by testing the BET over the designated distance of 50km in the same scenario.

3.1.3 Target drive cycle for long- haul drive

In the electric truck powertrain structures, it is crucial to base the study on a driving profile that closely reveals real driving behavior, including regenerative operations and transients, to examine the collaborative operation of energy systems.

In order to examine and compare the impact of the effective utilization of energy systems in a hybrid structure on the range, consumption, and battery life of the FCET application, the driving cycle considered is the VECTO long-haul mission from the tool developed by the European Commission for Heavy Duty Vehicles.

VECTO is a recently developed simulation tool by the European Commission, employed to assess CO_2 emissions and fuel consumption in Heavy Duty Vehicles (such as trucks, buses, and coaches) with a Gross Vehicle Weight exceeding 3500kg. Speed profile of the VECTO is presenten in Figure 3.4.

VECTO is a mandatory simulation tool for new trucks in certain vehicle categories since January 1, 2019, as part of certification legislation. The tool includes mission profiles for trucks, buses, and coaches, reflecting the current European fleet [61].

The European Commission has created a set of test cycles that aim to depict diverse Heavy-duty Vehicle (HDV) mission profiles, encompassing long hauls, regional deliveries, and urban deliveries.

To examine the thermal challenges in 40-ton FCEV applications, various driving profiles are considered. When comparing the loading conditions of the fuel-cell system, the VECTO cycle's prolonged duration and high slope angle necessitate the full operation of the fuel-cell system. Compared to other drive cycles, such as the Brenner cycle, the VECTO cycle present a more demanding thermal structure on the vehicle [63].

Table 3.5: Vecto long haul profile details [63].

Definition	Value
Trip length	100km
Average speed	80km/h
Stop time	67s

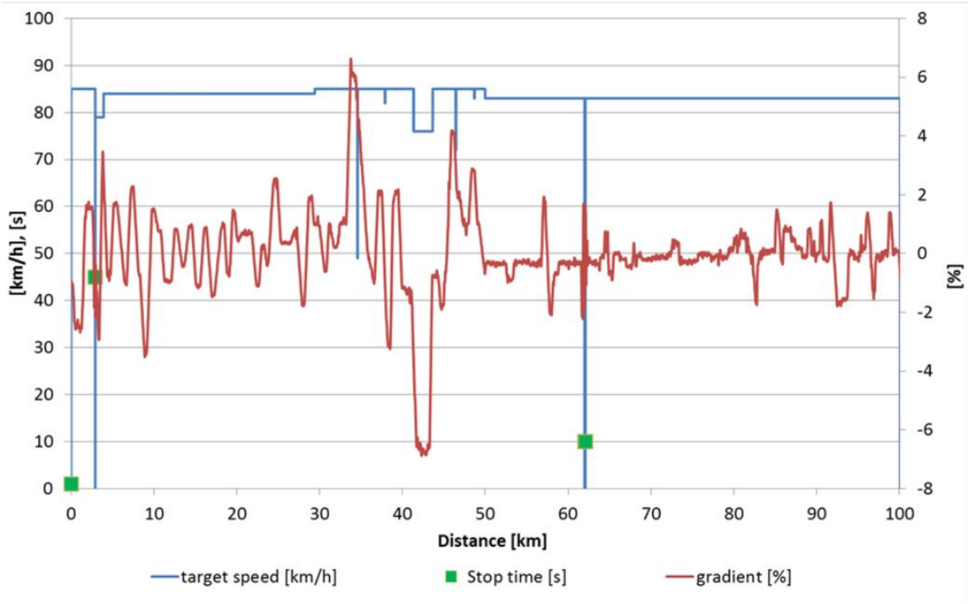

Figure 3.4: Vecto mission profile: Long-haul [62].

Within the scope of the thesis, 1000km of a cycled distance has been achieved via repeation of a 100km long VECTO long-haul cycle. The most relevant information of the VECTO long-haul cycle is given in Table 3.5.

3.1.4 Homologation requirements

During the vehicle modeling process, the approval tests set by the European Commission were taken into account. The main regulations applicable to heavy-duty BEVs and FCEVs include ECE R13 for Brake Systems, ECE R-10 for Electromagnetic Compatibility, and ECE R-100 for BEV safety. Each vehicle is tested in compliance with the regulations set to obtain approval for road traffic.

In this study, the regulation that needs to be considered for vehicle modeling and battery selection is UN ECE R-13. The ECE R13 standard sets the minimum Mean Fully Developed Deceleration (MFDD) at 2.5m/s^2 and the maximum acceptable Stopping Distance (SD) at 64.4 meters for secondary brake performance. In case the batteries are at a state that they will not accept charging such too high or too low SOC level or non-ideal environment temperatures, the braking torque which must be made available over regenerative braking shall be ensured. Beside this regulation, regenerative braking during normal driving conditions must be also taken consideration [64].

Within the scope of this thesis, BEV has been modelled with LFP and NMC batteries. The amounts of unrecoverable energy via regenerative braking were recorded for two vehicle models, with the intention of utilizing the high-recovery battery technology for the FCEV as well.

3.2 Energy Management System Optimization

In this study, a rule-based EMS is created to manage the power distribution in the FCEV. Key control parameters, such as non-recuperable energy, fuel-cell activation power, and SOC high and low set-points, are identified as important variables for optimization. The goal of the optimization is to reduce hydrogen consumption while extending battery life and keeping SOC fluctuations in check.

The SOC high and low thresholds indicate the levels of charge in the battery pack at which the operational conditions of the energy systems are adjusted based on changes in power demand. When the electric power demand reaches the specified fuel-cell activation power threshold and the power rating remains below a certain limit, the fuel-cell starts providing power in parallel with the battery packs to the electric motor. The FCS operates continuously to meet the vehicle’s ongoing power needs at maximum efficiency. Depending on the SOC status of the battery packs and the current vehicle power demand, the FCS may either charge the battery packs or assist in meeting vehicle power demands.

To find the best design point, the genetic algorithm is used to identify the most favorable combination of control strategy values. The main aim is to minimize hydrogen consumption and non-recuperable energy while ensuring consistent performance of both the fuel-cell and the battery system.

3.2.1 Optimum state-of-charge operation range of an $LiFePO_4$ battery

During the optimization of the EMS with GA selecting the SOC range with the lowest battery capacity degradation is crucial to extending the lifespan of the $LiFePO_4$ battery. Jiang et al. investigated the impact of the operating SOC range on the long-term cycling performance of $LiFePO_4$ batteries and illustrated the results as in the Figure 3.5. They subjected a 20Ah battery to charge and discharge cycles in SOC ranges of 0 to 25%, 25 to 50%, 50 to 75%, and 75 to 100%, respectively. At the conclusion of this study, batteries cycled within the mid-SOC ranges of 25 to 50% and 50 to 75%

exhibited superior cycle performance with reduced capacity loss. To further diversify the results, the battery was cycled again in SOC ranges including the mid-SOC range of 20 to 80%, the two SOC end points of 0 to 20% and 80 to 100%, and the full SOC range of 0 to 100%.

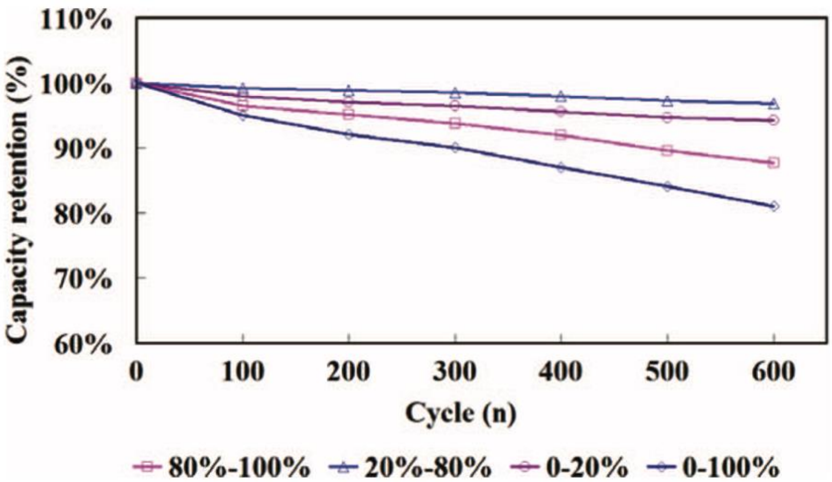

Figure 3.5: Effect of different SOC Ranges (0 to 20%, 80 to 100% and 0 to 100%) on the cycling life of a 20 Ah $LiFePO_4$ battery (charge/discharge at 1 C rate) [65].

The results clearly show that cycling the battery across the entire SOC range (0 to 100%) leads to early termination at 80% capacity. Similarly, batteries cycled at the extremes of SOC (0 to 20% or 80 to 100%) have similar outcomes. On the other hand, batteries cycled in the mid-SOC range of 20 to 80% (using 60% capacity in each cycle) retain capacity much better compared to others. This highlights how the SOC range affects battery life and suggests that cycling within the medium SOC range can significantly prolong battery life [65].

Manufacturers widely recommend maintaining a depth of discharge (DoD) between 40-60% for optimal battery performance. This range not only ensures maximum power output while minimizing stress on the battery, but also reduces the number of cycles over its lifespan. For $LiFePO_4$ batteries, an optimal DoD typically falls between 40% and 80%, preventing excessive discharge damage. However, going below 20% may lead to “memory effect” where capacity gradually drops without warning signs. While lower discharge levels may appear efficient, they require more frequent recharging and maintenance. Therefore, it is crucial to find a balance between battery lifespan and practicality when choosing the right depth of discharge (DoD) for a specific application [66]. Applied SOC boundries are shown in Table 3.6.

Table 3.6: SOC operation range for study.

Definition	Value
Initial SOC-Range	40 – 80 %
SOC Low Range	20 – 50 %
SOC High Range	50 – 80 %

3.2.2 Genetic algorithms optimization

Genetic algorithms are stochastic search techniques inspired by natural selection and genetics. Genetic algorithms have gained a lot of attention as tools for solving tough problems. Although they werenot well-known at first, they became popular for tasks like optimization, adaptation, and learning in many areas [67].

The process of genetic algorithms begins with a randomly generated initial population of individuals, each representing a potential solution to the problem. These individuals evolve through successive generations, where each generation undergoes evaluation based on a fitness measure. The next generation's population is created through genetic operators, and this cycle continues until a termination condition is met.

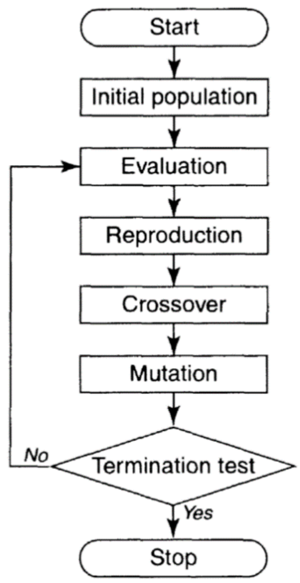

Figure 3.6: Flowchart of fundamental procedure of genetic algorithm.

The fundamental framework of genetic algorithms is shown in Figure 3.6 which involves initializing the population, evaluating individuals, selecting individuals for reproduction based on fitness, applying genetic operators like crossover and mutation, and repeating the process until termination criteria are satisfied. The main target is to converge to the best solution or an approximation of it.

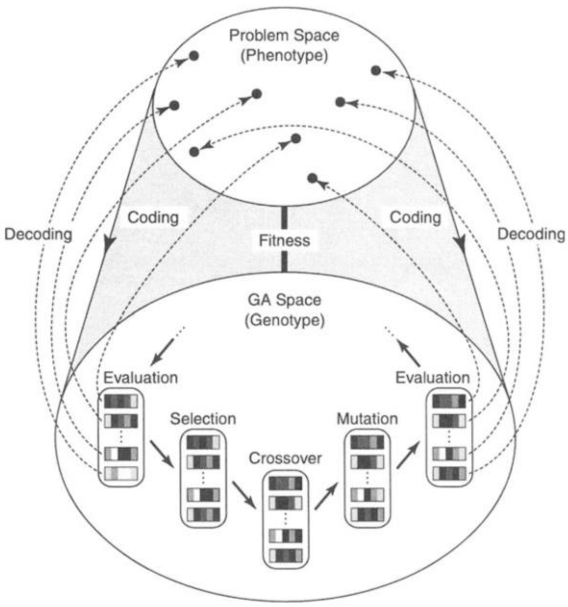

Figure 3.7: Fundamental structure of genetic algorithm [67].

Individuals in genetic algorithms are typically represented as strings of genes with each gene representing a potential solution component. The fitness of an individual is crucial, serving as the basis for selection and reproduction. In maximization problems, fitness aligns with the objective function value of the phenotype, while in minimization problems, fitness increases as the objective function value decreases.

The three main genetic operators—reproduction, crossover, and mutation—are essential for creating the next generation's population. Reproduction involves selecting individuals based on fitness for creating offspring, while crossover and mutation introduce variation by combining genetic material from parents and introducing random changes, respectively.

Various selection methods, such as roulette selection and ranking selection, determine which individuals contribute to the next generation. Crossover, a hallmark of genetic algorithms, involves combining genetic material from parents to produce offspring, with techniques like one-point crossover and multipoint crossover being common. Mutation adds randomness by making random alterations to individual genes, helping to explore different parts of the solution space.

In summary, genetic algorithms offer a powerful optimization approach that mimics natural selection and genetics, providing effective solutions to a wide range of problems across diverse domains [67].

4. MODELLING OF A LONG-HAUL BATTERY ELECTRIC AND FCELL HYBRID ELECTRIC TRUCK

Based on the literature review, the vehicle structure should be modeled with incremental targets to achieve decarbonization goals. Assuming the use of a common vehicle platform, a battery electric vehicle model was first created by taking longitudinal values and powertrain components as common for both battery and fuel-cell hybrid electric vehicle structures. After determining the appropriate battery chemistry, the vehicle was hybridized by applying the fuel-cell system and necessary modifications. Finally, an energy management system for the vehicle was established.

4.1 Vehicle Longitudinal Model

During the movement of vehicles, forces, also known as resistance forces, are defined in the opposite direction of the motion. These external forces vary depending on the direction, structure, movement, speed, road inclination, road condition, or acceleration of the vehicle. In the modeling of electric vehicles, these external forces are essentially grouped under four headings.

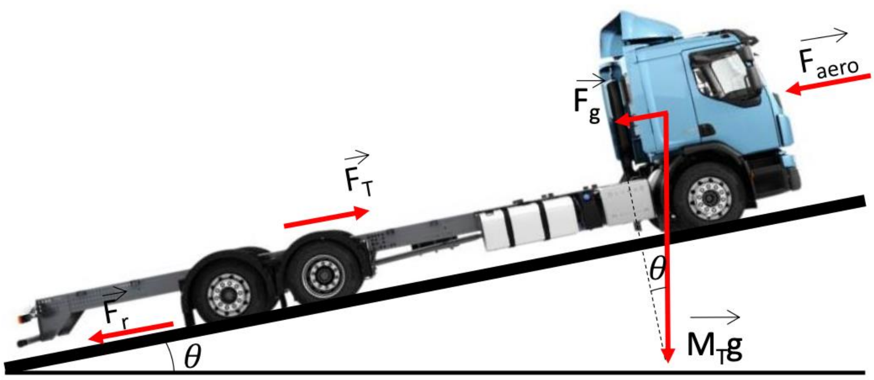

Figure 4.1: Truck scheme with the forces involved in the longitudinal vehicle simulation [68].

$$F_{traction}=F_{aerodynamic}+F_{gravity}+F_{roll\ friction}+F_i \tag{4.1}$$

Where $F_{gravity}$ represents gravitational force; $F_{traction}$ is the traction force which propels the vehicle forward; $F_{aerodynamic}$ denotes the aerodynmanic force which resists the vehicles motion; $F_{roll\ friction}$ is the rolling friction force that opposes motion due to vehicle's tires rolling on the surface; and F_i is the acceleration force which is required to change the speed of the vehicle.

The air friction force is a force that varies depending on the frontal area of the vehicle, the coefficient of air friction, the density of the air, and the speed. It originates from the friction of the vehicle body moving through the air. It is a force that varies proportionally with the square of the velocity of the vehicle during motion. The air friction force is expressed as in equation 4.2.

$$F_{aerodynamic} = \frac{1}{2}c_D c_r A_f (v_{veh} \pm v_0)^2 \tag{4.2}$$

The gradient force is a variable force that affects the vehicle and depends on the mass of the truck, gravitational acceleration, and the slope. This force can be positive or negative depending on the slope. The gradient force can be expressed as in equation 4.3.

$$F_{gravity}= M_{veh} g \sin(\theta) \tag{4.3}$$

The rolling resistance force is a resistance force that is directly proportional to the mass of the truck, gravitational acceleration, and the coefficient of rolling friction (c_r). The coefficient c_r is a value that represents the shape changes in the road and tires during rolling and the hysteresis losses of the tire. The rolling resistance force is expressed as in equation 4.4.

$$F_{roll\ friction}=c_r M_{veh} g \cos\theta \tag{4.4}$$

Finally, the acceleration force is another resistance force acting on the vehicle during motion. The acceleration force depends on the mass of the truck, the mass factor of the vehicle, and its acceleration. It affects the vehicle as the inertia of the rotating mass accelerates. The acceleration force and the vehicle mass factor can be expressed as in equations 4.5 and 4.6, respectively.

$$F_i=\delta.m.a \tag{4.5}$$

$$\delta = 1{,}04 + 0{,}0025i^2 \quad (4.6)$$

The vehicle speed (v_{veh}) is influenced by the aerodynamic drag coefficient (c_D), which characterizes the vehicle's resistance to air flow. The air density (c_r) and the wind speed (v_0) are environmental factors that alter the effective speed of the vehicle relative to the air. The frontal vehicle surface (A_f) affects the aerodynamic force exerted on the vehicle due to its interaction with the air. Additionally, the mass factor of the vehicle (δ) is indicative of the vehicle's inertia, and the total mechanical gear ratio (i) affects the torque delivered to the wheels, together influencing the vehicle's acceleration capability.

Coefficient c_w contains all the complex dependencies ($c_D.c_r$) and is usually determined experimentally.

$$F_{traction} = \frac{1}{2} c_D c_r A_f (v_{veh} \pm v_0)^2 + M_{veh} g \sin(\theta) + c_r M_{veh} g \cos\theta + \delta.m.a \quad (4.7)$$

The simulation of the electric truck model in the thesis was conducted using the MATLAB/Simulink program. To enhance the accuracy of estimating the energy consumption of the electric truck during its operation, VECTO Drive Cycle was utilized in the simulation. Together with these parameters, the total resistance force exerted on the electric truck was computed using the electric truck data presented in Table 4.1.

Table 4.1: Vehicle parameters.

Component	Parameter	Value
Truck body dimensions	Length max [21]	9605
	Width [21]	2550
	Wheel-base 4x2 [21]	5500
	r_{dyn}	0.492
	RRC	4.5%
	Height [21]	3.094
	Pitching moment coefficient	1
Truck nominal weight	Gross Vehicle Weight [kg]	40000
Max. Speed	km/h	89
Aerodynamic parameters	Drag coefficient (c_w) x Frontal Area (A_f)	6.2

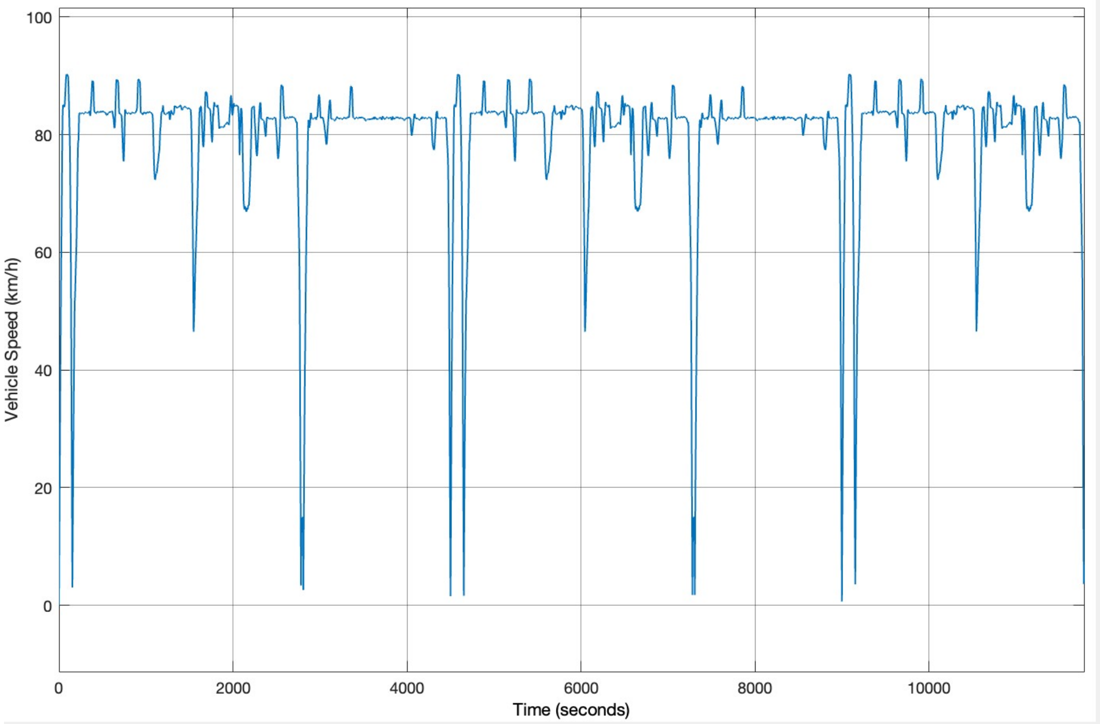

Figure 4.2: Battery electric truck speed.

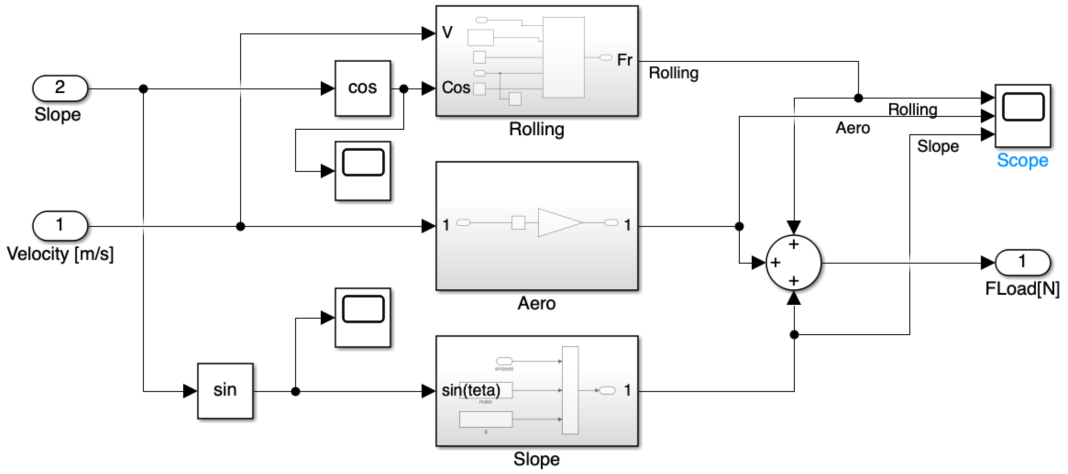

Figure 4.3: Total traction force calculation blocks.

Figure 4.3 shows the total traction force model, which calculates the total force acting on the vehicle along the direction of drive. The total force is the sum of all action forces against vehicle motion, such as rolling resistance, aerodynamic drag, and the component of gravitational force due to slope. This model is crucial for understanding vehicle energy consumption, performance in road conditions, and for developing control strategies for energy-efficient driving and vehicle stability. After running the model, the maximum force that traction motor should deliver is observed as 30kN as shown in Figure 4.4. For the traction motor design, it would be crucial to ensure that the motor can handle the peak demands consistently without overheating or degrading prematurely. The motor controller must also be capable of handling these variations smoothly to provide a comfortable driving experience and avoid unnecessary wear on the vehicle's components.

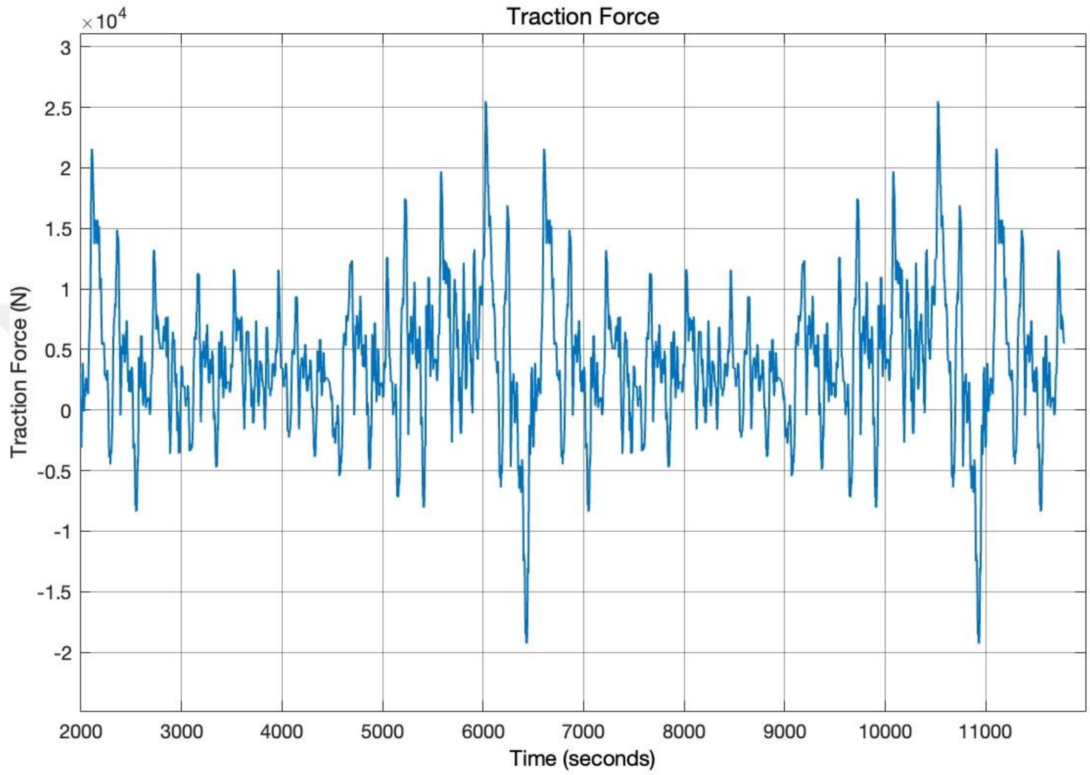

Figure 4.4: Simulated traction force**.**

4.2 Electric Traction Motor Specification

The calculations provided in Figure 4.5 have been utilized for the total traction power calculation based on the information of total traction force and truck speed.

In the simulation of this electric truck, a modular motor structure has been proposed. Based on the similar motor structures in the market, a modular electric axle, combining two oil cooled hairpin synchronous electric motors, transmission, and inverter has been modelled. This structure consists of two synchronous electric motors, two inverters and three speed transmissions. It can deliver continuously 380 kW maximum power and 54.8 kN of maximum torque. In this system, the power electronics and transmission efficiencies correspond to the modular system efficiency, and as such, the motor output power is assumed to be directly equal to the power demanded by the energy storage system. A constant block labeled “Transmission Ratio” is multiplying the electric motor torque. The motor torque is being adjusted by the transmission’s gear ratio to determine the effective torque output. The motor torque is then fed into feedback control loop that is modulating the motor torque based on efficiency. There is a lookup table block labeled 2-D Lookup Table which is used to determine the motor efficiency based on certain speed and torque inputs. Motor’s power output is calculated by multiplication of torque and angular velocity. This would be necessary to analyze the energy consumption or efficiency of the vehicle. Along with these calculations, the total drive power, motor output power, and motor output torque values have been obtained. The calculated motor output power is used to calculate the power demand of the energy storage system based on output torque, and truck speed information.

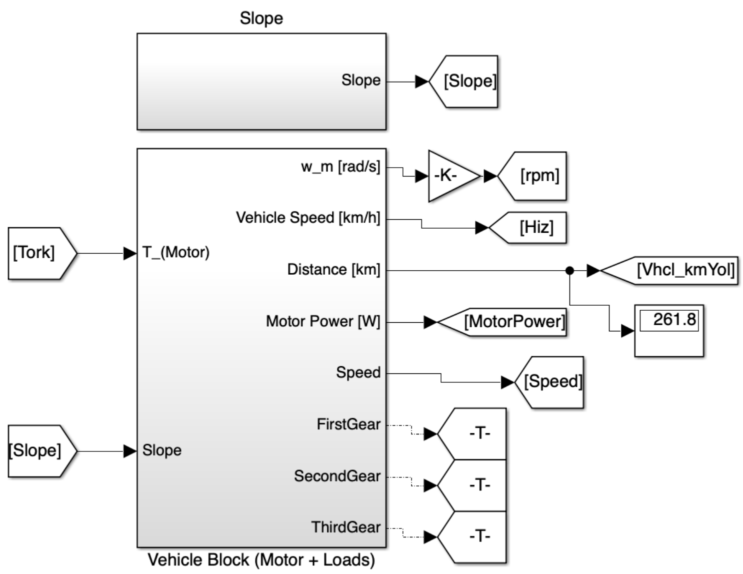

Figure 4.5: Total driving power and output torque calculation block.

Figure 4.6 shows the gearbox control system block which interfaces with the motor power block. It shows how the motor power output is managed based on the vehicle’s speed and the gear selection. The system uses conditional statements to select the gear based on the vehicle speed: If the speed is less than 30 km/h, the first gear is selected. If the speed is between 30 and 60 km/h, the second gear is selected. If the speed is above 60 km/h, the third gear is selected. For each gear, there is a corresponding 2-D lookup table that takes the vehicle speed and possibly the torque demand as inputs to output the appropriate motor torque and speed settings for that gear. These lookup tables are essentially maps of pre-calculated values that provide an efficient way to control the motor based on current operating conditions. The output from the merge block is then combined with the motor power and transmission power loss to calculate the total output power of the motor. The final output gives the motor power adjusted for the transmission losses. This is the net power available for propelling the vehicle.

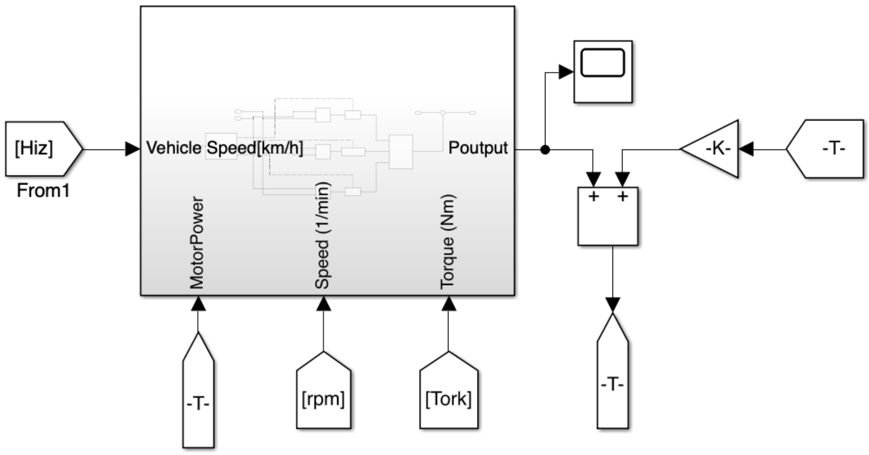

Figure 4.6: Electric traction motor control block.

After calculating the power demand for the vehicle's propulsion, the power requirements of auxiliary systems are gradually demanded from the ESS based on time and road data. To represent the load demand of Auxiliary loads, an overall energy demand of 57.5 kWh/100km has been gradually added according to the consumption of the Auxiliray per driven km into the demand from ESS via Auxiliary load block given in Figure 4.7.

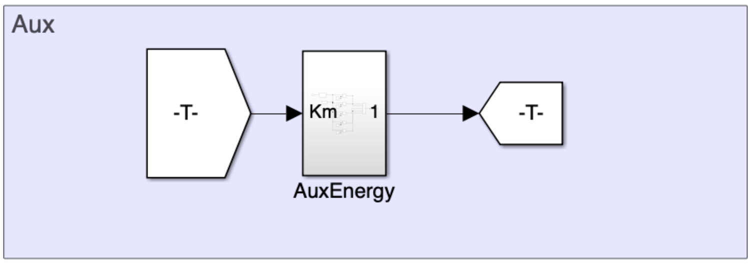

Figure 4.7: Auxiliary load block.

4.3 Battery Electric Truck Modelling

Within this study, LFP and NMC batteries have been deployed to determine the most suitable Li-ion battery type for FCELL-Battery Hybridization. A BET has been modeled using these two battery technologies and compared in terms of cost and waste energy that could not be recovered via regenerative braking due to the charge acceptance capabilities.

For lithium-ion batteries, a resistance circuit model is used to represent its operation, which [69, 70] is very simple and effective method. The battery's output current I_{bat} can be obtained by using its output power P_{bat}.

$$I_{bat}=\frac{V_{ocv}-\sqrt{V_{ocv}^{2}-4R_{bat}P_{bat}}}{2R_{bat}} \tag{4.7}$$

Where V_{ocv} is open circuit voltage and R_{bat} is battery resistance. They are all functions of the battery SOC and temperature. The state function of the battery is as follows:

$$\dot{SOC}=-\frac{I_{bat}\eta_{colm}}{Q_{bat}} \tag{4.8}$$

Where η_{colm} is coulombic efficiency, Q_{bat} is battery capacity [69].

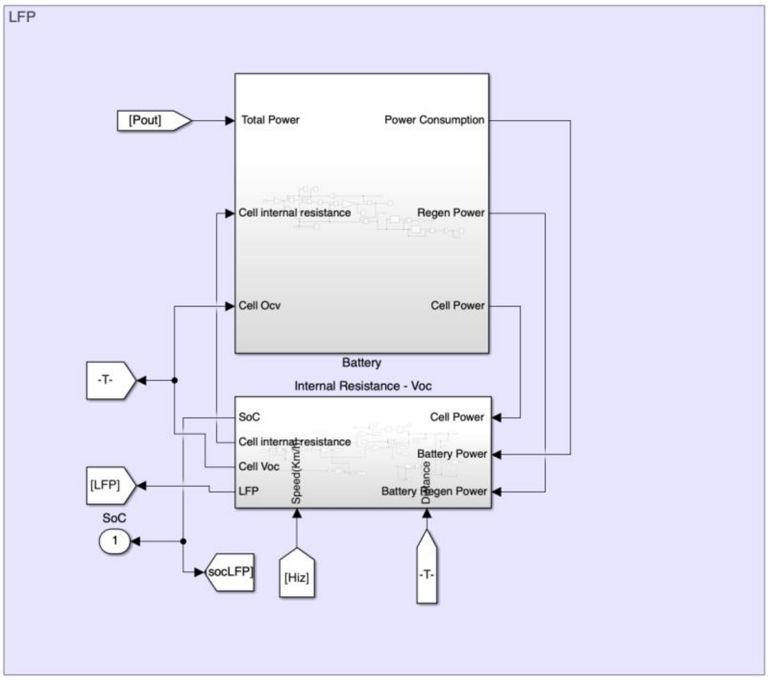

Figure 4.8: Battery block.

Figure 4.8 shows the battery block which includes the dynamics of charge and discharge processes, internal resistance, open-circuit voltage (OCV), state of charge (SOC), temperature effects, and energy consumption and recuperation. It also shows how the battery's stored energy is consumed during vehicle operation.

In the battery block, the current value to be demanded from the battery by the consumer is generated based on the output power, temperature, and operation status. Along with this value, the voltage information is provided to the battery according to the required battery current, and the terminal voltage, current value, and SOC information of the battery are obtained from its output. The power output of the battery in Figure 4.9 represents the load demand from the vehicle as explained in Chapter 4.2. Within the Internal Resistance Sub-block in Figure 4.10, the internal resistance of the battery cells are calculated. It influences the heat generation and overall efficiency of the battery. Temperature can significantly affect battery performance. This sub-block is used to account for temperature's impact on the battery's ability to charge and discharge, as well as its overall efficiency and lifespan. The open circuit voltage (OCV) is the voltage across the terminals of the battery when it is not connected to any load. It is a function of the SOC and temperature, indicating the health and charge level of the battery. This is modeled through lookup tables that relate SOC and temperature to OCV.

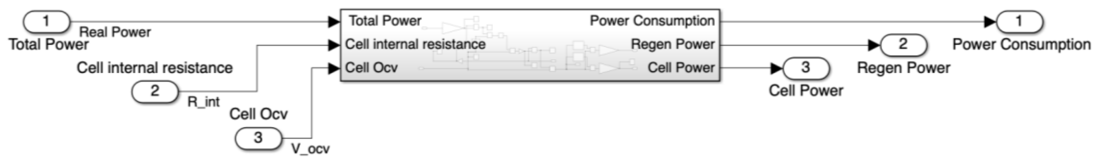

Figure 4.9: Battery sub-block.

The Low-Pass Filter is used to adjust the SOC signal to prevent abrupt changes or to simulate the delay in SOC measurement accurately.

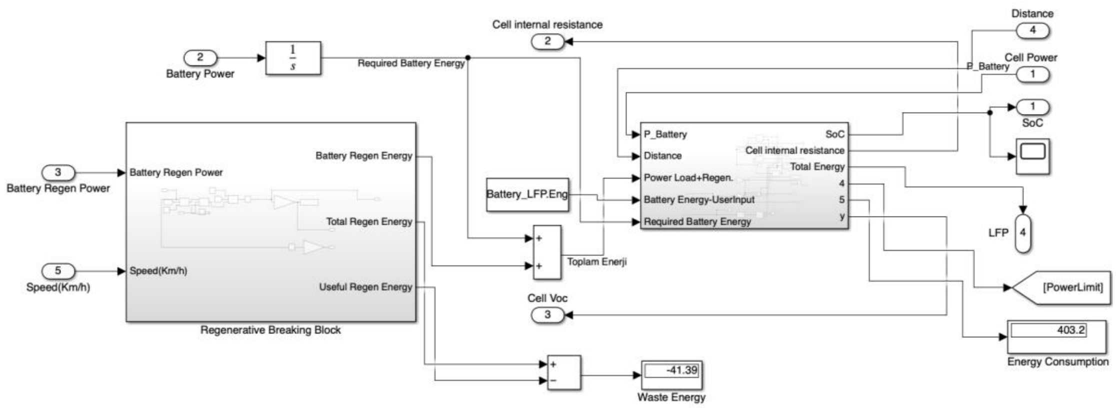

Figure 4.10: Internal resistance-voc sub-block.

4.3.1 Regenerative breaking

Figure 4.11 presents the regenerative braking block, which models the power recovered through driving. An integral component of energy management within EVs involves. To regulate the regenerative braking, the model considers critical conditions such as minimum battery charge power threshold of 5 kW and a minimum vehicle speed of 5 km/h in addition to SOC limit to avoid overcharging for the activation of this energy recovery mechanism. The useful regen energy is substracted from the available regenerative energy to find the unrecoverable/waste energy.

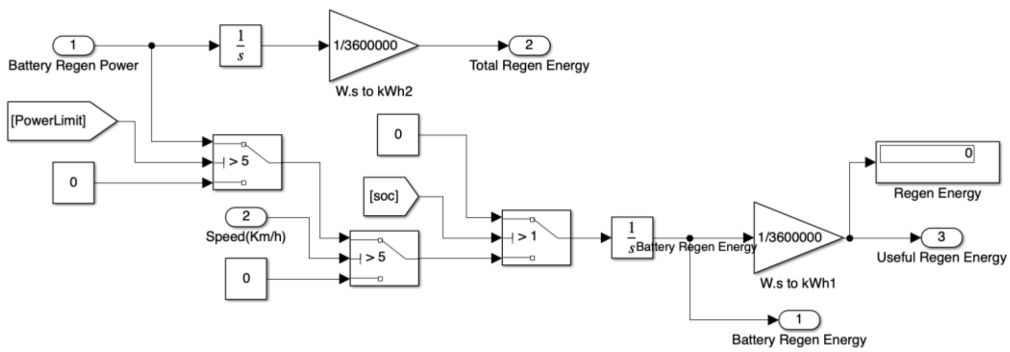

Figure 4.11: Regenerative breaking block.

4.4 Battery Technology Selection Based on BEV Model

In Fuel-cell Hybrid Electric Vehicle applications, the primary role of the battery is to meet transient and peak load demands that cannot be fulfilled by the FCS and to recover energy through regenerative braking.

Within the scope of this thesis, LFP and NMC performances are compared in terms of Regenerative Energy Recovery and Range. Installed Energy at the vehicle is considered to be equal regardless oft he packaging space needs in ordert o make a better forecast on costs and equivalent range.

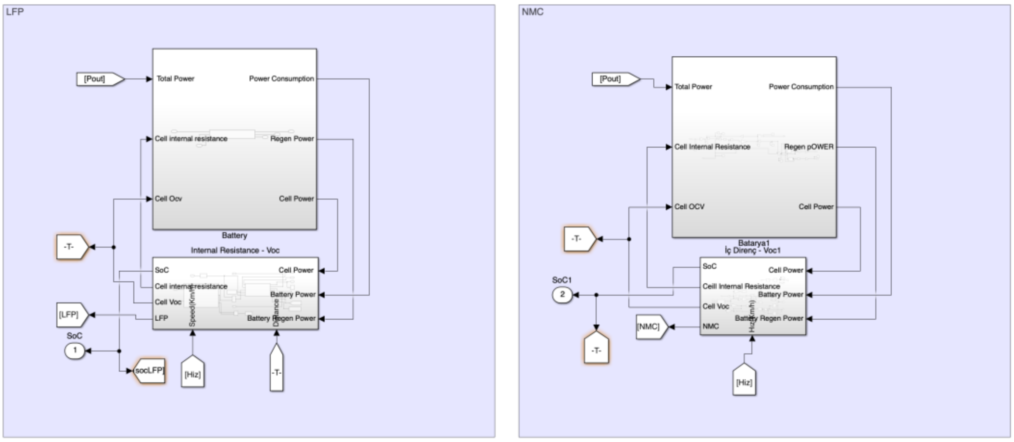

Figure 4.12: LFP and NMC battery blocks.

BEV-Model is respectively run with a 412 kWh NMC and LFP Batteries and the results of cycling performances are compared. Figure 4.12 shows the NMC and LFP battery blocks. Results are compared within Table 4.2.

Table 4.2: Comparison of LFP and NMC [71].

Parameter	NMC	LFP
Installed Energy (kWh)	412	412
Range (km)	261	261.8
Waste Energy (kWh)	0.848	0.124
Energy Regen. Breaking	46.87	49.23
Cost per kWh	~$100	$70

LFP batteries stand out in terms of ability to recover energy by providing the same range as NMC batteries. Besides, by the prices per kilowatt-hour, LFP provides a 30% initial advantage over NMC. Based on these results, it has been decided that the most suitable battery type for the FCHEV model is LFP.

4.5 Battery Capacity of FCHEV

To establish the required LFP battery capacity for a FCHEV, it is essential to consider the distance the vehicle can travel on a fully charged battery when the FCS is not operational. This analysis assumes that the vehicle must be capable of traveling at least 35 km to the nearest refueling station under such conditions. Employing the BEV model, the necessary LFP battery capacity to achieve this range has been calculated as 70 kWh. By the model in Figure 4.13, the covered distance has been observed as 35km when the SOC of the 70kWh battery reaches to zero.

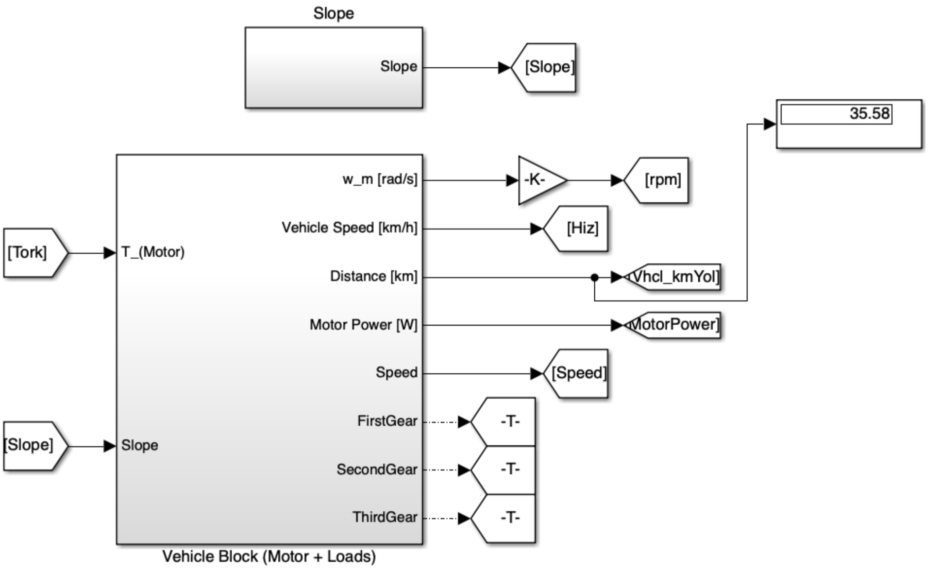

Figure 4.13: Battery capacity determination.

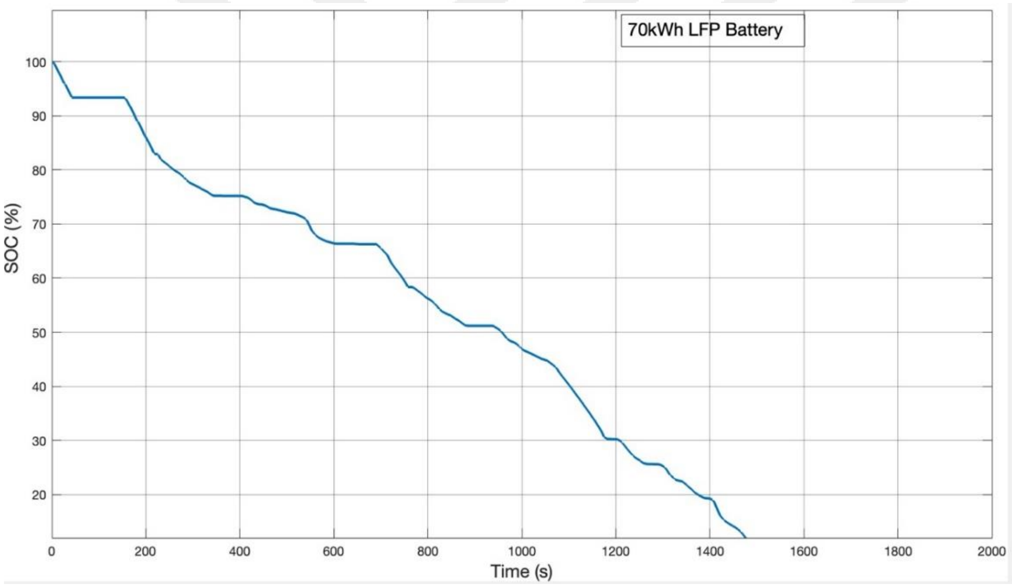

Figure 4.14: SOC change of 70kWh LFP battery.

4.6 Fuel-cell System Specifications

To specify the FCS power requirements, BEV model has been analysed. The power demand over traction motor is shown in the Figure 4.15. The analysis on the results shows that average power demanded from the motor is 142.2 kW. Additionally, the maximum instantaneous power demand has been determined to be 451.1 kW.

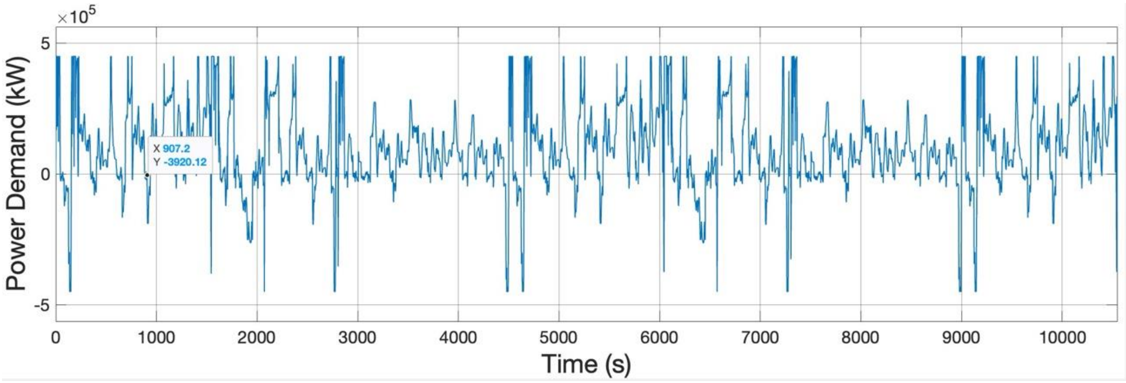

Figure 4.15: Power output of the battery electric vehicle.

Since the primary energy source in FCEVs is the FCS, the power of the FCS must be able to meet the continuous power demand of the vehicle. Considering the dynamic loads of BEV model, a FCS capable of meeting a continuous 150kW with high efficiency has been proposed.

According to the latest technological developments, FCS stacks for Heavy Duty applications can provide 150kW of output power at 800VDC with a scalable foundation. These systems can be placed in the engine compartment of heavy-duty commercial vehicles in two units, providing a total output power of up to 300kW [72].

4.7 Fuel-cell System Modelling

Due to the low technological maturity of hydrogen systems developed for Heavy Duty applications, companies keep the polarization graph information regarding hydrogen systems confidential.

Within the scope of this study, the Output Power-Efficiency and Power-Current graphs from the literature shown in Figure 4.16, Figure 4.17 and Figure 4.18 were considered. Data points of the graphs are subsequently scaled to project and achieve targeted efficiency values for the year 2025 and demonstrated in Figure 4.19. This data is implemented to the Look-up tables of the FCHEV Model.

According to Hydrogen and Fuel-cell Technologies Office, “Well” to Power Plant efficiency target for 2025 is set as 60%. The overall efficiency from “Well” to power plant includes both onboard and off-board efficiencies, taking into consideration various factors such as the energy efficiency of hydrogen production, transportation, liquefaction, compression, dispensing, and the regeneration process of chemical hydrogen storage materials, as applicable [73].

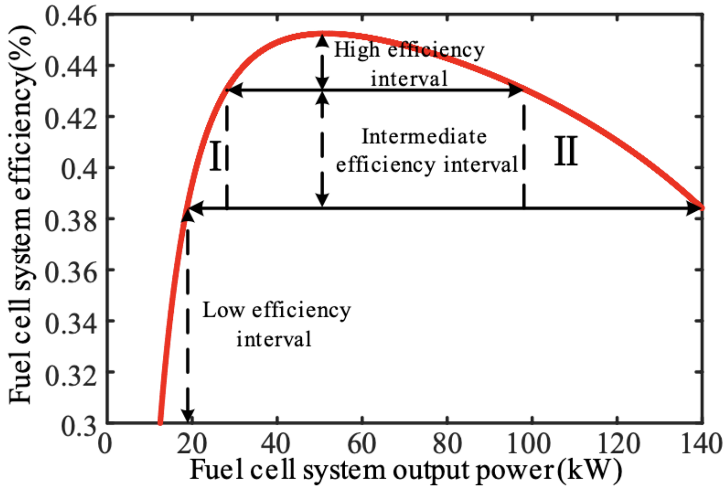

Figure 4.16: Working efficiency curve of fuel-cell system [74].

The FCS is designed to operate within an optimal efficiency range to minimize hydrogen consumption while simultaneously meeting the vehicle's power demands. Within the EMS three initial FCS operation points have been defined: idle power, continuous power, and maximum power. These points are subject to optimization by the EMS as part of this study.

As the FCS comprises two parallel fuel-cell stacks, it is referred to as the overall power of the fuel system, which consists of these two parallel fuel-cell system stacks. For a closer approximation to real driving conditions, a 2-second latency period is anticipated after the vehicle starts, to allow for the activation of the auxiliary loads within the FCS via the high-voltage (HV) battery. During this period, the overall load demands are supplied by the batteries.

To reflect the dynamic characteristics of fuel-cell, power flow rate limitation has been implemented to the FCS output via EMS. Load rate of the FCS is set as 10kW/s.

Table 4.3: FCS set points for energy management system.

Definition	Abbreviation	Value
Load Rate	Ratefc_load	10 kW/s
Idle Power	Pfc_idle	100 kW
Continous Power	Pfc_cont	140 kW
Maximum Power	Pfc_max	286 kW

To prevent frequent start-stop cycles of the Fuel-cell System (FCS), a non-stop mode has been implemented. This mode is facilitated through the establishment of an idle mode, which is defined as the minimum power output at which the system operates within its highest efficiency range. Based on the FCS efficiency curve, the idle power has been set at 100 kW. The system's continuous output power is 140 kW, with an upper limit of 286 kW. According to the predetermined algorithm, any load demands exceeding 10 kW/s or 286 kW are met by the battery. FCS operation points and power flow rate is listed in the table 4.3.

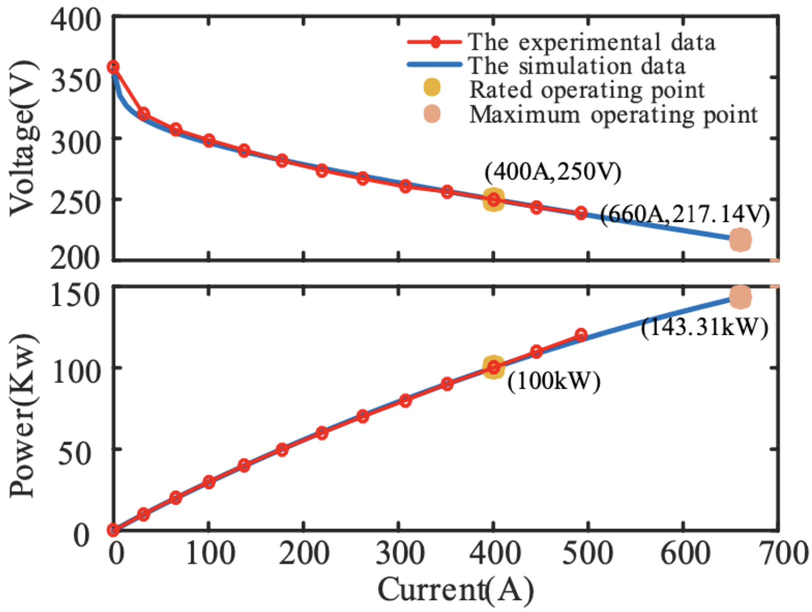

Figure 4.17: Curve fitting of polarization characteristics of fuel-cell [74].

In a PEMFC/battery hybrid power system, battery system is preferred to work in charge sustaining mode, where the battery charge and discharge are balanced so that the SOC variation is minimal throughout the driving cycle.

Fuel-cell system is considered as a device that only outputs voltage and current. This principle applies after system initiation, whereas the activation energy of auxiliries will be supplied by the HV battery-pack over DC-link [75].

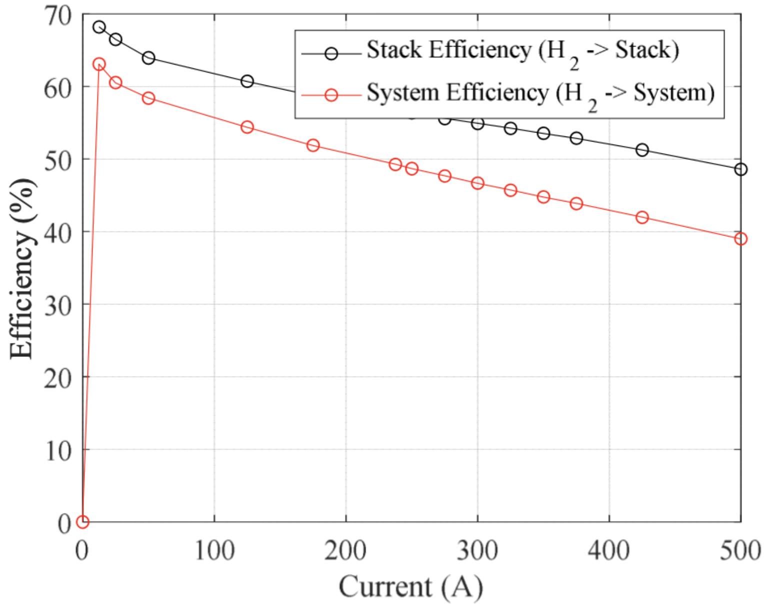

Figure 4.18: Similar stack extended to $\boldsymbol{P_{fc}}$, max=150kW [75].

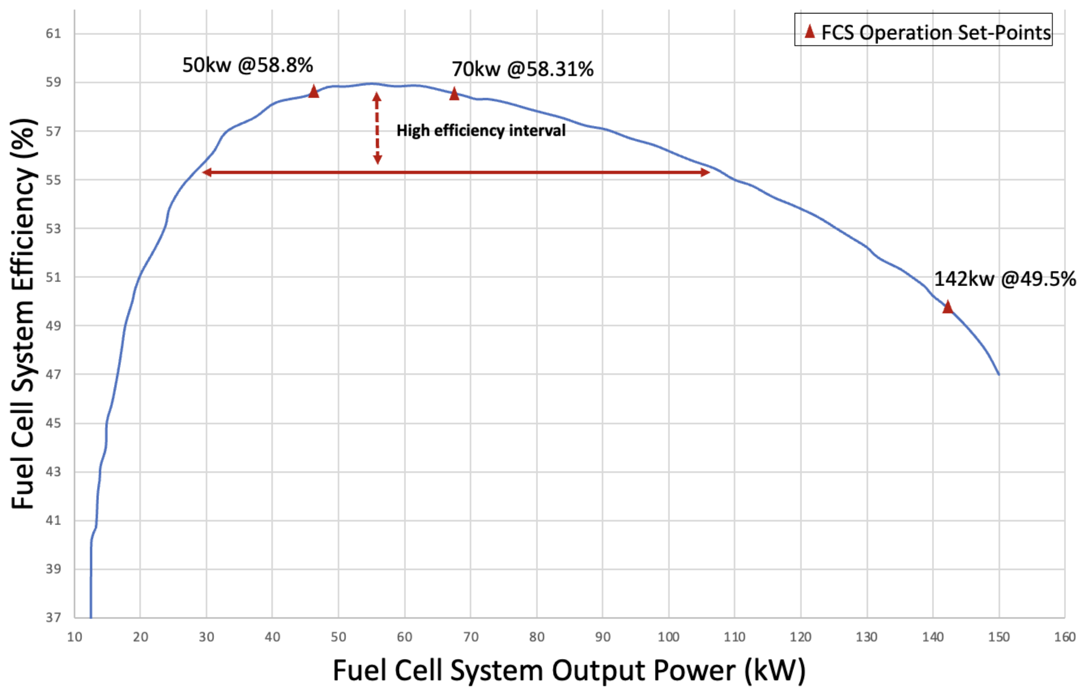

Figure 4.19: Scaled system efficiency curve of fuell cell system**.**

After cold start,

$$P_{fcs} = P_{fcs} - P_{aux} \tag{4.9}$$

Equation 4.9 expreses the net power output of the FCS. P_{fc} is the total power generated by the fuel-cell system. This includes the total electrical energy that the fuel-cell is capable of producing under operational conditions. P_{aux} refers to the auxiliary power demand, which includes the energy consumed by auxiliary components within the fuel-cell system. These auxiliary components might include pumps, controllers, fans, and other systems necessary for the operation of the fuel-cell but that do not contribute directly to the vehicle's propulsion.

The fuel net efficiency can be calculated as follows:

$$\eta = \frac{P_{fcs}}{\dot{m}H2LHV} \quad (4.10)$$

Where, $\dot{m}H2$ is the hydrogen fuel mass flow rate, *LHV* is the lower heating value of hydrogen (120 MJ kg^{-1}), M_{H2} is the hydrogen molar mass (2.02g/mol) [69].

P_{aux} value is expressed within the total FCS efficiency, hence auxiliary power is changing depending on the power demand. It is assumed that after starting the vehicle, an air-blower and compressor, which are auxiliary loads, will require 10 kW of power from the HV system for 2 seconds to activate the FCS.

Hydrogen consumption of the FCS is calculated as follows:

$$mfcs = \int_0^T \dot{m}_{H2}\, dt = \int_0^T \frac{P_{fcs}}{LHV \times \eta_{fc}} dt = \int_0^T \frac{P_{fcs}}{120 \times \eta_{fc}} dt \quad (4.11)$$

The resulting the FCS specification after scaling the literature data is shown in the table 4.4.

Table 4.4: Fuel-cell parameters [74, 76].

Characteristics	Values
Stack Peak power	150kW
Number of Stacks	2
Load Rate of stack	5kW/s
Rated power operating point	(400A, 250V)
Maximum power operating point	(660A, 217V)
Output current range	20A-660A
Number of cells	370
Rated efficiency	59%
Auxiliary Power	10kW (Activation Power)

4.8 Hydrogen and Battery Hybridization

Electric Power Train model of the BEV model has been extended by adding EMS and FCS blocks in order to achieve Battery-Fuel-Cell system hybridization for FCHEV.

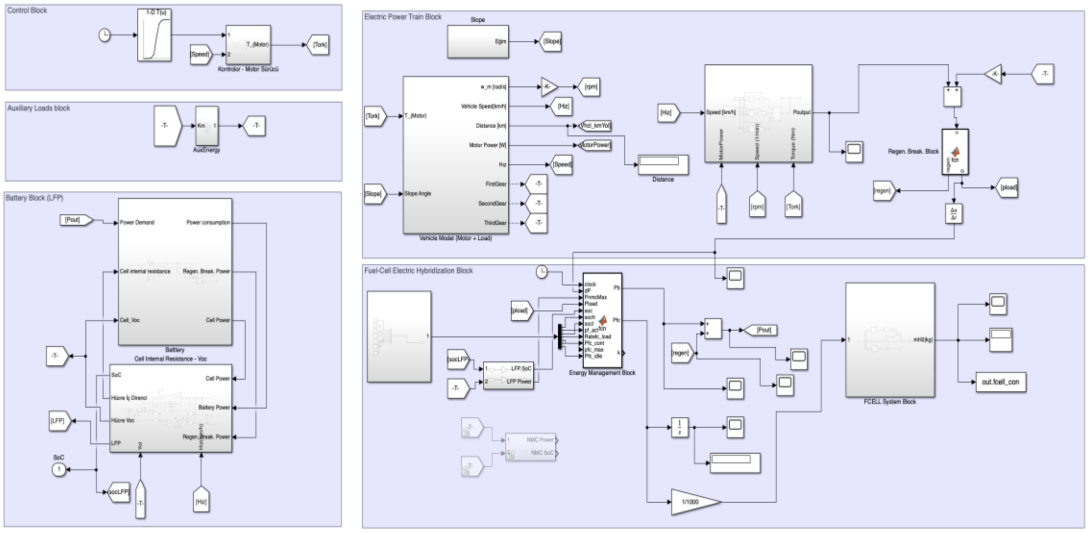

Figure 4.20: Fuel-cell electric truck model.

Figure 4.20 presents the FCHEV Model. Fuel-cell Electric Hybridization block represents the overall hybridization system that integrates the fuel-cell output with battery system. It contains the fuel-cell stacks and handles the generation of electricity from hydrogen and ensures optimal power management across different driving conditions.

Energy Management Block controls how energy is distributed between the fuel-cell, battery, and electric motors based on power needs and SOC of the battery. Recovered energy from regenerative breaking is is fed back into the battery thanks to the presence of the batteries in the system.

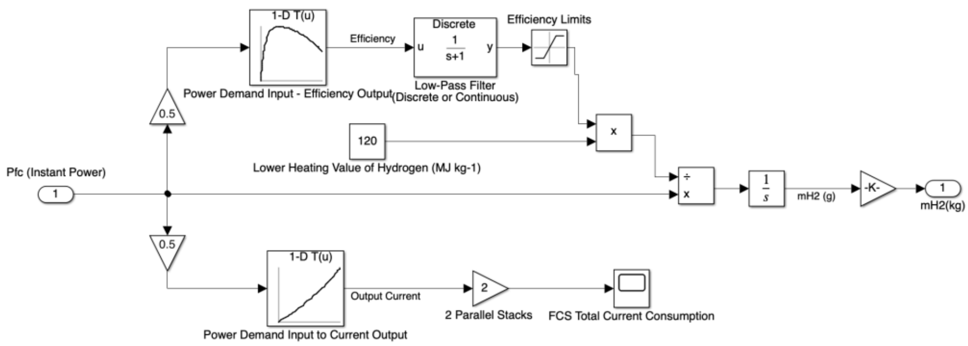

Figure 4.21: FCS block.

FCS block in Figure 4.21 utilizes the chemical energy content of hydrogen to calculate the amount needed based on energy demand over FCS.

4.8.1 Rule based-EMS

A rule-based EMS Algotihm is implementd via Matlab function into the model. Decision logic of the EMS Algorithm is shown in Figure 4.22. The system makes decisions primarily based on the SOC of the battery and the power demand of the vehicle.

The process starts when the vehicle is activated. If the power demand is lower than the battery's discharge limit, a further check is made to determine if it is below the FCS's minimum power output rate. If it is, the battery supplies the power, and any excess demand is recorded as un-recoverable energy. If the initial power demand is above the battery's discharge limit, vehicle shall wait for FCS activation. For the demands below discharge limits, system supplies power for the first 2 seconds from the battery to meet immediate demands while the FCS is bein activated. The system then checks if the power demand is below the maximum FCS power output. If it is, further decisions are made based on the SOC levels.

The system uses three SOC thresholds to make decisions. If the SOC is below the lower boundry, the battery and FCS work together to meet the power demand. If the demand is below the FCS maximum output, the FCS operates at maximum, and the battery supports in case of instantenous exceeding power demand. If SOC is between high and low boundries, decisions depend on whether the demand exceeds continuous power needs. If it does, the FCS and battery together meet the maximum demand; otherwise, the demand is met at the level of continuous power output of FCS. And if the SOC is above the upper boundry, the system prioritizes battery usage to drop the SOC to the defined level, with the FCS operating at idle or contributing to the power demand based on specific thresholds of demand.

For power demands exceeding power output rate (10 kW/s) and FCS max power, the battery supplies the additional required power.

This EMS aims to optimize the operation of the vehicle by strategically deploying the battery and FCS based on current power needs and battery condition. This helps in managing the efficiency of the system, prolonging the life of the battery, and ensuring that the vehicle can meet varying power demands efficiently.

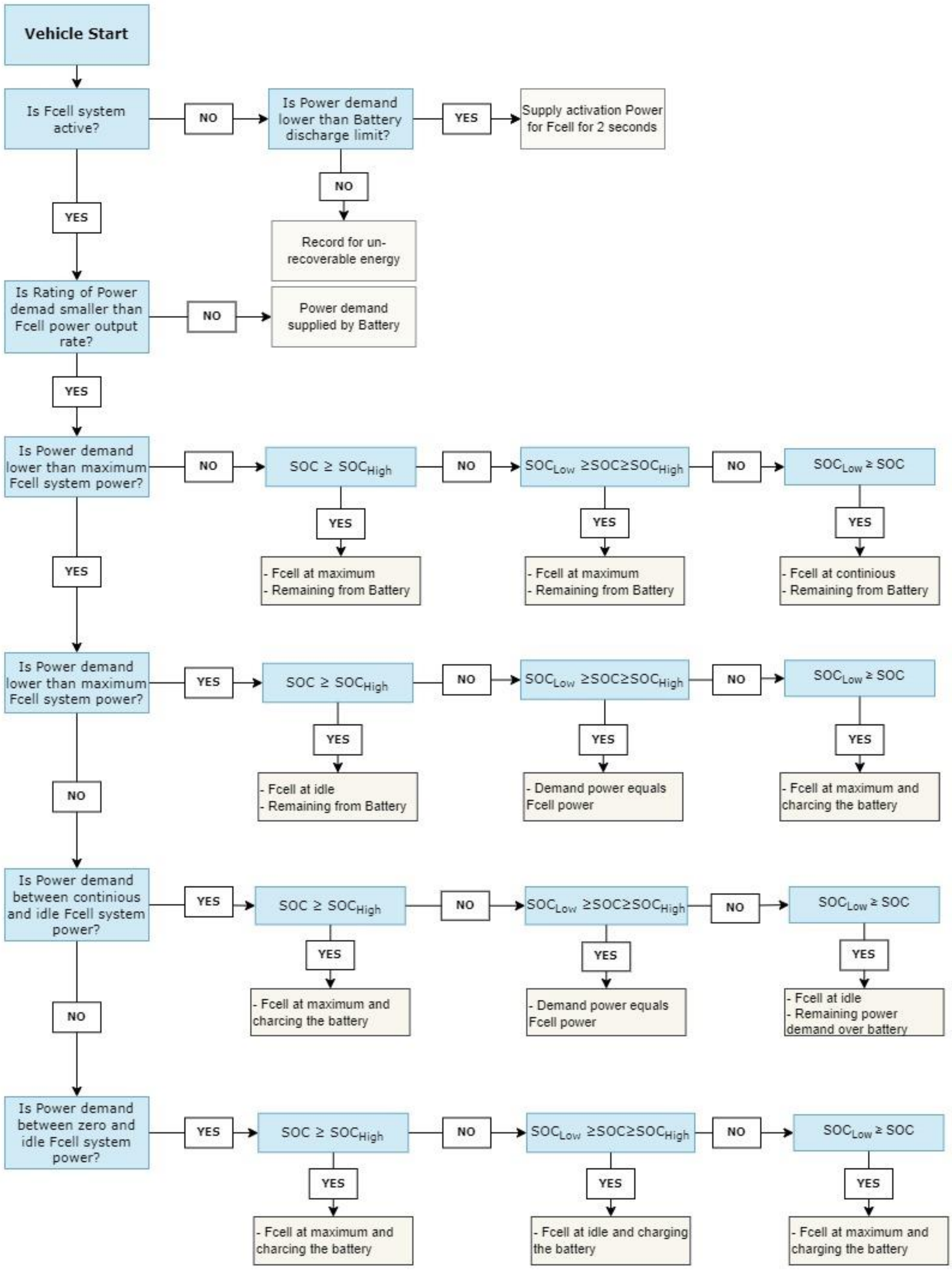

Figure 4.22: Rule-based energy management system algorithm.

4.8.2 FCHEV model aspects

FCHEV is run under initial defined values of the SOC limits and pre-defined FCS high efficiency operation points and results are shown in the Table 4.5.

Table 4.5: Fuel-cell electric truck design verification.

Parameters	Referenced Vehicle Aspects	Model Results
Vehicle Range (km)	1000	1000
Battery Capacity (kWh)	70	70
eDrive Power (kW)	330	380
Vehicle Weight (tonne)	40	40
LH_2 Consumption/Tank Capacity (kg)	88	80.17

After the first simulation, the amount of the hydrogen consumption is calculated as 80.17 kg based on the driving cycle to achieve the target range of 1000km. These results showed that the simulated model has comparable results with the referenced FCHEV.

4.8.2.1 FCHEV hydrogen tank

The mass and volume of the onboard hydrogen can be specified based on the energy generated by the fuel-cells. The gravimetric density of LH_2 is assumed to be 62 kg/1000 l at approximately 16 bar and −245°C. According to the model results, 80.17 kg would require a hydrogen tank with a volume of around 1293 l.

4.8.2.2 FCHEV unrecovered energy

The simulation results indicated that based on the initial system parameters, 0.552 kWh of energy remained unrecovered from regenerative braking. One of the primary objectives of this study is to reduce the amount of unrecoverable energy in alignment with homologation requirements.

4.8.2.3 SOC fluctuation of the initial design

One of the primary objectives of this study, as outlined in Chapter 3.2.1, is to improve the cycle life of the battery by mitigating stress through the limitation of DoD. Figure 4.23 shows the SOC changes of the model operating with the initially specified DoD values of 40% and 80% for the LiFePO4 battery. Despite the wide DoD range, when the battery’s SOC drops below the predetermined peak value, it is charged by the FCS before reaching the lower SOC limit, subsequently being elevated to the upper value. The actual DoD value has been measured at 22%.

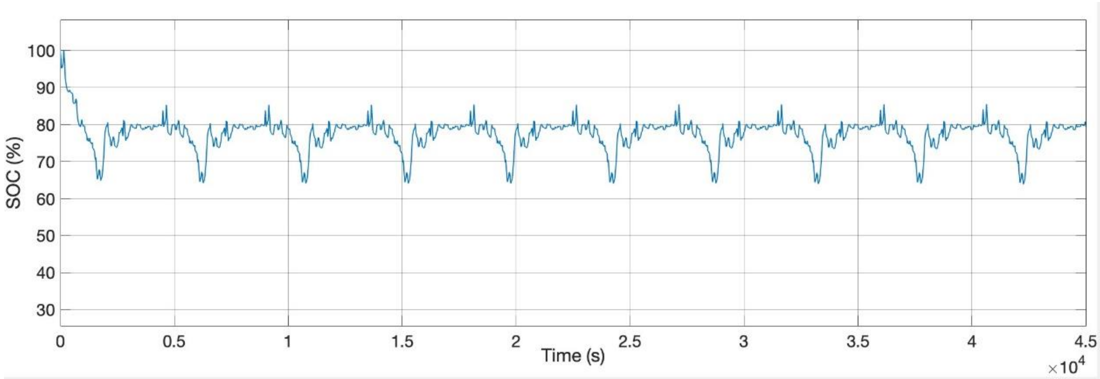

Figure 4.23: SOC fluctuation of the initial FCHEV Model.

5. ENERGY MANAGEMENT SYSTEM OPTIMIZATION

The rule-based EMS dynamically manages the distribution of power between the PEMFC and the battery system, guided by the power demand and batery SOC. To improve the system’s ability to adjust in real time, GA is integrated, which considers factors such as fuel-cell durability, efficiency, and battery charge sustainability.

In this study, multi-parameter optimization will be used to optimize FCS operation points and battery SOC ranges to minimize hydrogen consumption and unrecoverable energy (Waste_energy). The individual and combined impacts of these optimization parameters have also been tested and the results are provided in a comparative manner.

As a first step, the battery SOC boundaries will be fixed at their initial range, and the operating points of the hydrogen system that minimize hydrogen consumption and waste energy will be determined from the high-efficiency operating range using the Genetic Algorithm (GA) method.

Subsequently, the FCS operation points will be fixed at their initial state, and the SOC range that minimizes hydrogen consumption and waste energy will be determined using the GA method. After comparing the initial optimization results, these values will be integrated into the model.

Finally, in order to assess the combined impact of the optimized parameters on the GA objectives, the model will be rerun with the optimized FCS operation points and the resulting SOC range applied, and the results will be compared.

5.1 Optimization of FCS Operation Points

As a first step of EMS optimization, operation points of FCS are optimized focusing on the objectives of minimizing hydrogen consumption and unrecoverable energy during regenerative braking.

The FCS is designed to operate predominantly within its high-efficiency zone on the Efficiency-Power Output curve, identifying key operation points that include P_{idle} (the minimum output power required to keep the system active during driving), $P_{continuous}$ (the power output needed to meet the average vehicle power demands), and $P_{maximum}$ (the maximum power that the FCS can supply according to the rule-based energy management system). To optimize these points, the State of Charge (SOC) cyclic operation range is maintained between initial state of 40% and 90%. GA is utilized to determine the optimal FCS operation points that achieve the lowest hydrogen consumption and reduce unrecoverable energy, thereby enhancing the overall efficiency and sustainability of the FCHEV system.

As part of the GA Method, for each FCS operation point upper and lower boundries have been defined. Boundries for each FCS operation point threshold are shown as follows:

$$60kw < P_{idle} < 100kw \tag{5.1}$$

$$110kW < P_{continuous} < 160kw \tag{5.2}$$

$$160kW < P_{maximum} < 300kw \tag{5.3}$$

For both optimization steps, the same objective function is maintained. Which aims to minimize hydrogen consumption and unrecoverable energy to the lowest possible level. Table 5.1 shows the abbreviations of the GA objectives. Objectives are addressed to the variables to F1 and F2 and consitituted the obj ective function of J. W1 and W2 are weight constants which are defined as 1.

Table 5.1: GA objectives.

Parameters	Description
Fcell_con_final	Total Hydrogen Consumption
Waste_energy_final	Total Unrecoverable Energy

$$J_{fitness} = \frac{1}{\sum F.W_i} \tag{5.3}$$

$$F1 = fcel\_con\_final \tag{5.4}$$

$$F2 = waste\_energy\_final \tag{5.5}$$

$$W1 = W2 = 1 \tag{5.6}$$

Four parameters have been defined as termination criteria for the optimizations as shown in Table 5.2. These are reaching the maximum generation count (100), the best objective function results remaining unchanged for 1000 seconds, the best objective function result remaining unchanged for 50 generations and the Function Tolerance (1e-3).

Table 5.2: Parameters setting of GA.

Description	Value
Generations with unchanged result	50
Time with unchanged result (s)	1000
Function tolerance	1e-3
Generation number	100

Matlab Function and GA code is given in Appendix D and Appendix E. Following this optimization study, the FCS operation points, which minimize hydrogen consumption and unrecoverable energy, was determined. Resulting FCS operation points are shown in Figure 5.1.

```
ga stopped because it exceeded options.MaxTime.
Optimized parameters (Pfc_idle, Pfc_cont, Pfc_max):
       60000      110000      160000

Corresponding fitness value:
    0.0084
```

Figure 5.1: GA optimization results for FCS operation points.

The model was then updated with these values and rerun. The outcome of the simulation is shown in Table 5.3.

Table 5.3: Vehicle outcome with optimized FCS operation points.

Parameters	H_2 Consumption (kg)	Unrecoverable Energy (kWh)
Initial State	80.17	0.552
Optimized FCS Operation Points	76.96	0.547

SOC Fluction of the Battery is shown in Figure 5.2. The results showed that when the battery SOC changes were examined with an extended SOC operating range and the new FCS operation points were considered as inputs, the hydrogen consumption is reduced significantly about 3.21kg but the DoD was observed to be 35%. To lower the stress on the battery and extend the cycle life, further optimization is performed on SOC set points.

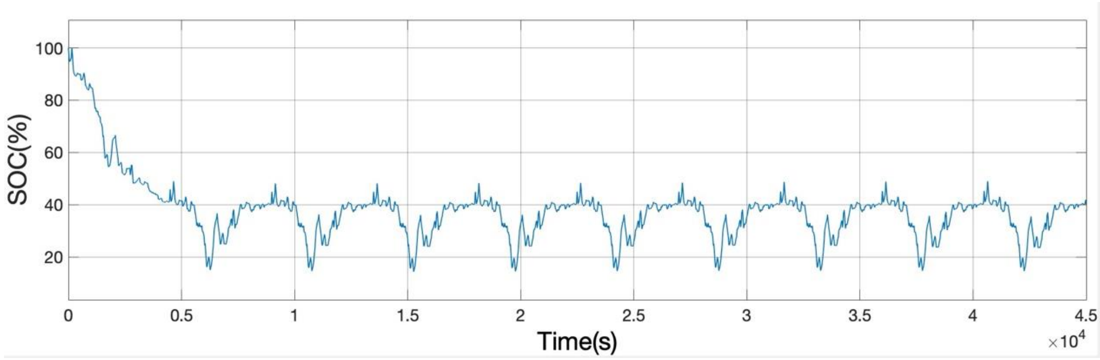

Figure 5.2: SOC fluctuation with the optimized FCS range.

5.2 Optimization of SOC Range

In various driving scenarios, power allocation under the rule-based EMS relies heavily on SOC thresholds (SOC_{Low}, SOC_{High}), which directly impact hydrogen consumption and SOC fluctuations in the system. A lower SOC_{High} may lead to battery over-discharge, while a higher SOC_{Low} can result in the fuel-cell overcharging the battery. Both extremes negatively affect hydrogen consumption and the health of the PEMFC and battery.

Minimizing SOC variation (ΔSOC) helps prevent battery overcharging and over-discharge, thus saving hydrogen consumption. GA optimizes SOC variation under load conditions, with SOC_{Low} and SOC_{High} coefficients subject to GA optimization.

Furthermore, constraints for each SOC threshold are outlined as follows:

$$40\% \leq SOC_{Low} < 60\% \tag{5.7}$$

$$60\% < SOC_{High} < 80\% \tag{5.8}$$

The objective function and GA parameters are maintained as the first optimization aiming to minimize hydrogen consumption and unrecoverable energy to the lowest possible level. Multiple Parameter GA optimization code and the matlab function are given in Appendix-A and Appendix-B.

Optimization has been terminated automatically when the defined conditions are met. The Fitness value change over generation number is shown in Figure 5.3. Following this optimization study, the SOC range, which minimizes hydrogen consumption and unrecoverable energy, was determined and presented in Figure 5.4. The model was then updated with these values and rerun to obtain optimized results. The outcome of the vehicle model is shown in Table 5.4.

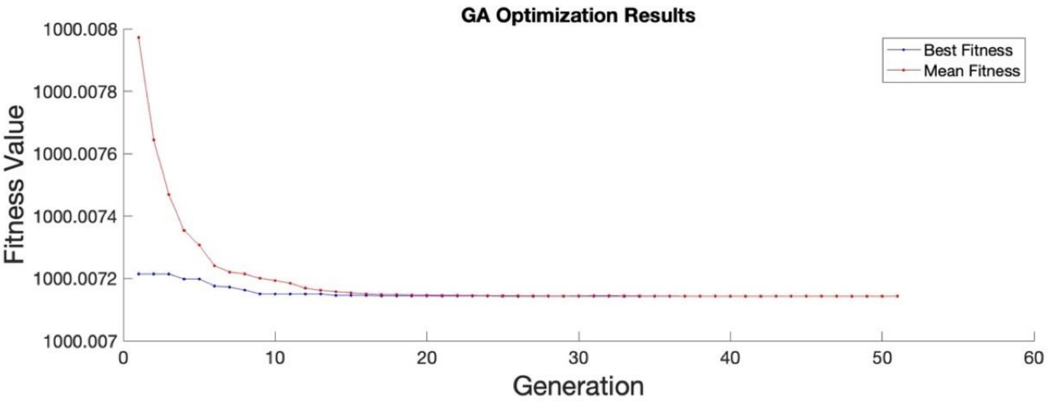

Figure 5.3: GA optimization results**.**

```
ga stopped because it exceeded options.MaxTime.
Optimized parameters (soch, socl):
    40    60

Corresponding fitness value:
   1.0000e+03
```

Figure 5.4: GA optimization of SOC range.

Table 5.4: Vehicle outcome with the optimized SOC range.

Parameters	H_2 Consumption (kg)	Unrecoverable Energy (kWh)
Initial State	80.17	0.552
Optimized FCS Operation Points	79.15	0.5517

The simulation results showed that when the battery SOC changes were examined with the FCS operation points kept at initial conditions and the optimized SOC range applied, the system managed to maintain the Battery SOC approximately within the 40% to 60% range and the DoD was observed to be restricted to about 20% as shown in Figure 5.5. Nevertheless, the impact of the SOC Set-point optimization on the hydrogen consumption reduction seemed to be limited with 1.02 kg.

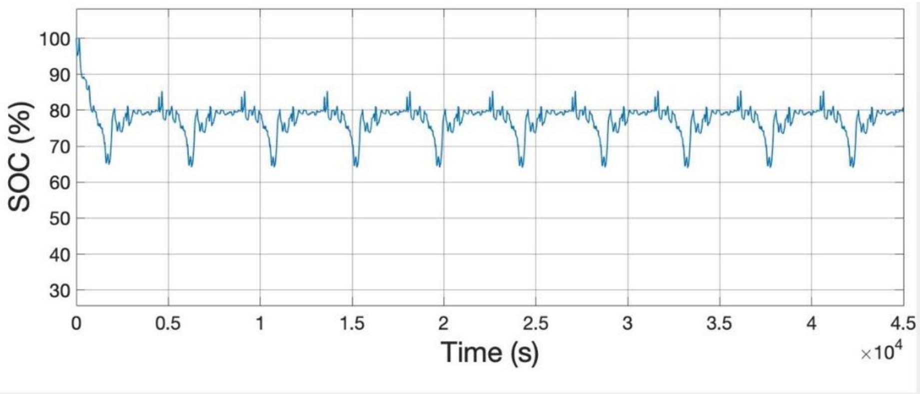

Figure 5.5: SOC fluctuation with the optimized SOC range.

5.3 Combined Impact of Optimization Parameters

To observe the combined effect of the investigated optimization parameters, the FCS operation points determined by the optimization result have been integrated into the model and the SOC operation range has been re-optimized. The optimization result showed similarities with the initial SOC range optimization. The optimized SOC range and FCS operation points were applied to the vehicle model, and the results are displayed in Table 5.5.

Table 5.5: Vehicle outcome with the optimized SOC range.

Parameters	H_2 Consumption (kg)	Unrecoverable Energy (kWh)
Initial State	80.17	0.552
Optimized FCS Operation Points	76.99	0.5468

Similarly, when looking at the SOC fluction of the vehicle in Figure 5.6, when both FCS and SOC optimized parameter are implemented to the mode, the system was unable to maintain the Battery SOC within the 40% to 60% range. Despite the DoD is limited with 20% the battery was utilized near the deep discharge zone.

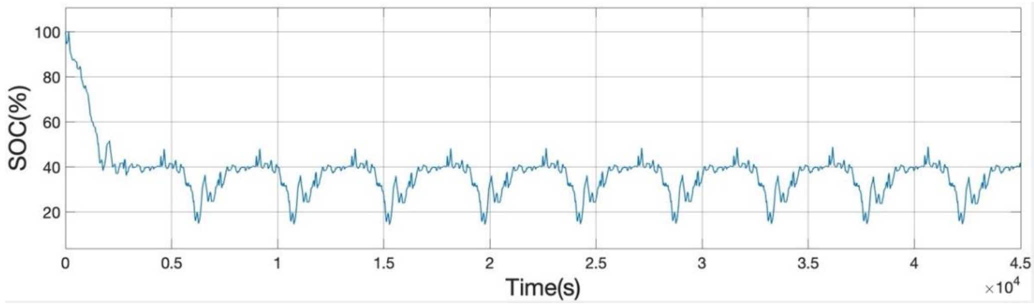

Figure 5.6: SOC fluctuation with the optimized SOC range.

Table 5.6 shows the overview of all simulation results after each optimization step. The scenario in which the FCS operation points are optimized independently of the SOC operating range results in the lowest hydrogen consumption. However, when considering the impact of Battery DoD on battery life together with with Hydrogen consumption, a scenario where both FCS operation points and SOC operating range are optimized together shows a negligible increase in hydrogen consumption, yet a significant reduction in Battery DoD has been observed.

Table 5.6: Results of each optimization step.

Optimization parameters	Initial	FCS	FCS and SOC	SOC
P_idle (kW)	100	60	60	100
P_con (kW)	140	110	110	140
P_max (kW)	286	160	160	286
SOC_high (%)	40	40	40	40
SOC_low (%)	80	80	60	60
LH_2 cons. (kg)	80.17	76.96	76.99	79.15
E_waste (kWh)	0.552	0.5469	0.5468	0.5517
DoD (%)	22	35	20	20

As a result of the optimization, considering the combined impact of both FCS and SOC parameters, there have been a 3.97% (3.18kg) reduction in hydrogen consumption and a 0.94% (5.2Wh) improvement in unrecoverable energy. Additionally, by maintaining the DoD at 20% contribution has been made to extending battery life. Considering the gravimetric density of liquid hydrogen an improvement of 51.3 liters in the hydrogen storage tank volume is expected. Table 5.7 highlights the states of the objectives before and after the optimazation is applied.

Table 5.7: Optimization impact on hydrogen storage tank and range

Parameters	Initial Design	After Optimization
Unrecoverable Energy (kWh)	0.552	0.5468
DoD (%)	22	20
LH_2 Consumption (kg)	80.17	76.99
LH_2 Tank Volume (l)	1293	1241.7

6. CONCLUSIONS AND RECOMMENDATIONS

This thesis discusses the operational optimization of an energy management system used in FCHEV. A comprehensive literature review has been conducted, considering the requirements of battery electric trucks and other vehicle needs. Various hydrogen systems, types of hydrogen fuel, energy storage systems, and hybridization methods were analyzed to determine the optimal FCHEV structure. The research focused on an FCHEV architecture where the battery is directly connected to the DC bus, and the FCS is indirectly connected.

In the later sections of the thesis, a longitudinal dynamic model of a battery electric vehicle was developed in a Matlab/Simulink environment. By using the battery electric vehicle model, energy storage systems were compared to select the appropriate battery type for the FCHEV. The comparison considered parameters like regenerative braking energy recovery, range, and cost, which are also used as objectives in optimization work. Using the longitudinal dynamic model of the battery electric vehicle, an FCHEV model was created.

The energy management system used in this study, the optimization targets, and the genetic algorithm as the optimization method were defined and explained. Different scenarios were explored using the dynamic model for optimization.

In the final phase of the study, the FCS operating points within its efficient range were optimized using GA. These FCS operating points were set as the optimization parameters in the energy management system. The objectives of the optimization were to minimize hydrogen consumption and unrecoverable regenerative energy. The initial optimization results are integrated into the model and lead to a reduction of 3.97% in hydrogen consumption (3.21 kg) and 0.9% in unrecoverable energy (5.1 Wh) by keeping the battery DoD at 35%. As a second step of the optimization, the operation setpoints of the FCS were kept constant at their initial values, while the high and low thresholds of the SOC at EMS were optimized using GA. The optimized SOC high and low thresholds were determined to be 60% and 40%, respectively, and integrated into the model. The model was then re-run. In this setup, while maintaining the battery DoD at 20%, a reduction in hydrogen consumption of 1.27% (1.02 kg) and a reduction in non-recoverable energy were achieved. At the last step of the optimization, the initial FCS operation setpoints have been replaced with the optimized FCS operating points and the battery's SOC operation boundries have been optimized with respect to the same GA objectives. The new SOC operation boundaries are found, similar to the second step, between 40% and 60% and implemented to the model. After running the model with optimized FCS and SOC paramaters, the simulation showed a reduction of % in hydrogen consumption (3.17 kg) and 3.96% in unrecoverable energy (5.2 kWh) by keeping the battery DoD at 20%.

Cycling a LFP battery between 40% and 60% SOC significantly reduces the DoD, which also reduces the stress on battery cells and slows down degradation. This limited cycling range avoids the damaging high voltages that occur at full charge or discharge, thereby stabilizing the electrode materials and preventing harmful chemical reactions. Consequently, such a practice can more than double the cycle life of the battery by reducing wear and allowing for more cycles before the capacity significantly declines.

Reducing hydrogen consumption by 3.17 kg in the FCHEV increases the vehicle's range by 40 km. This efficiency translates to a fuel economy of approximately 12.62 km per kilogram of hydrogen. The initial total hydrogen capacity of the vehicle is around 80.17 kg, and the 3.17 kg reduction frees up about 51.3 liters of space within the vehicle. This saved space, previously dedicated to hydrogen storage, can now be utilized for additional packaging or system components, improving vehicle utility.

Considering the optimization studies, the scenario where both the FCS and the SOC setpoints were optimized together has been found as the most effective approach for extending battery life, reducing hydrogen consumption, and minimizing non-recoverable energy.

Further research should be conducted on different ways to improve energy management system like using artificial intelligence. Simple energy management systems can be effective and easy to use, helping truck drivers save energy. Testing new battery types with better charge acceptance and longer lifespans can help improve truck efficiency. Battery design can be further optimized as FCSs become more efficient and more refueling stations become available on the road by reducing the on-board battery capacity.

REFERENCES

[1] **European Environment Agency (EEA),** (2022). Retrieved September 2023 from https://www.eea.europa.eu/ims/emissions-of-air-pollutants-from.

[2] **International Energy Agency (IEA),** (2021). Key World Energy Statistics 2021. Retrieved September 2023 from https://www.iea.org/reports/key-world-energy-statistics-2021.

[3] **United Nations Sustainable Development**, **(**2020). Amid worsening climate crisis, UN Secretary-General sets out top ten climate action priorities for 2020, vows to stay on frontlines. Retrieved September 2023 from https://www.un.org/sustainabledevelopment/blog/2019/12/ 77358/.

[4] **European Environment Agency (EEA),** (2022). Retrieved September 2023 from https://www.mckinsey.com/industries/automotive-and-assembly/our-insights/hydrogen-the-next-wave-for-electric-vehicles.

[5] **Bethoux, O.** (2020). Hydrogen Fuel-cell Road Vehicles: State of the Art and Perspectives. *Energies 2020, 13, 5843.*

[6] **Ambel, C.C**. (2015). Too Big to Ignore-Truck CO_2 Emissions in 2030. *Transport & Environment.*

[7] **European Commission** (2019). EU Regulation 2019/1242 Setting CO_2 emission performance standards for new heavy-duty vehicles and amending Regulations (EC) No 595/2009 and (EU) 2018/956 of the European Parliament and of the Council and Council Directive 96/53/EC. Off. J. Eur. Union 2019, 202–239.

[8] **Becker, H., Bichucher, V., Dwyer, J., Engstrom, S., Farrag-Thibault, A., Hamdi-Cherif, C., Heid, B., Hertzke, P., De Monts, A. and Östgren, E.** (2022). Road Freight Global Pathways Report. Retrived December 2023 from: https://www.mckinsey.com/industries/automotive-and-assembly/our-insights/road-freight-global-pathways-report#/

[9] **Cui, H., Gode, P. and Wappelhorst, S.** (2021). A Global Overview of Zero-Emission Zones in Cities and Their Development Progress. International Council on Clean Transportation. Retrieved September, 2023 from https://theicct.org/publication/a-global- overview-of-zero-emission-zones-in-cities-and-their-development-progress/.

[10] **Sigle, S. and Hahn R.** (2022). Energy Consumption Comparison of Current Powertrain Options in Autonomous Heavy Duty Vehicles (HDV). Second International Conference on Sustainable Mobility Applications, Renewables and Technology (SMART).

[11] **Wilkins, S.** (2020). Challenges and Opportunities For Highly Electrified Heavy Duty Vehicles. Decarbonisation of Heavy-Duty Vehicle Transport: Zero-Emission Heavy Goods Vehicles TNO. Retrieved December 2023 from https://www.scribd.com/document/525429500/Steven-Wilkins-Challenges-and-Opportunities-for-Highly-Electrified-Heavy-Duty-Vehicles-Public.

[12] **Ruf, Y.** (2020). Study on European business cases for fuel-cells and hydrogen trucks. *In EU Hydrogen Week: Roland Berger GmbH: Munich, Germany, 2020.*

[13] **Bethoux, O.** (2020). Hydrogen Fuel-cell Road Vehicles and Their Infrastructure: An Option towards an Environmentally Friendly Energy Transition. *Energies 2017, 13, 6132*.

[14] **Verbruggen, F., Hoekstra, A. and Hofman, T.** (2018). Evaluation of the state-of-the-art of full-electric medium and heavy-duty trucks. *World Electric Vehicle Symposium and Exhibition 2018.*

[15] **Kast, J.; Morrison, G., Gangloff, J.J., Vijayagopal, R. and Marcinkoski, J**. (2018). Designing hydrogen fuel-cell electric trucks in a diverse medium and heavy duty market. *Research in Transportation Economics 70 (2018) 139-147.*

[16] **Pizzutilo, E., Acher, T., Reuter, B., Will, C. and Schäfer, S.** (2024).Subcooled Liquid Hydrogen Technology for Heavy-Duty Trucks. *World Electric Vehicle Journal (2024), 15, 22.*

[17] **Naylor, S.M., Pickert, V. and Atkinson, D.J.** (2006). Fuel-cell Drive Train Systems-Driving Cycle Evaluation of Potential Topologies. University of Newcastle upon Tyne Merz Court. *IEEE 2006 1-4244-0159-3/06/$20.00.*

[18] **Pardhi, S. Chakraborty, S., Tran, D., El Baghdadi, M., Wilkins, S. and Hegazy, O.** (2022). A Review of Fuel-cell Powertrains for Long-Hail Heavy-Duty Vehicles: Technology, Hydrogen, Energy and Thermal Management Solutions. *Energies 2022, 15, 9557.*

[19] **Ragab, A., Marei, M. and Mokthar, M**. (2023). Comprehensive Study of Fuel-cell Hybrid Electric Vehicles: Classification, Topologies, and Control System Comparisons. *Pre-prints 2023*, doi:10.20944/preprints202310.1459.v1.

[20] **Bauman J.** (2008). A Comparative Study of Fuel-Cell–Battery, Fuel-Cell–Ultracapacitor, and Fuel-Cell–BatteryUltracapacitor Vehicles. *IEEE 2008 Transactions on Vehicular Technology, Vol. 57, No.2*, doi:10.1109/TVT.2007.906379.

[21] **Zhao, X., Wang, L., Zhou, Y., Pan, B., Wang, R. Wang, L. and Yan, X**. (2022). Energy management strategies for fuel-cell hybrid electric vehicles: Classification, comparison, and outlook. *Energy Conversion and Management. 270 (2022) 116179,* doi: 10.1016/j.enconmann.2022.116179.

[22] **Yuan, H., Zou W., Jungi S. and Kim Y**. (2022). A Real-Time Rule-Based Energy Management Strategy With Multi-Objective Optimization for a Fuel-cell Hybrid Electric Vehicle. *IEEE VOL.10, 2022,*pp. 102618-102628, doi: 10.1109/ACCESS.2022.3208365.

[23] **Salek, F., Abouelkhair E., Babaie M., Cunliffe F. and Nock W.** (2023). Multi-Objective Optimization of the Fuel-cell Hybrid Electric Powertrain for a Class 8 Heavy-Duty Truck. *SAE Technical Paper 2023-01-0473,* doi: 10.4271/2023-01-0473

[24] **European Environment Agency (EEA),** (2022). Retrieved October, 2023 from https://ec.europa.eu/commission/presscorner/detail/en/MEMO_14_36.

[25]**Virta Global**. Retrieved October, 2023 from https://www.virta.global/blog/electrification-of-heavy-duty-fleets-the-time-is-right

[26] **Volvo HD 4x2 diesel powertrain topplogy**. Retrieved February, 16 2024 from www.volvotrucks.com. Accessed in 16.02.2024.

[27] **Zhao, H., Burke A., Zhu L.** (2013). Analysis of Class 8 Hybrid-Electric Truck Technologies Using Diesel, LNG, Electricity, and Hydrogen, as the Fuel for Various Applications. *EVS27 International Battery, Hybrid and Fuel Cell Electric Vehicle Symposium 2013*.

[28] **Cabazuelo, D., Andreu, Z., Kortabarria I.** (2017). Powertrain systems of electric, hybrid and fuel-cell vehicles: state of technology. *IEEE 2017 978-1-5090-1412-5/17/$31.00* pp.1445-1450.

[29] **Boer. E, Aarnink, S., Kleiner, F., Pagenkopf, J.** (2013) An overview of state of the art technologies and their potential. *Delft, July 2013, Zero emission trucks 13.4841.21*.

[30] **Battery Electric Truck with Near-Wheel Drive.** Retrieved February, 17 2024 from https://cenicesk.life/product_details/51325753.html.

[31] **Mercedes-Benz Actros**. Retrieved February, 17 2024 from https://www.mercedes-benz-trucks.com/en_NZ/models/actros.html.

[32] Tesla Semi Retrieved 17.02.2024 from https://www.tesla.com/semi

[33] Volvo Trucks Long Range Retrieved 17.02.2024 from https://www.volvotrucks.com/en-en/news-stories/press-releases/2023/jun/volvo-presents-electric-trucks-with-longer-range.html

[34] **Mercedes-Benz eActros 600.** Retrieved February, 16 2024 from https://www.daimlertruck.com/newsroom/pressemitteilung/mercedes-benz-trucks-feiert-weltpremiere-des-batterieelektrischen-fernverkehrs-lkw-eactros-600-52428265.

[35] MAN TGX Retrieved 17.02.2024 from https://www.man.eu/de/en/truck/all-models/the-man-tgx/the-man-etgx/overview.html

[36] SCANIA Battery Electric Truck Retrieved 17.02.2024 from https://www.scania.com/group/en/home/products-and-services/trucks/battery-electric-truck.html

[37] IVECO HD BEV Retrieved 17.02.2024 from https://www.iveco.com/en-us/press-room/release/Pages/IVECO-to-produce-and-market-its-Heavy-Duty-Battery-Electric-Vehicle-and-Heavy-Duty-Fuel-Cell-Electric-Vehicle.aspx

[38] BYD Class 8 Day Cab https://en.byd.com/truck/class-8-day-cab/

[39]**Hayes, G.J., Goodarzi, A.G.** (2018). Book: Electric Power Train. ISBN 9781119063667.

[40]**Quantron.** BEV or FCEV. Retrieved October, 2023 from https://www.quantron.net/wp-content/uploads/2023/01/Quantron-AG_Whitepaper-BEV-or-FCEV.pdf.

[41] **Selmi., T., Khadhraoui, A., Cherif, A.** (2022). Fuel-cell-based electric vehicles technologies and challenges. *Environmental Science and Pollution Research* (2022) 29:78121-78131, doi: 10.1007/s11356-022-23171-w.

[42] **Fuel-cell Hydrogen Electric Truck**. Retrieved February, 17 2024 from: https://nikolamotor.com/tre-fcev/.

[43] **Fuel-cell Electric Truck – Mercedes-Benz -GenH2 with liquid Hydrogen Storage.** Retrieved February, 17 2024 from: https://www.daimlertruck.com/en/newsroom/pressrelease/fuel-cell-technology-daimler-truck-builds-first-mercedes-benz-genh2-truck-customer-trial-fleet-52552943.

[44] **Hu, X., Zou, C., Zhang, C., Li, Y.** Technological developments in batteries: A survey of principal roles, types, and management needs. *IEEE Power Energy Mag. 2017, 15, 20–31*.

[45] **Main Characteristics of Li-Ion Batteries**: Retrieved February,16 2024 from https://zecar.com/resources/what-are-lfp-nmc-nca-batteries-in-electric-cars.

[46] **Main Characteristics of Li-Ion Batteries**: Retrieved February, 16 2024 from https://www.lithiumstoragebattery.com/news-lithium-ion-battery-classification-future-trend.htm.

[47] **Knibbe, R., Harding, D., Burton, J., Coopera E., Zadeh, Z.A., Sagulenkoa, M., Meehan, P.A., Buckley, R.** (2023). Optimal battery and hydrogen fuel-cell sizing in heavy-haul locomotives, *Journal of Energy Storage. Journal of Energy Storage 71(2023) 108090*, doi:1016/j.est.2023.108090.

[48] **What factors will define the Lithium-Ion battery technology of the future?** Retrieved February, 16 2024 from https://energydmmanagement.com/what-factors-will-define-the-lithium-ion-battery-technology-of-the-future/.

[49] **Lukic, S., Cao, J., Bansal, R., Rodriguez, F., Emadi, A.** (2009). Energy storage systems for automotive applications, *IEEE Transactions on Industrial Electronics, vol. 55, no. 6, ss. 2258-2267, June 2008, doi: 10.1109/TIE.2008.918390.*

[50] **Ultracapacitor from Maxwell**: Retrieved February,15 2024 from https://maxwell.com/products/ultracapacitors/cells.

[51] **Ultracapacitor from Maxwell**: Retrieved February, 15 2024 from https://maxwell.com/products/ultracapacitors/48v-module-with-durablue.

[52] **Ribeiro, P., Johnson, B., Crow, M., Arsoy, A., Liu, Y.** (2001). Energy Storage Systems for Advanced Power Applications. *PROCEEDINGS OF THE IEEE*, vol. 89, no.12 December 2001 pp.1744-1756.

[53] **Wang, Y., Yuan, H., Martinez, A., Hong, P., Xu, H., & Rockmiller, F.** (2021). Polymer electrolyte membrane fuel-cell and hydrogen station networks for automobiles: Status, technology, and perspectives. *Elsevier Enhanced Reader. Advances in Applied Energy.*

[54] Modern Electric, Hybrid Electric, and Fuel-cell Vehicles, CRC Press LLC , 2005.

[55] **Basma, H. Rodriguez, F.** (2022). The ICCT: Fuel-cell electric tractor-trailers: Technology overview and fuel economy.*International Council on Clean Transportation Working Paper* 2022-23.

[56] **CNHI.** (2020). Truck Architecture and Hydrogen Storage.

[57] **H2 Mobility.** (2021). Overview Hydrogen-Refuelling For Heavy-Duty Vehicles. storage systems for advanced power applications, *Proceedings of the IEEE*, vol. 89, no. 12, ss. 1744-1756, December 2001, doi: 10.1109/5.975900.

[58] **K. Kawashima, T. Uchida, and Y. Hori.** (2009).Development of a novel ultra-capacitor electric vehicle and methods to cope with voltage variation," in Proc. *IEEE VPPC, 2009, pp. 724–729*.

[59] **Townsend, A., Gouws, R.,**. A Comparative Review of Lead-Acid, Lithium-Ion and Ultra-Capacitor Technologies and Their Degradation Mechanisms, 2022, p-9.vEnergies 2022, 15, 4930.

[60]ZF Electric Axle. Retrieved 28.04.2024 from: https://www.zf.com/products/en/cv/products_75912.html

[61] **Vehicle Energy Consumption Calculation Tool – VECTO.** Retrieved January, 10 2024 from https://climate.ec.europa.eu/eu-action/transport/road-transport-reducing-co2-emissions-vehicles/vehicle-energy-consumption-calculation-tool-vecto_en).

[62] The European Commission's science and knowledge service Joint Research Centre 2018 VECTO Workshop Ispra. (2018)

[63] **Doppler, C., Lindner, B.** (2023) Fuel-cell Trucks: Thermal Challenges in Heat Exchanger Layout. Energies 2023, 16, 4024. https://doi.org/10.3390/en16104024

[64] **Cruz, L.,Rudek, C., Freire, R.** (2019) Different approaches on how to improve braking performance in M3 vehicles to meet secondary brake requirements from ECE R13 regulation through low cost solutions. *SAE International 2019-36-0011.*

[65] **Jiang, J., Shi, W., Zhen, J., Zuo, P., Xiao, J., Chen, X., Xu, W., Zhan, J.** (2014). Optimized Operating Range for Large-Format LiFePO4/Graphite Batteries. *Journal of The Electrochemical Society, 161(3):A336-A341,* doi:10.1149/2.052403jes

[66] Lifepo4 Battery Depth of Discharge: Best Usable Capacity To Maximizing Battery Life. Retrieved March, 02 2024 from https://harveypoweress.com/lifepo4-battery-depth-of-discharge/.

[67] **Sakawa, M**. (2002). Genetic Algorithms and Fuzzy Multiobjective Optimization. Doi: 10.1007/978-1-4615-1519-7.

[68] **Martinez-Boggio, S., Monsalve-Serrano, J., Garcia, A., Curto-Risso, P.** (2023). Energies 2023, 16 (8), 3565, doi: 10.3390/en16083565.

[69] **Zhang, J., Xu, L., Liang, C., Jianqiu, L. , Ouyang, M.**. (2020). Optimal sizing of fuel cell electric vehicle powertrain considering multiple objectives. *IEEE* 317-322. 10.1109/IECON43393.2020.9254713.

[70] **Ruan, J., Zhang, B., Liu, B., Wang, S.** (2021). The Multi-objective Optimization of Cost, Energy Consumption and Battery Degradation for Fuel Cell-Battery Hybrid Electric Vehicle. *IEEE* 50-55. 10.1109/CPEEE51686.2021.9383396, pp.317-322.

[71] LFP or NMC. Retrieved March 2024 from: https://www.eetimes.com/lithium-batteries-for-evs-go-nmc-or-lfp/

[72] Cellcentric Fuel-cell System: https://cellcentric.net/en/technology/

[73]Fuel-cell System Targets. Retrieved from https://www.energy.gov/eere/fuelcells/doe-technical-targets-onboard-hydrogen-storage-light-duty-vehicles

[74] **Yuan, H., Zou, W., Jung, S., Kim,Y.** (2022) Optimizes rule-based energy management for a polymer electrolyte membrace fuel-cell/battery hybrid power system using genetic algorithm. *International Journal of Hydrogen Energy*, Volume 47, Issue 12, pp. 7932-7948, doi: 10.1016/j.ijhydene.2021.12.121.

[75] **Zhang, Z., Wang, F., Guo, H., Shi, T., Hu, L.** (2022) Hierarchical Control Strategy for Hybrid Heavy-duty Trucks Considering Equivalent Hydrogen Consumption and Fuel-cell Life. *IEEE Transportation Electrification Conference and Expo 2022,* doi: 10.1109/ITECAsia-Pacific56316.2022.9942135.

[76] **Tran, H.N., Le, T., Jeong H., Kim, S., Kieu, H., Choi, S.** (2021). High Power Density DC-DC Converter for 800V Fuel Cell Electric Vehicles. *2021 IEEE 12th Energy Conversion Congress & Exposition - Asia (ECCE-Asia),*, pp. 2224-2228, doi: 10.1109/ECCE-Asia49820.2021.9479257.

APPENDICES

APPENDIX – A: FCS Optimization Simulink Function

```
function Output = Multiobjectives2(input, LB, UB)
    % Extract input arguments
    Pfc_cont = input(1);
    pfc_max = input(2);
    Pfc_idle = input(3);

    % Run the simulation
    simOut = sim("Fuel_Cell_opt.slx");

    % Get simulation data for fcell_con and waste_energy
    fcell_con_data = simOut.fcell_con;
    waste_energy_data = simOut.waste_energy;

    % Extract the final numerical data from timeseries objects
    fcell_con_final = fcell_con_data.Data(end);
    waste_energy_final = waste_energy_data.Data(end);

    % Calculate F1 and F2 based on the final values
    F1 = fcell_con_final;
    F2 = waste_energy_final;

    % Define weights for each objective
    w1 = 1; % Weight for F1
    w2 = 1; % Weight for F2

    % Calculate weighted sum fitness
    Fitness = 1 / (w1 * F1 + w2 * F2);

    % Penalty for violating bounds
    penalty = 0;
    if any(input < LB) || any(input > UB)
        penalty = 1000; % Large penalty for out-of-bound values
    end

    % Return the output
    Output = Fitness + penalty; % Apply penalty to fitness
end
```

APPENDIX – B: FCS GA Optimization Code

```
% Define the number of variables (parameters)
numVariables = 3;

% Define lower and upper bounds for the parameters
LB = [60000, 110000, 160000]; % Lower bounds for Pfc_idle, Pfc_cont, Pfc_max
UB = [100000, 160000, 300000]; % Upper bounds for Pfc_idle, Pfc_cont, Pfc_max

% Set up options for the genetic algorithm
options = optimoptions(@ga, ...
    'MaxGenerations', 20, ... % Limit iterations to 20
    'MaxTime', 1000, ... % Set maximum time to 1000 seconds
    'StallGenLimit', 50, ... % Set maximum stall generations to 50
    'PopulationSize', 50, ... % Set population size as 50
    'PlotFcn', []); % Remove plot function

% Call the genetic algorithm function
[x, fval] = ga(@(x) Multiobjectives2(x, LB, UB), numVariables, [], [], [], [], LB, UB,
[], options);

% Display the optimized parameters and corresponding fitness value
disp('Optimized parameters (Pfc_idle, Pfc_cont, Pfc_max):');
disp(x);
disp('Corresponding fitness value:');
disp(fval);
```

APPENDIX – C: FCHEV Energy Management System Function

```
function [Pb, Pfc,k] = fcn(clock, dP, PnmcMax, Pload,
soc,soch,socl,pf_act,Ratefc_load,Pfc_cont,pfc_max,Pfc_idle)
k=0;
Pb = 0;
Pfc = 0;

% If Fuel-cell is not active due to Activation routine.
if clock < 2 && PnmcMax >= Pload

    if soc > soch
        Pb = Pload + pf_act;
        Pfc = 0;
        k=0;
    elseif soc >= socl && soc <= soch
        Pb = Pload + pf_act;
        Pfc = 0;
        k=1;
    elseif soc < socl
        Pb = Pload+pf_act;
```

```
        Pfc = 0;
        k=2;
    end
else

    %If Fuel-cell is not active due to Power Rating.
    if clock > 2 && PnmcMax >= Pload

        if (Ratefc_load <= dP / 1000)
            Pb = Pload;
            Pfc = 0;
            k=3;
            %If Fuel-cell is active due to Power Rating.
        elseif Pload >= pfc_max
            if soc > soch
                Pb = Pload-Pfc_cont;
                Pfc = Pfc_cont;
                k=4; %battery %supports because SOC>SOCh
            elseif soc >= socl && soc <= soch
                Pb = Pload - pfc_max;
                Pfc = pfc_max;
                k=5;
            elseif soc < socl
                Pfc = pfc_max;
                Pb = Pload - pfc_max;
                k=6;
            end
        elseif pfc_max>= Pload && Pload >= Pfc_cont %inefficient working range
            if soc > soch
                Pb = Pload - Pfc_idle;
                Pfc = Pfc_idle;
                k=7;
            elseif soc >= socl && soc <= soch
                Pb = 0;
                Pfc = Pload;
                k=8;
            elseif soc < socl
                Pfc = pfc_max;
                Pb = -abs(pfc_max - Pload);
                k=9;
            end
        elseif Pfc_cont >= Pload && Pload >= Pfc_idle
            if soc > soch
                Pb = Pload- Pfc_idle;
                Pfc = Pfc_idle;
                k=13;
            elseif soc >= socl && soc <= soch
                Pb = 0;
                Pfc = Pload;
                k=14;
```

```
        elseif soc < socl
          Pfc = pfc_max;
          Pb = -abs(pfc_max - Pload);
          k=15;
        end
      elseif Pfc_idle > Pload && Pload >= 0
        if soc > soch
          Pb = 0;
          Pfc = Pload;
          k=16;
        elseif soc >= socl && soc <= soch
          Pb = -abs(Pload-Pfc_idle);
          Pfc = Pfc_idle;
          k=17;
        elseif soc < socl
          Pfc = pfc_max;
          Pb = -abs(pfc_max - Pload);
          k=18;
        end
        end
    end

end
```

APPENDIX – D: Battery SOC Range Optimization Simulink Function

```
function Output = Multiobjectives2(input, LB, UB)
    % Extract input arguments
    soch = input(1);
    socl = input(2);

    % Run the simulation
    simOut = sim("Fuel_Cell_opt.slx");

    % Get simulation data for fcell_con and waste_energy
    fcell_con_data = simOut.fcell_con;
    waste_energy_data = simOut.waste_energy;

    % Access data
    fcell_con_final = fcell_con_data(end);
    waste_energy_final = waste_energy_data(end);

    % Calculate F1 and F2 based on the final values
    F1 = fcell_con_final;
    F2 = waste_energy_final;

    % Define weights for each objective
    w1 = 1; % Weight for F1
    w2 = 1; % Weight for F2
```

```
    % Calculate weighted sum fitness
    Fitness = 1 / (w1 * F1 + w2 * F2);

    % Penalty for violating bounds
    penalty = 0;
    if socl < LB(2) || soch < UB(2) || socl >= soch
        penalty = 1000; % adjust penalty weight as needed
    end

    % Return the output
    Output = Fitness + penalty; % Apply penalty to fitness
end
```

APPENDIX – E: Battery SOC Range GA Optimization Code

```
% Define the number of variables (parameters)
numVariables = 2;

% Define lower and upper bounds for the parameters
LB = [40,60]; % Define lower bounds for soch and socl
UB = [60,90]; % Define upper bounds for soch and socl

% Set up options for the genetic algorithm
options = optimoptions(@ga, ...
    'MaxGenerations', 20, ... % Limit iterations to 20
    'MaxTime', 1000, ... % Set maximum time to 1000 seconds
    'StallGenLimit', 50, ... % Set maximum stall generations to 50
    'PopulationSize', 50, ... % Set population size as 50
    'PlotFcn', []); % Remove plot function

% Call the genetic algorithm function
[x, fval] = ga(@(x) Multiobjectives_1703(x, LB, UB), numVariables, [], [], [], [], LB,
UB, [], options);

% Display the optimized parameters and corresponding fitness value
disp('Optimized parameters (soch, socl):');
disp(x);
disp('Corresponding fitness value:');
disp(fval);
```

CURRICULUM VITAE

Name Surname : Baturay Gürsel

EDUCATION:

- **B.Sc.:** 2015, Istanbul Technical University, Electrical-Electronics Faculty, Electrical Engineering, Istanbul, Turkey

PROFESSIONAL EXPERIENCE AND REWARDS:

- 2019-Present, R&D Engineer – Daimler Truck AG
- 2017-2019, R&D Engineer – Mercedes-Benz Türk A.S
- 2015-2017, R&D Engineer – Arcelik A.S.

PUBLICATIONS, PRESENTATIONS AND PATENTS ON THE THESIS:

OTHER PUBLICATIONS, PRESENTATIONS AND PATENTS:

- WO 002020057842 - AN ELECTRIC MOTOR
- DE 102022118087 - HOCHVOLTKOMPONENTE